AD-A267 265

1. AGENCY USE ONLY (Leave blank)	2. REPORT DATE	3. REPORT TYPE AND DATES COVERED
	09/20/92	Final, 5/15/90 - 8/31/92

4. TITLE AND SUBTITLE

(U) A Numerical Investigation of Energy Transfer and Subgrid-Scale Eddy-Viscosity in Homogeneous, Isotropic and Shear Turbulence

5. FUNDING NUMBERS

PE - 61102F
PR - 2307
SA - BS
G - AFOSR-90-0300

6. AUTHOR(S)

Principal Investigator: J.A. Domaradzki

7. PERFORMING ORGANIZATION NAME(S) AND ADDRESS(ES)

Department of Aerospace Engineering
University of Southern California
University Park, RRB 215
Los Angeles, CA 90089-1191

8. PERFORMING ORGANIZATION REPORT NUMBER

AFOSR-TR- 93 0479

9. SPONSORING/MONITORING AGENCY NAME(S) AND ADDRESS(ES)

AFOSR/NA
Building 410
Bolling AFB DC 20332-6448

10. SPONSORING/MONITORING AGENCY REPORT NUMBER

AFOSR-90-0300

11. SUPPLEMENTARY NOTES

12a. DISTRIBUTION/AVAILABILITY STATEMENT

Approved for public release; distribution is unlimited

12b. DISTRIBUTION CODE

13. ABSTRACT (Maximum 200 words)

Using results of direct numerical stimulation we have analyzed nonlinear energy transfer between scales of motion in isotropic and homogeneous shear turbulence in both spectral and physical space representation. In all cases we find that the transfer is local, occurring between similar scales, but is always moderated by scales from the energy containing range (local transfer through nonlocal triad interaction). Such local energy exchanges dominate also subgrid-scale energy transfer which was found to be composed os a forward and an inverse transfer components, both being significant in dynamics of large scales. The spatial structure of the subgrid-scale transfer was compared with the structure of a number of physical quantities which are considered important in the dynamics of large scales giving usually poor correlations. Moderate correlations were observed only for the large scale energy and the Smagorinsky's transfer. Finally, a new theory of spectral energy dynamics was developed. The theory provides a plausible physical mechanism of the observed transfer process and predicts the energy spectrum in the inertial and the dissipation range in agreement with experiments and simulations.

14. SUBJECT TERMS

15. NUMBER OF PAGES 79

16. PRICE CODE

17. SECURITY CLASSIFICATION OF REPORT	18. SECURITY CLASSIFICATION OF THIS PAGE	19. SECURITY CLASSIFICATION OF ABSTRACT	20. LIMITATION OF ABSTRACT
Unclassified	Unclassified	Unclassified	UL

Contract No. AFOSR-90-0300

A NUMERICAL INVESTIGATION OF ENERGY TRANSFER AND SUBGRID-SCALE EDDY-VISCOSITY IN HOMOGENEOUS, ISOTROPIC AND SHEAR TURBULENCE

Principal Investigator:
J.A. Domaradzki

Department of Aerospace Engineering
University of Southern California
University Park
Los Angeles, California 90089-1191

September 16, 1992

Final Technical Report
Period: May 15, 1990 to August 31, 1992

Air Force Office of Scientific Research
Bolling Air Force Base
Washington, D.C. 20332-6448

1 Summary of the Research Results

The following goals have been accomplished in the course of this research:

1. We have analyzed nonlinear energy transfer between scales of motion in homogeneous isotropic and uniform shear turbulence using results of direct numerical simulations. The main conclusion drawn from these analyses is that the transfer is local in the spectral space i.e. occurs between two similar small scales, but results from interactions of these scales with much larger and energetic scales from the energy containing range (local energy transfer through nonlocal triad interactions).

2. The results of this investigation were used to develop a new theory of spectral energy dynamics. The theory properly accounts for properties of interscale energy transfer observed in the simulations, predicts the form of the energy spectrum in the dissipation range in agreement with experiments and simulations, predicts correctly the form of the energy spectrum in the inertial range, and provides a plausible physical mechanism responsible for the observed transfer process.

3. We have devised a physical space representation of the spectral energy transfer among scales with predefined sizes and found that the interscale energy transfer is spatially intermittent and local in the physical space.

4. The physical space representation of the spectral energy transfer was used in an analysis of subgrid-scale nonlinear interactions. The subgrid-scale transfer was found to be composed of a forward and an inverse transfer components, both being significant in dynamics of resolved scales. Energy exchanges between the resolved and unresolved scales from the vicinity of the cutoff wave number dominate the subgrid-scale processes and the energetics of the resolved scales are unaffected by the modes with wave numbers greater than twice the cutoff wave number. The dominance of nonlinear interactions among the largest scales in the subgrid-scale energy transfer process suggests that the resolved nonlinear term may serve as a basis of a new approach to the subgrid-scale modeling.

5. The physical space representation of the subgrid-scale transfer was used in assessing the dynamical importance of large scales of motion (coherent structures) in isotropic turbulence. The spatial structure of the exact subgrid-scale transfer was qualitatively compared with the spatial structure of a number of physical quantities which are considered to govern the dynamics of the large scales of turbulence. It was found that all quantities determined by the first derivatives of the velocity field correlate poorly with the transfer which is largest at the peripheries of regions characterized by large values of these quantities. The spatial structure of the transfer correlates much better with the large scale energy and the Smagorinsky's subgrid-scale energy transfer which is determined by the second derivatives of the velocity field. None of the considered quantities was capable of predicting sign of the subgrid-scale transfer.

6. The interscale energy transfer analysis in both spectral and physical representation has been performed using results of direct numerical simulations of the Kida flow performed by Dr. Pelz at Rutgers University. The results of this analysis will serve to supplement an ongoing investigation at Rutgers of the process of generation of small scales in such a flow.

2 Publications/Presentations

Refereed Journals

1. J.A. Domaradzki, "Nonlocal triad interactions and the dissipation range of isotropic turbulence", Phys. Fluids **4**, 2037-2045 (1992).

2. J.A. Domaradzki, W. Liu, and M.E. Brachet, "An analysis of subgrid-scale interactions in numerically simulated isotropic turbulence", submitted to Phys. Fluids (1992).

3. J.A. Domaradzki and R.M. Kerr, "Subgrid-scale energy transfer and large scales of motion in isotropic turbulence", to be submitted to Phys. Fluids (1992).

Conference Proceedings/Abstracts

1. J.A. Domaradzki, R.S. Rogallo, and A.A. Wray, "Interscale Energy Transfer in Numerically Simulated Homogeneous Turbulence", in *Proceedings of the Center for Turbulence Research, Summer Program 1990*, NASA Ames/Stanford University, 319-329 (1990).

2. J.A. Domaradzki, R.S. Rogallo, and A.A. Wray, "Interscale Energy Transfer in Numerically Simulated Homogeneous Turbulence", Bull. Am. Phys. Soc. **35**, 2305 (1990).

3. J.A. Domaradzki, R.S. Rogallo, and A.A. Wray, "Physical Space Representation of Spectral Energy Transfer in Homogeneous Turbulence", in *Proceedings of 13th IMACS World Congress on Computation and Applied Mathematics*, Dublin, 1986-1987 (1991).

4. J.A. Domaradzki, "Energy transfer in dissipation range", Bull. Am. Phys. Soc. **36**, 2649 (1991).

5. J.A. Domaradzki, W. Liu, and M.E. Brachet, "An analysis of subgrid-scale interactions in numerically simulated isotropic turbulence", Bull. Am. Phys. Soc. **37**, (1992).

Invited Talks

1. J.A. Domaradzki, "Energy transfer and nonlocal interactions in turbulent flows", Department of Mechanical Engineering, University of Southern California, Los Angeles, CA (September 1990).

2. J.A. Domaradzki, "Subgrid-scale interactions in numerically simulated turbulence". Geophysical Turbulence Program, National Center for Atmospheric Research, Boulder, CO (July 1992).

3 Research Personnel

1. J.A. Domaradzki (Principal Investigator), Associate Professor, Department of Aerospace Engineering, University of Southern California, Los Angeles, CA 90089-1191. Dates supported: 05/15/90 - 08/31/92.
2. W. Liu, Research Associate, Department of Aerospace Engineering, University of Southern California, Los Angeles, CA 90089-1191. Dates supported: 06/01/91 - 08/31/92.

Our research had a collaborative character and during its course we have collaborated with the following scientists:

1. Professor M.E. Brachet, École Normale Supérieure, 75231 Paris CEDEX 05, France.
2. Dr. R.M. Kerr, National Center for Atmospheric Research, Boulder, CO 80307-3000.
3. Professor R.B. Pelz, Mechanical and Aerospace Engineering, Rutgers University, Piscataway, N.J. 08855.
4. Dr. R.S. Rogallo, NASA Ames Research Center, Moffett Field, CA 94035.
5. Dr. A.A. Wray, NASA Ames Research Center, Moffett Field, CA 94035.

This collaboration is reflected in joint authorship of papers, either published or submitted for publication.

4 Honors/Awards

1. J.A. Domaradzki, Northrop Junior Faculty Research Award, University of Southern California, School of Engineering, 1991.
2. J.A. Domaradzki, Alexander von Humboldt Research Award for Senior U.S. Scientists, Alexander von Humboldt Foundation, Germany, 1992.

5 Research Papers

This section consists of three journal papers (one published, one submitted, and one in preparation for publication) and two conference proceedings, all in chronological order, which provide detailed information about research results summarized in section 1.

Interscale Energy Transfer in Numerically Simulated Homogeneous Turbulence

By J. A. Domaradzki[1], R. S. Rogallo[2], and A. A. Wray[2]

Energy transfer is investigated for flows obtained by direct numerical simulations of low Reynolds number homogeneous-shear and isotropic turbulence and by large-eddy simulations of high Reynolds number isotropic turbulence. The transfer in spectral space is found to be local but results from interaction between separated scales. The transfer among small scales is highly intermmitent in physical space. The measurements suggest an important correlation between transfer among small scales and the energy of large scales.

1. Introduction

Using results of low-Reynolds-number direct numerical simulations (DNS) Domaradzki and Rogallo (1988, 1990) analyzed the energy transfer in isotropic turbulence and concluded that beyond the energy containing range the energy was transferred among scales of motion similar in size but that the interactions responsible for this local energy transfer were nonlocal in k-space. The same transfer mechanism was also found when the eddy-damped quasinormal Markovian (EDQNM) approximation was applied to high Reynolds number flows which are inaccessible to the DNS technique.

The conclusions concerning the apparent universality of this transfer mechanism are extended in this work to homogeneous shear flows and to high Reynolds number isotropic flows obtained by large-eddy simulation. We also devise a physical-space representation of the spectral energy transfer calculated in k space that allows us to estimate the spatial intermittency of the energy transfer and the spatial correlation between quantities defined using only large-scales flow information and the dynamically important energy transfer among different scales. In particular this is useful in evaluating the performance of subgrid-scale models formulated in physical space e.g. the classical Smagorinsky eddy viscosity model.

2. Numerical Velocity Fields

We have used velocity fields generated by numerical simulations that were run for sufficiently long times to fully establish nonlinear interactions.

The velocity field C128U8 is the result of a DNS of uniformly sheared homogeneous turbulence performed by Rogers (1986) and LES128 is the result of a

1 University of Southern California
2 NASA Ames Research Center

large-eddy simulation of forced isotropic turbulence, at nominally infinite Reynolds number, performed by Chasnov (1990). The energy spectrum of LES128 exhibits a $k^{-5/3}$ law over the entire range of simulated wavenumbers. The field K128 is obtained from a DNS of isotropic turbulence performed by Rogallo (unpublished). Its use is motivated primarily by the fact that the two dynamically important processes that determine the evolution of the energy spectrum, i.e. viscous dissipation and nonlinear transfer, are very well resolved. This resolution is obtained at the expense of lowering the Reynolds number as compared with the two other cases.

3. Basic Quantities

The Navier-Stokes equations, in the Fourier spectral representation, for the fluctuating velocity field u_n subjected to uniform shear $\mathbf{U} = (sx_2, 0, 0)$ are

$$\left(\frac{\partial}{\partial t} + \nu k^2\right) u_n(\mathbf{k},t) = (-i/2)P_{nlm}(\mathbf{k}) \int u_l(\mathbf{p},t)u_m(\mathbf{k}-\mathbf{p},t)d\mathbf{p}$$

$$+2s\frac{k_1 k_n}{k^2}u_2(\mathbf{k},t) + sk_1\frac{\partial}{\partial k_2}u_n(\mathbf{k},t) - s\delta_{n1}u_2(\mathbf{k},t) \tag{1}$$

$$ik_n u_n = 0 \tag{2}$$

where

$$P_{nlm}(\mathbf{k}) = k_m(\delta_{nl} - k_n k_l/k^2) + k_l(\delta_{nm} - k_n k_m/k^2), \tag{3}$$

ν is the kinematic viscosity, and the summation convention is assumed. In subsequent formulae explicit time dependence will be omitted.

The equation for the energy amplitudes $\frac{1}{2}|u(\mathbf{k})|^2 = \frac{1}{2}u_n(\mathbf{k})u_n^*(\mathbf{k})$ is obtained from (1)

$$\frac{\partial}{\partial t}\frac{1}{2}|u(\mathbf{k})|^2 = -2\nu k^2\frac{1}{2}|u(\mathbf{k})|^2 + T(\mathbf{k}) + sk_1\frac{\partial}{\partial k_2}\frac{1}{2}|u(\mathbf{k})|^2 - sRe\{u_1(\mathbf{k})u_2^*(\mathbf{k})\} \tag{4}$$

where the asterisk denotes complex conjugate.

The nonlinear energy transfer is

$$T(\mathbf{k}) = \frac{1}{2}Im\left[u_n^*(\mathbf{k})P_{nlm}(\mathbf{k})\int u_l(\mathbf{p})u_m(\mathbf{k}-\mathbf{p})d\mathbf{p}\right] \tag{5}$$

and the following two terms in (4) containing s describe energy transfer due to the mean shearing deformation of turbulent eddies and turbulent energy production by the mean shear respectively. A detailed description of these effects is given by Deissler (1961), Fox (1964), and Lumley (1964), and is summarized in Hinze's (1975) monograph. Note that the corresponding equations for isotropic turbulence are obtained from (1) by taking $s = 0$. In particular, the nonlinear transfer term (5) has the same form for both homogeneous shear turbulence and isotropic turbulence.

The principal quantity of interest here is the energy exchange between a given mode k and all pairs of modes p and q = k − p that form a triangle having k as one of the legs and where p and q lie in prescribed regions $\mathcal{P}$ and $\mathcal{Q}$ of the spectral space respectively. For a given k, confining p and q to $\mathcal{P}$ and $\mathcal{Q}$ is equivalent to selecting a specific set of triangles from all of the possible triangles contributing to the energy transfer at the wavevector k in (5).

In this work we choose $\mathcal{P}$ and $\mathcal{Q}$ as shells in the wavenumber space $k - \frac{1}{2}\Delta k < |\mathbf{k}| < k + \frac{1}{2}\Delta k$ with a shell thickness Δk. This choice is natural for isotropic turbulence and is also convenient for other homogeneous fields as first suggested by Batchelor (1953).

The net nonlinear energy transfer to wavenumber band k is denoted by $T(k)$ and the contribution to this transfer resulting from nonlinear interactions between wavenumbers in the band k and wavenumbers in the bands p and q is denoted by $T(k|p,q)$. According to this definition

$$T(k) = \sum_p \sum_q T(k|p,q) = \sum_p P(k|p) \tag{6}$$

where the $P(k|p)$ is the result of summation of $T(k|p,q)$ over all bands q and is interpreted as the contribution to the net energy transfer into band k due to all interactions involving band p.

The functions $T(k)$, $P(k|p)$, and $T(k|p,q)$ give progressively more detailed information about energy transfer among different scales of motion in a turbulent field. The method of computing these functions is described by Domaradzki and Rogallo (1990).

4. Analysis of Energy Transfer in Spectral Space

All of the contributing terms of (4), computed for the field C128U8 and averaged over spherical shells with thickness $\Delta k = 1$, are plotted in figure 1. The calculation of the linear transfer $sk_1 \frac{\partial}{\partial k_2} \frac{1}{2}|u(\mathbf{k})|^2$ suffers from low accuracy due to the coarse resolution of k, and we believe that this term is close to zero for $k > 40$, contrary to the plotted results. Despite this numerical error a few important conclusions can be drawn from these results. Nonlinear transfer, viscous dissipation, and mean shear all make significant contributions to the energy balance for wavenumbers $k < 40$ which comprise the energy containing range and a significant fraction of the dissipation range. Energetics of the smaller eddies ($k > 40$) is affected only by nonlinear transfer and viscous dissipation which are roughly in balance. Thus the energetics of turbulence in about half of the spectral domain ($k > 40$) is not affected directly by the large scale mean shear.

The triad structure of the nonlinear energy transfer term is illustrated by plotting $P(k|p)$ in figure 2a as a function of k for p fixed in a wavenumber band beyond the peak of the energy spectrum. The contributions $T(k|p,q)$ to $P(k|p)$, from all significant bands q, is also included. The peaks of $P(k|p)$ are located in the vicinity of the band p indicating that the energy transfer is primarily between comparable scales of motion. However, the decomposition into functions $T(k|p,q)$ reveals that

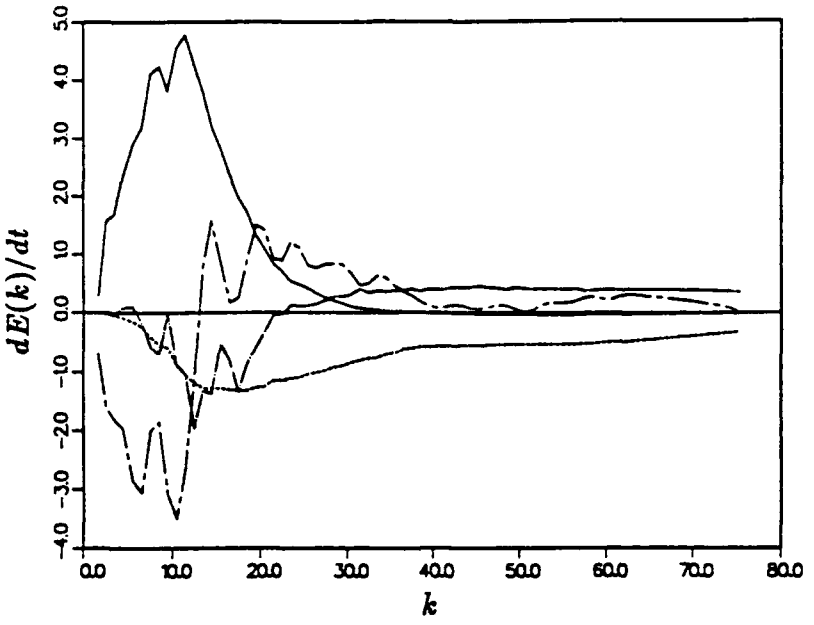

FIGURE 1. Spectral energy balance for the field C128U8. ——— production, - - - - dissipation, —·— nonlinear transfer, - - - - linear transfer. The linear transfer data has been smoothed.

the largest contributions to this local transfer come from the interactions involving a scale in the energy containing range $5 < q < 20$. Thus for homogeneous shear flow we obtain the same result as previously reported by Domaradzki and Rogallo (1988, 1990) for isotropic flows: local energy transfer between two scales beyond the energy containing range results from nonlocal interactions with scales in the energy containing range.

Analysis of the nonlinear transfer for the two remaining velocity fields, LES128 and K128, provided the same qualitative results.

An attempt was made to find a similarity scaling for the functions $T(k|p,q)$. For a given energy spectrum the following transformation collapses reasonably well all curves $T(k|p,q)$ for a band p beyond the energy containing range.

$$T(k|p,q) = pE(p)E(q)T_s(\frac{k-p}{q}) \tag{7}$$

The similarity variable $\xi = (k-p)/q$ is deduced from geometric relations for a triad with legs k, p, and q and the scaling factor $pE(p)E(q)$ is ad hoc (but is found in the EDQNM theory for power-law spectra in the disparate-scale limit). In figure 2b we show the result of scaling (7) applied to the measured functions $T(k|p,q)$ of figure 2a. Interestingly, the transfer scales with the energy $E(q)$ of the large eddies rather than with their rate-of-strain $qE(q)^{1/2}$ which is the scaling postulated by a number of classical closure hypotheses (Monin and Yaglom, 1975). We have not been able to propose a convincing dynamical model of transfer processes which would provide scaling (7).

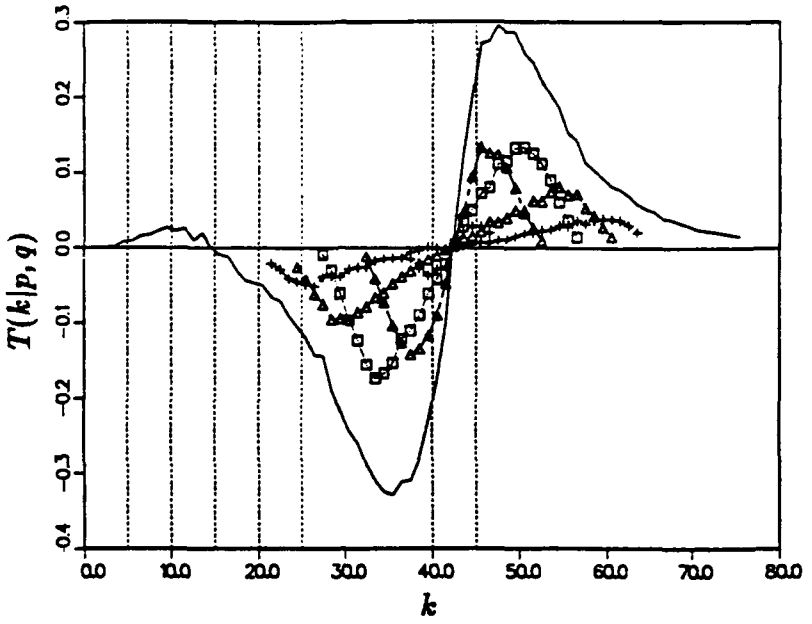

(a)

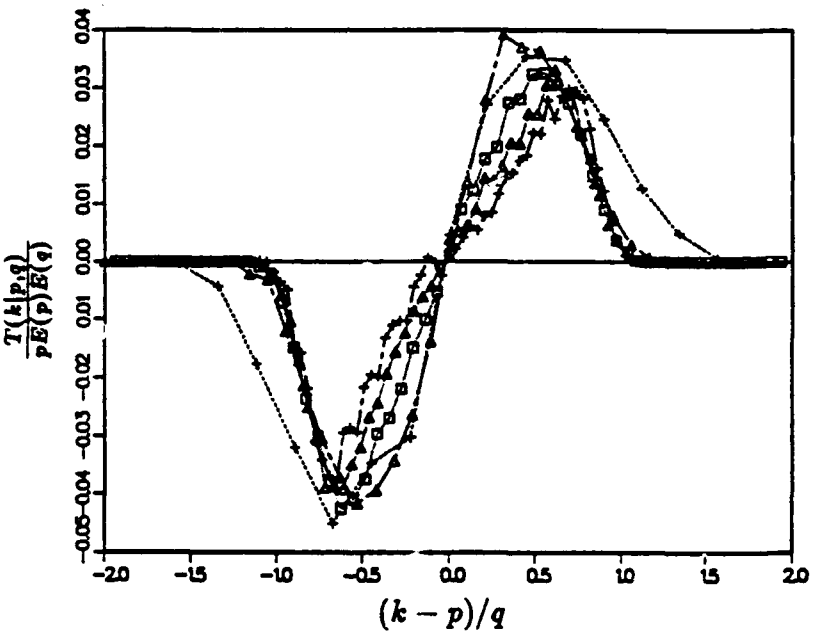

(b)

FIGURE 2. Detailed triad contributions to energy transfer for case C128U8: (a) unscaled, (b) scaled by (7). The transfer spectra $T(k|p,q)$ are shown for band $40 < p < 45$, and all bands q that make a significant contribution to $P(k|p)$. +---- $0 < q < 5$, △ —-- $5 < q < 10$, □ ····· $10 < q < 15$, △ ····· $15 < q < 20$, +—-- $20 < q < 25$, —— $P(k|p)$.

5. Physical Space Representation of Spectral Energy Transfer

Let us denote by $N_n^{\mathcal{PQ}}(\mathbf{k})$ the contribution to the integral (the nonlinear term) in (1) from only those interactions between modes $\mathbf{p}$ and $\mathbf{q} = \mathbf{k} - \mathbf{p}$ such that each of them is confined to one of the two prescribed wavenumber bands $\mathcal{P}$ and $\mathcal{Q}$. This quantity is computed using the method described by Domaradzki and Rogallo (1990). Its Fourier transform to physical space, $N_n^{\mathcal{PQ}}(\mathbf{x})$ say, gives the contribution to the rate of change of velocity in physical space $u_n(\mathbf{x}, t)$ caused by the nonlinear interactions involving two scales from the respective wavenumber bands $\mathcal{P}$ and $\mathcal{Q}$ in the spectral space. Note that these interactions influence all modes $\mathbf{k}$ that can form a triangle with modes such that one is in $\mathcal{P}$ and the other in $\mathcal{Q}$. Consider next a velocity field truncated to a prescribed wavenumber band $\mathcal{K}$, i.e.

$$u_n^{\mathcal{K}}(\mathbf{k}) = \begin{cases} u_n(\mathbf{k}), & \text{if } \mathbf{k}\epsilon\mathcal{K} \\ 0, & \text{otherwise.} \end{cases} \tag{8}$$

The Fourier transform of (8) to physical space, $u_n^{\mathcal{K}}(\mathbf{x})$ say, represents the contribution in physical space that scales from band $\mathcal{K}$ make to the total velocity. The contracted product of these two physical space quantities

$$T^{\mathcal{KPQ}}(\mathbf{x}) = u_n^{\mathcal{K}}(\mathbf{x}) N_n^{\mathcal{PQ}}(\mathbf{x}) \tag{9}$$

gives a physical space representation of the energy transfer to/from modes in the k-band due to their nonlinear interactions with modes in the p- and q-bands.

An interesting case is obtained by dividing wavenumber space into two disjoint regions $\mathcal{K}$ ($k < k_c$) and $\mathcal{P}$ ($k > k_c$). The quantity

$$T_{SGS}(\mathbf{x}|k_c) = T^{\mathcal{KPP}}(\mathbf{x}) + T^{\mathcal{KKP}}(\mathbf{x}) \tag{10}$$

provides a physical space representation of the rate of change of energy of large scales $k < k_c$ due to nonlinear interactions involving small scales $k > k_c$. This is precisely the energy transfer process which is the subject of subgrid-scale modelling.

We have computed transfer functions (9) and (10) for various wavenumber bands of the field K128. The low wavenumber band $\mathcal{Q}$ is chosen to cover the entire energy containing range $0 < q < 10$. Figure 3a shows one plane from the full transfer (9) representing in physical space the energy transfer to eddies in the band $23 < k < 28$ caused by their interactions with eddies in the bands $20 < p < 25$ and $0 < q < 10$. The transfer function is spatially intermittent and is predominantly positive indicating a flow of energy from the larger scales p to the smaller scales k. In figure 4b we plot the same function for $17 < k < 22$. The transfer is now predominantly negative as expected and occurs at roughly the same locations as the transfer of figure 3a. We thus conclude that the local energy transfer between similar wavenumber modes in spectral space is intermittent in physical space.

We have attempted to correlate this spatial distribution of energy transfer with a number of simpler quantities (rate-of-strain, dissipation, energy, etc.) calculated from the velocity field truncated to contain only either large or small scales. In figures 4a and 4b we show the physical-space distribution of energy for the velocity

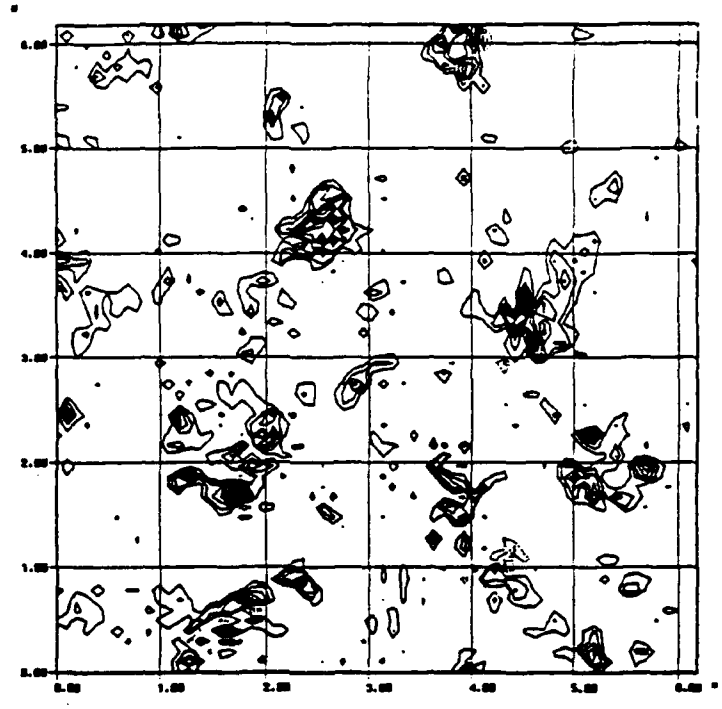

(a)

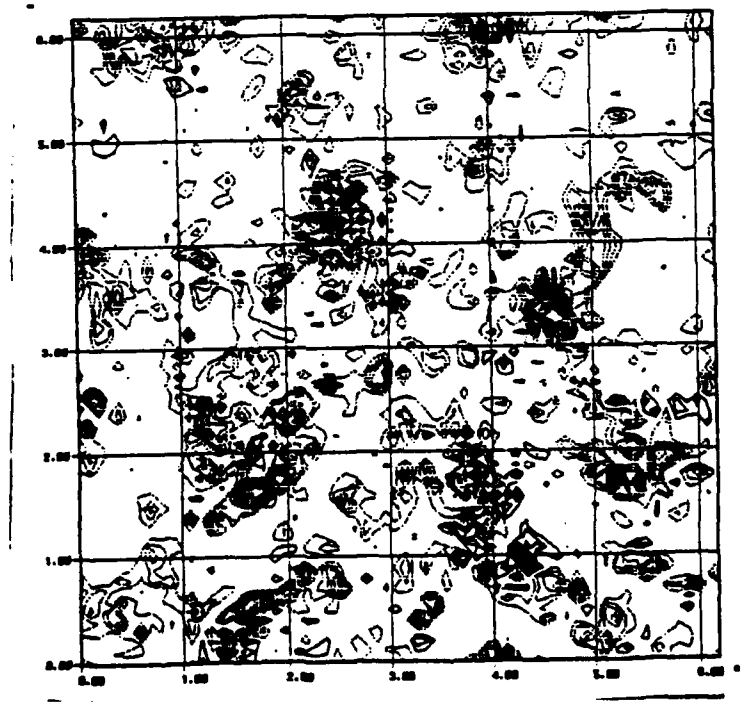

(b)

FIGURE 3. Energy transfer $T^{KPQ}(\mathbf{x})$ of K128 in physical space for $20 < p < 25, 0 < q < 10$: (a) $23 < k < 28$, (b) $17 < k < 22$.

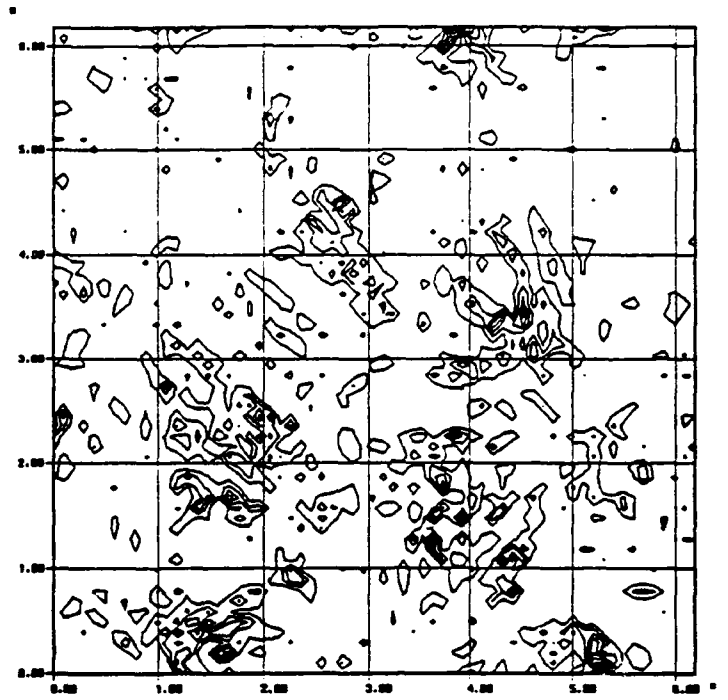

(a)

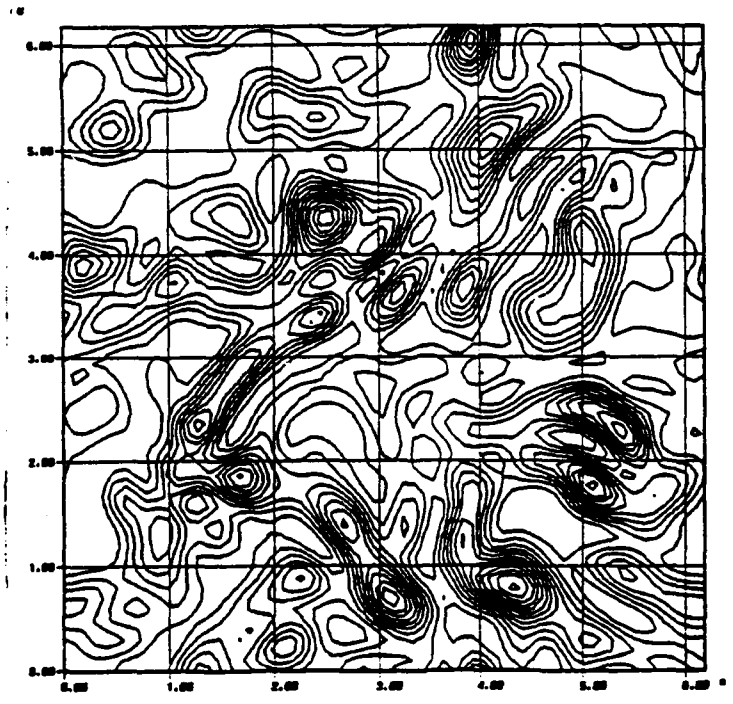

(b)

FIGURE 4. Turbulent energy in physical space for the velocity field truncated in spectral space to wavenumber band: (a) $23 < k < 28$, (b) $0 < k < 10$.

field truncated to $23 < k < 28$ and $0 < k < 10$, respectively. Both energy fields correlate very well with the energy transfer among small scales shown in figure 3. Correlation of other calculated quantities with the energy transfer, notably the square of the rate-of-strain tensor, was generally much worse. Therefore we conclude that the energy transfer among small scales occurs mostly at those physical locations that contain large amounts of turbulent energy rather than at the locations of high strain rate. This correlation is the physical space counterpart of the observed importance of the nonlocal triads in the energy transfer process in spectral space.

We have used formula (10) to calculate subgrid-scale (SGS) energy transfer for the field K128 with the cutoff wavenumber $k_c = 10$. The full SGS transfer field, plotted in figure 5a for a typical plane, is characterized by the presence of both negative and positive regions. These indicate energy flux from and to the large scales respectively due to subgrid-scale interactions. The classical Smagorinsky model (Smagorinsky, 1963) for this transfer, based on the velocity field truncated to the large scales $0 < k < 10$, is plotted in figure 5b. Note that the model captures properly the locations of the regions where the transfer is most intense but fails completely to predict the inverse energy transfer from small to large scales.

6. Conclusions

Using results of direct numerical simulations of homogeneous shear turbulence we have shown that the nonlinear energy transfer in spectral space beyond the energy containing range has the same character as reported previously for isotropic turbulence: *local* energy transfer caused by *nonlocal* triad interactions. The same conclusion was reached for velocity fields obtained in large-eddy simulations of isotropic turbulence at high Reynolds numbers.

An ad hoc scaling roughly collapses the transfer $T(k|p,q)$ to a self-similar form. This scaling implies an important role which the energetic scales play in the energy transfer among small scales, but the process does not appear to be simply straining of the small scales by the large ones.

We have devised a physical space representation of the energy transfer processes among scales of motion belonging to three distinct wavenumber bands in spectral space and conclude from it that the energy transfer among small scales is highly intermittent in physical space. Furthermore, regions of significant transfer appear to correlate better with regions of significant large-scale energy than with those of significant large-scale strain rate.

As a particular case we have calculated the subgrid-scale energy transfer in isotropic turbulence. This SGS transfer exhibits regions of energy drain from large to small scales as well as significant regions of reversed energy transfer from small to large scales. The Smagorinsky eddy viscosity model captures the locations of the most intense transfer but predicts that it is always from large to small scales, contrary to the measurements from direct calculations.

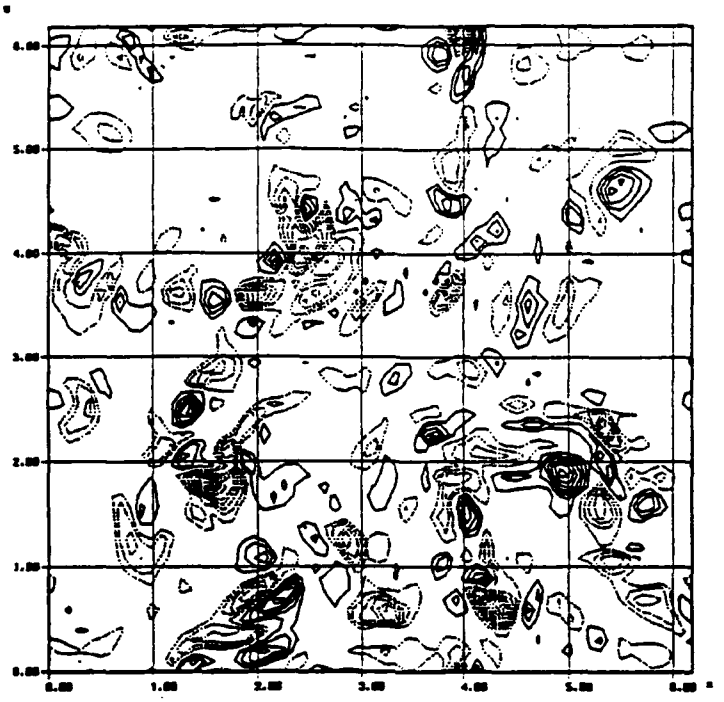

(a)

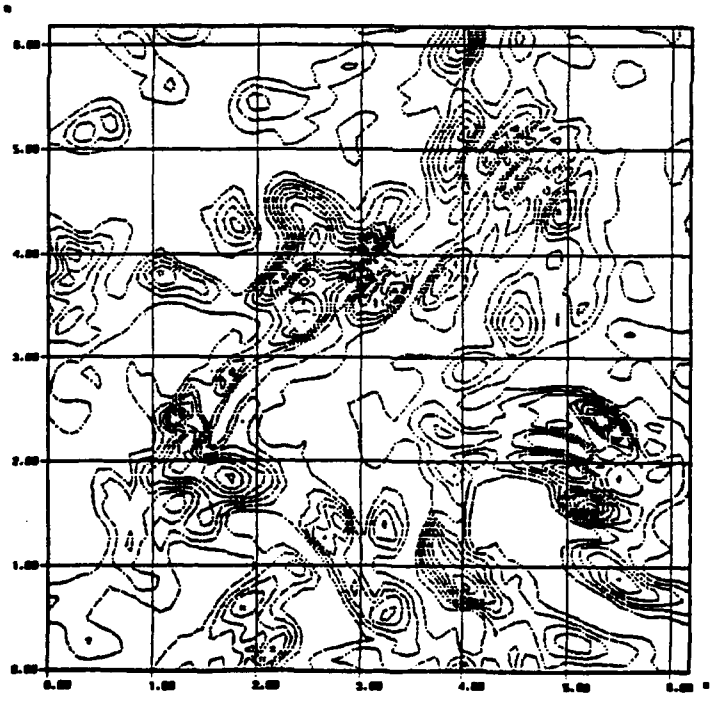

(b)

FIGURE 5. Subgrid scale energy transfer in physical space $T_{SGS}(\mathbf{x}|k_c)$ for $k_c = 10$: (a) measured, (b) computed using the Smagorinsky eddy viscosity model for the velocity field truncated to wavenumber band $0 < k < 10$.

REFERENCES

BATCHELOR, G.K. 1953, *The Theory of Homogeneous Turbulence*, Cambridge University Press.

CHASNOV, J.R. 1990 Ph.D. Dissertation, Columbia University

DEISSLER, R.G. 1961, *Phys. Fluids* **4**, 1187.

DOMARADZKI, J.A. & ROGALLO, R.S. 1988, in *Proceedings of Center for Turbulence Research, Summer Program 1988.*

DOMARADZKI, J.A. & ROGALLO, R.S. 1990, *Phys. Fluids* **A2**, 413.

FOX, J. 1964, *Phys. Fluids* **7**, 562.

HINZE, J.O. 1975, *Turbulence*, McGraw-Hill.

LUMLEY, J.L. 1964, *Phys. Fluids* **7**, 190.

MONIN, A.S. & YAGLOM, A.M. 1975, *Statistical Fluid Mechanics*, Vol. 2, The MIT Press, pp.212-241.

ROGERS, M. M., MOIN, P., & REYNOLDS, W. C. 1986 Report TF-25, Department of Mechanical Engineering, Stanford University

SMAGORINSKY, J. 1963, *Mon. Weath. Rev.* **91**, 99.

IMACS '91

13TH WORLD CONGRESS ON COMPUTATION AND APPLIED MATHEMATICS

JULY 22 - 26, 1991
TRINITY COLLEGE DUBLIN
IRELAND

PROCEEDINGS

IN FOUR VOLUMES

VOLUME 4

PHYSICAL SPACE REPRESENTATION OF SPECTRAL ENERGY TRANSFER IN HOMOGENEOUS TURBULENCE

J. ANDRZEJ DOMARADZKI
University of Southern California
Los Angeles, CA 90089-1191 U.S.A.

AND

ROBERT S. ROGALLO, ALAN A. WRAY
NASA-Ames Research Center
Moffett Field, CA 94035 U.S.A.

Abstract-Direct numerical simulations of homogeneous turbulence are used to analyze energy transfer among scales of motion in spectral space. A physical space representation of such a spectral energy transfer is devised and applied to the analysis of an eddy viscosity with a sharp spectral cut-off.

1 Introduction

Statistically homogeneous turbulent flows are conveniently represented in spectral (Fourier) space. In such a representation dynamically important, elementary nonlinear interactions involve three distinct modes with their wavenumbers forming a closed triad. Understanding these interactions is of paramount importance in the theory of turbulence since essentially all turbulence closures rely on assumptions about the nature of the nonlinear interactions. Recently, using results of direct numerical simulations (DNS) Domaradzki and Rogallo [1] [2] analyzed the energy transfer in homogeneous turbulence. They concluded that beyond the energy containing range the energy was transferred among scales of motion similar in size but that the interactions responsible for this local energy transfer were nonlocal in k-space. The importance of such nonlocal triadic interactions in the evolution of turbulent flows has been confirmed by Yeung and Brasseur [3] who also provided analytical arguments [4] supporting conclusions drawn from DNS.

Despite the usefullness of spectral representation as a theoretical and numerical tool in turbulence research, various quantities (velocity, energy, vorticity, etc.) in the physical space often provide a more natural description of turbulent flows. Thus it is of interest to have *the physical space* representation of the nonlinear transfer processes that dominate *the spectral space* dynamics. One such representation has been proposed by Domaradzki et al. [5]. In this paper we discuss other possible ways of representing detailed spectral energy transfer in the physical space.

2 Interscale Energy Transfer in Spectral Space

The equation for the energy amplitudes $\frac{1}{2}|u(\mathbf{k})|^2 = \frac{1}{2}u_n(\mathbf{k})u_n^*(\mathbf{k})$ is:

$$\frac{\partial}{\partial t}\frac{1}{2}|u(\mathbf{k})|^2 = -2\nu k^2\frac{1}{2}|u(\mathbf{k})|^2 + T(\mathbf{k}) \tag{1}$$

where $u_n(\mathbf{k})$ is the velocity field in spectral space, with the explicit dependence on time omitted, the asterisk denotes complex conjugate, ν is the kinematic viscosity, and $T(\mathbf{k})$ is the nonlinear energy transfer

$$T(\mathbf{k}) = Re(u_n^*(\mathbf{k})N_n(\mathbf{k})). \tag{2}$$

In the last equation $N_n(\mathbf{k})$ is the nonlinear term in the Navier-Stokes equation

$$N_n(\mathbf{k}) = (-i/2)P_{nlm}(\mathbf{k})\int d^3p u_l(\mathbf{p})u_m(\mathbf{k}-\mathbf{p})\,, \tag{3}$$

where tensor $P_{nlm}(\mathbf{k})$ accounts for the pressure and incompressibility effects. The summation convention is assumed throughout.

Detailed energy transfer to/from mode $\mathbf{k}$ caused by its interactions with wavenumbers $\mathbf{p}$ in a prescribed region $\mathcal{P}$ of the wavenumber space and $\mathbf{q} = \mathbf{k} - \mathbf{p}$ in another region $\mathcal{Q}$ is

$$T^{\mathcal{P}\mathcal{Q}}(\mathbf{k}) = Re(u_n^*(\mathbf{k})N_n{}^{\mathcal{P}\mathcal{Q}}(\mathbf{k})) \tag{4}$$

where $N_n{}^{\mathcal{P}\mathcal{Q}}$ is (3) calculated with one of the contributing velocity fields truncated to $\mathcal{P}$ and the other to $\mathcal{Q}$. Details of such calculations are provided in [2]. For homogeneous turbulence the regions $\mathcal{P}$ and $\mathcal{Q}$ are usually chosen as spherical wavenumber bands. Similarly truncating velocity $u_n^*(\mathbf{k})$ in (4) to a spherical shell $\mathcal{K}$ results in a quantity $T^{\mathcal{K}\mathcal{P}\mathcal{Q}}(\mathbf{k})$ which, after averaging over $\mathcal{K}$, is interpreted as the energy transfer to the band $\mathcal{K}$ resulting from nonlinear interactions of scales in $\mathcal{K}$ with scales in $\mathcal{P}$ and $\mathcal{Q}$.

3 Interscale Energy Transfer in Physical Space

Inverse Fourier transform, signified by tilde, of $N_n(\mathbf{k})$ is the sum of the convection and pressure terms in the Navier-Stokes equation in the physical space coordinates

$$\tilde{N}_n(\mathbf{x}) = -\tilde{u}_i(\mathbf{x})\frac{\partial \tilde{u}_n(\mathbf{x})}{\partial x_i} - \frac{\partial \tilde{p}(\mathbf{x})}{\partial x_n}. \tag{5}$$

Similarly, using $N_n{}^{\mathcal{P}\mathcal{Q}}(\mathbf{k})$ we can define its physical space counterpart $\tilde{N}_n^{\mathcal{P}\mathcal{Q}}(\mathbf{x})$ as well as $\tilde{N}_n^{\mathcal{K}\mathcal{P}\mathcal{Q}}(\mathbf{x})$ which is the inverse Fourier transform of $N_n{}^{\mathcal{P}\mathcal{Q}}(\mathbf{k})$ truncated to the band $\mathcal{K}$. $\tilde{N}_n^{\mathcal{P}\mathcal{Q}}(\mathbf{x})$ can be interpreted as the contribution to the rate of change of the velocity field $\tilde{u}_n(\mathbf{x})$ at a point $\mathbf{x}$ made by the nonlinear interactions involving modes from the bands $\mathcal{P}$ and $\mathcal{Q}$. Note that these interactions influence all modes $\mathbf{k}$ which can form a triangle with two other modes such that one is in $\mathcal{P}$ and the other in $\mathcal{Q}$. $\tilde{N}_n^{\mathcal{K}\mathcal{P}\mathcal{Q}}(\mathbf{x})$ represents a contribution to the rate of change of $\tilde{u}_n(\mathbf{x})$ which is made by all modes from $\mathcal{K}$ interacting nonlinearly with modes in $\mathcal{P}$ and $\mathcal{Q}$.

The rate of change of the turbulent energy $e(\mathbf{x}) = \frac{1}{2}\tilde{u}_n(\mathbf{x})\tilde{u}_n(\mathbf{x})$ at a point $\mathbf{x}$ caused by the nonlinear interactions is

$$\frac{\partial e(\mathbf{x})}{\partial t} = \tilde{u}_n(\mathbf{x})\tilde{N}_n(\mathbf{x})\,. \tag{6}$$

Our goal is to decompose (6) into contributions from the interactions among modes from predefined wavenumber bands $\mathcal{K}$,$\mathcal{P}$, and $\mathcal{Q}$ i.e. to find a physical space counterpart of $T^{\mathcal{K}\mathcal{P}\mathcal{Q}}(\mathbf{k})$ which itself is the result of such a decomposition of the transfer $T(\mathbf{k})$ performed in the spectral space. Despite uniqueness of such a decomposition in the spectral representation, the procedure is ambiguous in the physical space. Possible definitions are:

$$\tilde{T}_1^{\mathcal{K}\mathcal{P}\mathcal{Q}}(\mathbf{x}) = \tilde{u}_n^{\mathcal{K}}(\mathbf{x})\tilde{N}_n^{\mathcal{P}\mathcal{Q}}(\mathbf{x})\,, \tag{7}$$

$$\tilde{T}_2^{\mathcal{K}\mathcal{P}\mathcal{Q}}(\mathbf{x}) = \tilde{u}_n^{\mathcal{K}}(\mathbf{x})\tilde{N}_n^{\mathcal{K}\mathcal{P}\mathcal{Q}}(\mathbf{x})\,, \tag{8}$$

$$\tilde{T}_3^{\mathcal{K}\mathcal{P}\mathcal{Q}}(\mathbf{x}) = \tilde{u}_n(\mathbf{x})\tilde{N}_n^{\mathcal{K}\mathcal{P}\mathcal{Q}}(\mathbf{x})\,, \tag{9}$$

where $\tilde{u}_n^{\mathcal{K}}(\mathbf{x})$ is the inverse Fourier transform of $u_n(\mathbf{k})$ truncated to the band $\mathcal{K}$.

Function $\tilde{T}_1^{\mathcal{K}\mathcal{P}\mathcal{Q}}(\mathbf{x})$ is a straightforward counterpart of $T^{\mathcal{K}\mathcal{P}\mathcal{Q}}(\mathbf{k})$, with a product of $\tilde{u}_n^{\mathcal{K}}$ and $\tilde{N}_n^{\mathcal{P}\mathcal{Q}}$ taken in the physical rather than in the spectral space. However, since $u_n{}^{\mathcal{K}}(\mathbf{k})$ vanishes outside $\mathcal{K}$, the multiplication in the spectral space implicitly truncates $N_n{}^{\mathcal{P}\mathcal{Q}}(\mathbf{k})$ to the same band so that $T^{\mathcal{K}\mathcal{P}\mathcal{Q}}(\mathbf{k})$ expresses transfer to the modes in $\mathcal{K}$ only. In $\tilde{T}_1^{\mathcal{K}\mathcal{P}\mathcal{Q}}(\mathbf{x})$ the effect of nonlinear transfer to modes outside $\mathcal{K}$ is present in the term $\tilde{N}_n^{\mathcal{P}\mathcal{Q}}$.

An explicit truncation of $N_n{}^{\mathcal{P}\mathcal{Q}}(\mathbf{k})$ to $\mathcal{K}$ and multiplication by $\tilde{u}_n^{\mathcal{K}}$ seems to rectify this problem resulting in (8). The drawback of this definition is that it does not satisfy a natural condition:

$$\sum_{\mathcal{K},\mathcal{P},\mathcal{Q}} \tilde{T}^{\mathcal{K}\mathcal{P}\mathcal{Q}}(\mathbf{x}) = \frac{\partial e(\mathbf{x})}{\partial t}\,, \tag{10}$$

which is satisfied by both (7) and (9).

Function $\hat{T}_3^{\mathcal{KPQ}}(\mathbf{x})$ may be interpreted as a fraction of the rate of change of the total energy $e(\mathbf{x})$ due to variation of modes in $\mathcal{K}$ as they are affected by nonlinear interactions with modes from $\mathcal{P}$ and $\mathcal{Q}$.

Thus none of the above definitions is an exact counterpart of the spectral transfer $T^{\mathcal{KPQ}}(\mathbf{k})$ but (9) is the most appealing candidate.

An interesting special case is obtained by dividing a wavenumber space into two disjoint regions $\mathcal{K}$ ($k \leq k_c$) and $\mathcal{P}$ ($k > k_c$). Quantity

$$T_{SGS}(\mathbf{x}|k_c) = \hat{T}^{\mathcal{KPP}}(\mathbf{x}) + \hat{T}^{\mathcal{KKP}}(\mathbf{x}) \qquad (11)$$

provides a physical space representation of the rate of change of energy of large scales ($k \leq k_c$) due to their nonlinear interactions through wavenumber triads which have at least one of the legs in the region $\mathcal{P}$. This is precisely the energy transfer process which is the subject of the subgrid-scale modeling.

We have computed transfer functions (7) and (11) for the statistically isotropic velocity field obtained in direct numerical simulations performed with a resolution of 128^3 modes (maximum wavenumber $k = 64$). The low wavenumber band $\mathcal{Q}$ remains always fixed and is chosen to cover the entire energy containing range ($0 < q < 10$). Figure 1 shows one plane from the full transfer (7) representing in the physical space the energy transfer to eddies in the band $23 < k < 28$ caused by their interactions with eddies in the bands $20 < p < 25$ and $0 < q < 10$. The transfer function is spatially intermittent and is predominantly positive, indicating a flow of energy from the larger scales p to the smaller scales k.

We have attempted to correlate this physical energy transfer with a number of simpler quantities (rate-of-strain, dissipation, energy, etc.) calculated from the velocity field truncated in such a way as to contain only either large or small scales. We found that the energy of the velocity field truncated to large scales $0 < k < 10$ correlates very well with the energy transfer among small scales shown in figure 1. Correlation of other calculated quantities with the energy transfer, notably the square of the rate-of-strain tensor, was generally much worse. Therefore we conclude that the energy transfer among small scales occurs mostly at those physical locations which contain large amounts of turbulent energy rather than at the locations of high strain rate, an unexpected result. Indeed, until this paradox is resolved, we can not be confident that the particular measure of energy transfer that we have used is the appropriate one.

We have used formula (11) to calculate subgrid-scale (SGS) energy transfer for the same field with the cutoff wavenumber $k_c = 10$. A plane from the full SGS transfer field is plotted in figure 2. The transfer is characterized by the presence of both negative and positive regions. These indicate energy flux from and to the large scales respectively due to their interactions with the smaller scales. Standard subgrid-scale eddy viscosity models predict transfer in one direction only, from large to small scales.

4 Conclusions

We have devised a physical space representation of the energy transfer processes among scales of motion belonging to three distinct wavenumber bands in the spectral space and conclude from it that the energy transfer among small scales is highly intermittent in the physical space and correlates well with regions of significant large-scale energy.

As a particular case we have calculated a subgrid-scale energy transfer in isotropic turbulence. The SGS transfer exhibits regions of energy drain from large to small scales as well as significant regions of reversed energy transfer from small to large scales. Classical eddy viscosity models assume that transfer is always from large to small scales, contrary to the results of direct calculations.

Acknowledgments- Work of one of the authors (JAD) was supported by the AFOSR Contract No. 90-0300 and by the NASA-Ames/Stanford Center for Turbulence Research.

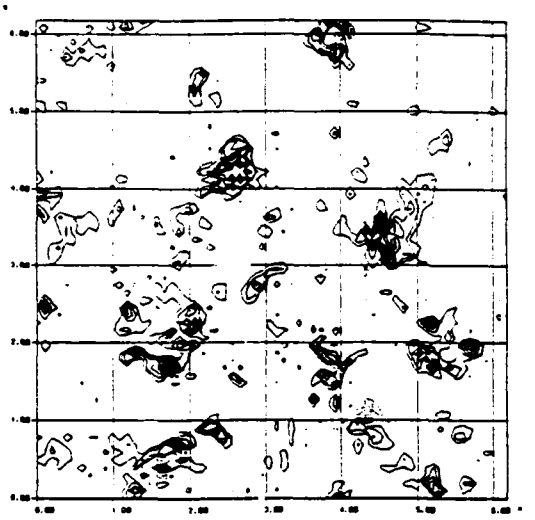

Fig.1. Energy transfer in physical space $\hat{T}^{\mathcal{KPQ}}$ for $23 < k < 28, 20 < p < 25, 0 < q < 10$.

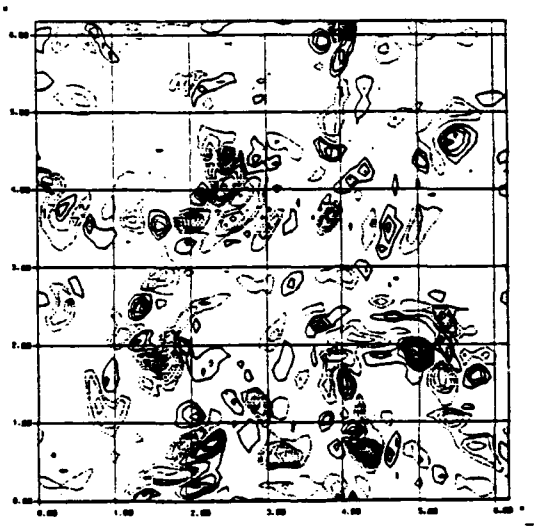

Fig.2. Subgrid scale energy transfer in physical space $T_{SGS}(\mathbf{x}|k_c)$ for $k_c = 10$.

References

[1] J.A. Domaradzki and R.S. Rogallo, in *Proceedings of Center for Turbulence Research, Summer Program 1988.*

[2] J.A. Domaradzki and R.S. Rogallo, *Phys. Fluids* A2, 413 (1990).

[3] P.K. Yeung and J.G. Brasseur, submitted to *Phys. Fluids* A.

[4] J.G. Brasseur and P.K. Yeung, *AIAA Paper No. 91-0230* (1991).

[5] J.A. Domaradzki, R.S. Rogallo and A.A. Wray, in *Proceedings of Center for Turbulence Research, Summer Program 1990.*

Nonlocal triad interactions and the dissipation range of isotropic turbulence

J. Andrzej Domaradzki
Department of Aerospace Engineering, University of Southern California, Los Angeles, California 90089-1191

(Received 29 January 1992; accepted 14 May 1992)

Detailed transfer functions $T(k|p,q)$, which express turbulent energy transfer rate to modes k caused by their nonlinear interactions with modes p and q, are analyzed using results of direct numerical simulations of homogeneous turbulence. A previously found phenomenological scaling for the functions $T(k|p,q)$, which brings them into a self-similar form, is used to deduce the form of the energy spectrum in the dissipation range proportional to $k^{-2}\exp(-ak)$ and the transfer spectrum proportional to $\exp(-ak)$. A physical mechanism of the energy transfer process consistent with the self-similarity scaling is proposed.

I. INTRODUCTION

Navier–Stokes equations for an incompressible, homogeneous turbulent flow have the following form in spectral (Fourier) representation (see, e.g., Lesieur,[1] pp. 92–94):

$$\frac{\partial}{\partial t}u_n(\mathbf{k}) = -\nu k^2 u_n(\mathbf{k}) + N_n(\mathbf{k}). \tag{1}$$

Here, $u_n(\mathbf{k})$ is the velocity field in spectral space, with the explicit dependence on time omitted, ν is the kinematic viscosity, and $N_n(\mathbf{k})$ is the nonlinear term

$$N_n(\mathbf{k}) = \left(\frac{-i}{2}\right) P_{nlm}(\mathbf{k}) \int d^3p\, u_l(\mathbf{p}) u_m(\mathbf{k}-\mathbf{p}), \tag{2}$$

where tensor $P_{nlm}(\mathbf{k})$ accounts for the pressure and incompressibility effects. The summation convention is assumed throughout.

The equation for the energy amplitudes $\frac{1}{2}|u(\mathbf{k})|^2 = \frac{1}{2}u_n(\mathbf{k})u_n^*(\mathbf{k})$, where the asterisk denotes a complex conjugate, is obtained from (1) and has the following form:

$$\frac{\partial}{\partial t}\frac{1}{2}|u(\mathbf{k})|^2 = -2\nu k^2 \frac{1}{2}|u(\mathbf{k})|^2 + T(\mathbf{k}). \tag{3}$$

In the last equation $T(\mathbf{k})$ is the nonlinear energy transfer

$$T(\mathbf{k}) = \mathrm{Re}[u_n^*(\mathbf{k})N_n(\mathbf{k})], \tag{4}$$

expressing the rate of change of energy of the mode $\mathbf{k}$ caused by its nonlinear interactions with all other modes in the system.

Detailed energy transfer to/from mode $\mathbf{k}$ caused by its interactions with wave numbers $\mathbf{p}$ in a prescribed region $\mathscr{P}$ of the wave-number space and $\mathbf{q}=\mathbf{k}-\mathbf{p}$ in another region $\mathscr{Q}$ is

$$T^{\mathscr{P}\mathscr{Q}}(\mathbf{k}) = \mathrm{Re}[u_n^*(\mathbf{k})N_n^{\mathscr{P}\mathscr{Q}}(\mathbf{k})], \tag{5}$$

where N_n^{PQ} is given by formula (2), calculated with one of the contributing velocity fields truncated to $\mathscr{P}$ and the other to $\mathscr{Q}$. Details of such calculations are provided by Domaradzki and Rogallo.[2,3] For homogeneous turbulence the regions $\mathscr{P}$ and $\mathscr{Q}$ are usually chosen as spherical wave-number bands centered at wave numbers p and q, respectively. Similarly, truncating velocity $u_n^*(\mathbf{k})$ in (5) to a spherical shell $\mathscr{K}$, centered at a wave number k, results in a quantity $T^{\mathscr{K}\mathscr{P}\mathscr{Q}}(\mathbf{k})$, which is nonzero only for those modes $\mathbf{k}$ that belong to the region $\mathscr{K}$. Summing this last quantity over all modes in $\mathscr{K}$ results in a function denoted as $T(k|p,q)$, which is interpreted as the energy transfer to the band $\mathscr{K}$ resulting from nonlinear interactions of scales in $\mathscr{K}$ with scales in $\mathscr{P}$ and $\mathscr{Q}$.

Total nonlinear energy transfer $T(k)$ to a wave-number band k (i.e., the region $\mathscr{K}$) is obtained by summing contributions $T(k|p,q)$ from all possible bands p and q:

$$T(k) = \sum_p \sum_q T(k|p,q) = \sum_p P(k|p). \tag{6}$$

Here, the function $P(k|p)$ is a result of summation of $T(k|p,q)$ over all q bands and is interpreted as the energy transfer between wave-number bands k and p. Also note that $T(k)$ can be obtained from (4) by summing $T(\mathbf{k})$ over all modes in the wave-number shell k.

Functions $T(k)$, $P(k|p)$, and $T(k|p,q)$ give progressively more detailed information about energy transfer among different scales of motion in the turbulent field.

For low Reynolds number homogeneous, isotropic, and shear turbulence, the same qualitative result for the function $T(k|p,q)$ was reported by Domaradzki and Rogallo[2,3] and Yeung and Brasseur[4] (isotropic turbulence), and by Domaradzki *et al.*[5] (shear turbulence): local energy transfer between two scales k and p outside the energy containing range caused by nonlocal interactions with the third scale q in the energy containing range. For high Reynolds number flows, similar behavior of the function $T(k|p,q)$ was observed by Ohkitani and Kida,[6] using results of direct numerical simulations of a high symmetry flow, and by Domaradzki *et al.*,[5] using velocity fields obtained in large eddy simulations of Chasnov.[7] Moreover, the function $T(k|p,q)$ computed by Domaradzki and Rogallo[3] and Ohkitani and Kida[6] in the framework of the analytical theories of turbulence exhibits the same features as observed in the simulations.

 0899-8213/92/092037-09$04.00

Even though there is little disagreement concerning properties of the function $T(k|p,q)$, there is a serious disagreement concerning physical interpretation and significance of the observed form of $T(k|p,q)$, in particular, for the energy transfer process in the inertial range of turbulence. Using an asymptotic analysis of triad interactions, Brasseur[8] argued that the dynamical couplings between large and small scales strengthen with increasing Reynolds number, and this effect casts doubt on the validity of the classical assumptions of local isotropy and, consequently, may require modifications in Kolmogorov's arguments, leading to the universal form of the inertial range spectrum. On the other hand, Waleffe[9] dismisses physical significance of such interactions entirely, asserting that "... the nonlocal interactions with local transfer character of triadic interactions is not property of turbulence physics, but rather a general feature of the Fourier representation." Others (Zhou and Rogallo[10]) are inclined to treat as physically interpretable quantities only certain integrals of $T(k|p,q)$, e.g., net energy flux across the spectrum, and not the function $T(k|p,q)$ itself.

To some extent, these controversies are caused by a fairly qualitative character of the above referenced analyses and our poor understanding of the relation between dual pictures of turbulence, one using a physical space and the other a spectral (Fourier) space representation. In this paper we draw several quantitative conclusions about the energy and the transfer spectra from the observed form of the function $T(k|p,q)$ and propose a particular mechanism of interactions between scales in the physical space, which is consistent with the observed behavior of the function $T(k|p,q)$ in the spectral space.

II. SELF-SIMILARITY SCALING FOR THE FUNCTION $T(k|p,q)$

In Ref. 5 three different velocity fields generated by numerical simulations were considered. The velocity field C128U8 was the result of a direct numerical simulation of uniformly sheared homogeneous turbulence performed by Rogers *et al.*[11] and LES128 was the result of a large-eddy simulation of forced isotropic turbulence, at a nominally infinite Reynolds number, performed by Chasnov.[7] The energy spectrum of LES128 exhibits the Kolmogorov $k^{-5/3}$ law over the entire range of simulated wave numbers. The field K128 was obtained from a direct numerical simulation of isotropic turbulence performed by Rogallo.[12]

For all three fields the functions $T(k|p,q)$ were computed. In Fig. 1(a) we show the functions $T(k|p,q)$ computed for the field C128U8 for p fixed outside the energy-containing range. The triad structure of the nonlinear energy transfer term is best understood by considering in this figure $P(k|p)$ as a function of k (for p fixed) and decomposing $P(k|p)$ into functions $T(k|p,q)$ for all possible wave-number bands q. Peaks of $P(k|p)$ are located in the vicinity of the prescribed p band, indicating that the energy transfer is most effective among comparable scales of motion. However, the decomposition into functions $T(k|p,q)$ reveals that the largest contributions to this local transfer come from the triad interactions with the third

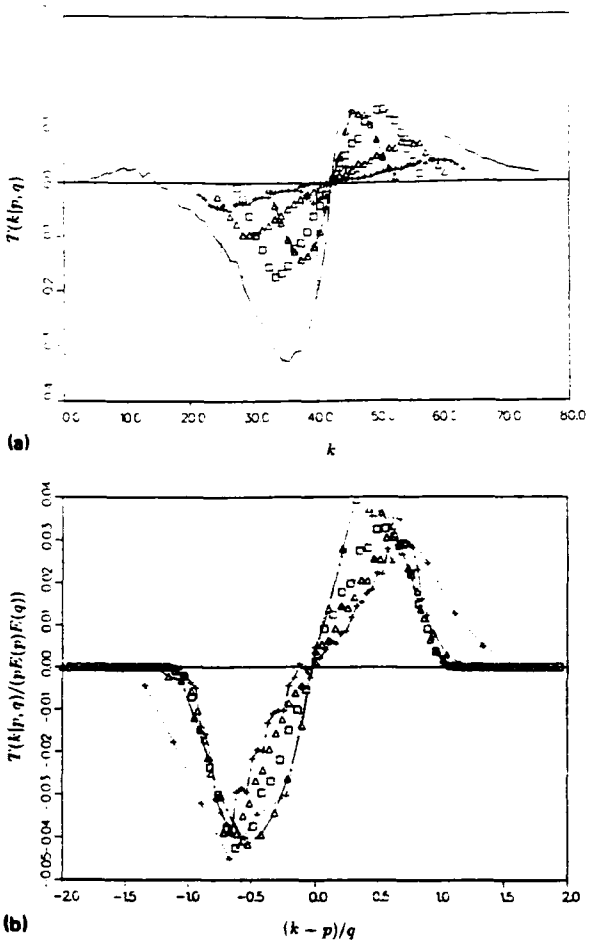

FIG. 1. Detailed energy transfer functions $T(k|p,q)$ for field C128U8: (a) unscaled, (b) scaled using Eq. (7). The transfer spectra $T(k|p,q)$ are shown for band $40<p<45$, and all bands q that make a significant contribution to $P(k|p)$ [the solid line in (a)]. The vertical dashed lines delineate the band p and different bands q for which transfer curves $T(k|p,q)$ are plotted: dashed line and plus symbols, $0<q<5$; double-dashed line and triangles, $5<q<10$; dotted line and squares, $10<q<15$; dotted line and triangles, $15<q<20$; double-dashed line and plus symbols, $20<q<25$. In (a) peaks of the transfer curves broaden for increasing q.

interacting scale in the energy-containing range (here, $5<q<20$). Thus we observe local energy transfer between two scales outside the energy-containing range caused by nonlocal interactions with the third scale in the energy-containing range.

In Ref. 5 it was found that for a given energy spectrum the following transformation collapsed reasonably well all curves $T(k|p,q)$ for all bands p outside the energy-containing range:

$$T_s\left(\frac{k-p}{q}\right)=\frac{T(k|p,q)}{pE(p)E(q)}. \tag{7}$$

The similarity variable $\xi=(k-p)/q$ is deduced from geometric relations for triads with legs k, p, and q. For a fixed p and q, with $p>q$, the range of wave numbers k that can form a triangle with those wave numbers is $p-q<k<p+q$. Therefore, for any such pair of fixed wave numbers p and q the variable ξ will always be in the range $-1<\xi$

< 1. The scaling factor $pE(p)E(q)$ is phenomenological. The result of scaling (7) applied to the functions $T(k|p,q)$ is plotted in Fig. 1(b). The quality of the scaling was comparable for all three fields considered and it was the only scaling, among those tried, that had any success in collapsing the numerical data. We must emphasize that the above relation applies to a particular combination of two fixed wave numbers, q being in the energy-containing range and $p > q$ outside this range. Therefore, even though the function $T(k|p,q)$ is symmetric in p and q the scaling is not, since this particular ordering of the wave numbers p and q is assumed in (7).

No explanation for the scaling (7) exists and at this stage it must be treated as a purely phenomenological result akin to experimental fitting procedures. Scatter in the data in Fig. 1(b) is caused partially by this approximate nature of the scaling and partially by the fact that in our numerical procedure we are dealing with wave-number bands of finite thickness ($\Delta k = 1, \Delta p = \Delta q = 5$) and not with sharply defined wave numbers k, p, and q. Despite these shortcomings of the scaling relation (7) in what follows we will assume that it holds for the functions $T(k|p,q)$ and we will explore its consequences and a possible physical interpretation.

It is important to note that according to (7) the transfer scales formally with the *energy* $E(q)$ of the large eddies rather than with their *rate of strain* $qE(q)^{1/2}$, which is the scaling postulated by a number of classical closure hypotheses.[13] At the present time the dependence of the energy transfer process among small scales on the *energy* of large scales observed in the simulations lacks a clear physical explanation. Direct coupling between large and small scales is postulated in the linear theories of the viscous-convection range of Batchelor[14] and Kraichnan[15] and the far dissipation range of Novikov[16] and Saffmann,[17] but these theories assume that the small scales are affected by the strain of the large scales, not their energy. For turbulence in the inertial range the classical theories predict that the energy transfer is dominated by the local interactions. For instance, theories of Obukhov and of Heisenberg (see Monin and Yaglom[13]) express a spectral energy flux through a wave number k as a product of two wave-number integrals involving the energy spectrum $E(k)$ with the largest contributions to both integrals coming from the wave numbers in the vicinity of k. Thus the nonlocal interactions discussed here are considered to be of little importance in those theories. Similar conclusions are also reached in the analytical theories of turbulence (see the monographs of Lesieur[1] and McComb[18]), which predict that the energy flux through a wave number k in the inertial range is dominated by scales from the spectral vicinity of k. However, these conclusions are not necessarily inconsistent with the nonlocal character of the detailed transfer function $T(k|p,q)$ found by Domaradzki and Rogallo[2,3] since the energy flux across the energy spectrum is obtained as a wave number integral of $T(k|p,q)$, and because of the cancellation effects, the integral may not reflect the nonlocal character of the integrand. One must therefore be cautious in drawing conclusions about the detailed transfer $T(k|p,q)$ from the analyses of integrated quantities.

Some of these theories may provide a partial explanation of features of the transfer process observed in the simulations, but none of them is fully satisfactory. As already noted, the classical theories based on the spectral energy flux assumptions do not account explicitly for the nonlocal interactions. On the other hand, the linear theories of the far dissipation range, which have nonlocal character, lead to the form of the energy spectrum proportional to $\exp(-ak^2)$, contrary to the form $\exp(-ak)$, which is observed in the dissipation range of low Reynolds number experiments (Ling and Huang[19] and Comte-Bellot and Corrsin[20]), simulations (Kerr[21] and Kida and Murakami[22]), and is also predicted theoretically by Foias *et al.*[23] and the analytical theories of turbulence (Kraichnan[24]). Among linear theories only Kraichnan's analysis[15] shows a possibility of the behavior $\exp(-ak)$ for the spectrum of the scalar field in the viscous–conductive range. However, this result is obtained under assumptions of unknown validity, and no parallel result for the far dissipation range behavior exists. The asymptotic analysis of Brasseur[8] results in a scaling of the energy transfer rate between two small scales by the square root of the energy of the remaining large scale rather than by its energy, as suggested by the phenomenological relation (7). Also, Waleffe's analysis[9] is unable to produce this scaling. The EDQNM theory reproduces properly the scaling (7) for power law spectra in the disparate-scale limit (Domaradzki and Rogallo[3]), in particular, the dependence of $T(k|p,q)$ on the energy $E(q)$ of the large scales. However, the physical interpretation of the observed transfer mechanism is not made easier by referring to the EDQNM theory, which is derived using assumptions about statistical properties of turbulent fields and formal structure of the Navier–Stokes equations rather than an intuitive picture of the physical processes occurring in turbulent flows.

III. PHYSICAL INTERPRETATION OF THE SELF-SIMILARITY SCALING

Dimensional analysis of the phenomenological relation (7) indicates that T_s has the dimension of time. Since the function T_s is the same for all pairs of wave numbers p and q it must scale with a time scale of turbulence that does not depend explicitly on p and q. It is thus natural to assume that it is a certain integral time scale of turbulence, e.g., large eddy turnover time,

$$\Theta \sim \left(\int_0^{k_c} k^2 E(k) dk \right)^{-1/2}, \tag{8}$$

where k_c denotes the wave number at the end of the energy-containing range. The quantity (8) has been computed for all three velocity fields considered in this paper and is compared in Table I with the values of the positive peaks of the function T_s for these fields. The peak values are within a factor 2 of the computed integral time scales. This is probably as good an agreement as could be expected, in view of the fact that the formula (8) provides only an order-of-magnitude estimate of the large eddy turnover time.

TABLE I. Large eddy turnover times Θ and the peak values of the self-similar function T, for three different, numerical velocity fields.

Field	Θ	$T_1^{\max}$
K128	0.11	0.230
C128U8	0.02	0.026
LES128	0.04	0.077

Consider now the energy transfer rate to all wave numbers $k>p$ interacting with the wave-number bands $(p,p+\Delta p)$ and $(q,q+\Delta q)$. This transfer rate is equal to an area under the positive peak of the function $T(k|p,q)$ and its estimate, using (7), is

$$\Pi(p,q)\sim\sum_{k>p}T(k|p,q)\Delta p\,\Delta q\sim qpE(p)E(q)\Delta p\,\Delta q\,\Theta. \tag{9}$$

The factor q in the last equality appears because the range of wave numbers $k>p$ affected by the wave-number bands p and q is $p<k<p+q$, as discussed after formula (7). Due to the localness of the energy transfer process, the quantity $\Pi(p,q)$ may also be interpreted as the energy transfer rate from the scales in the band $(p,p+\Delta p)$ caused by their interactions with scales from the bands $(q,q+\Delta q)$ and $(p,p+q)$.

The classical spectral energy transfer hypotheses usually invoke dimensional arguments, eddy viscosity concepts, or analogies with the turbulent energy production by the mean flow gradients in the turbulent kinetic energy balance equation. The last approach, used by Obukhov[25] and Ellison,[26] is the most appealing because it is based on the formally correct equation. The main difficulty in this approach is a proper interpretation of the equation in terms of spectral quantities.

The turbulent energy production term is

$$P=-\overline{u_iu_j}\frac{\partial U_i}{\partial x_j}, \tag{10}$$

where $\overline{u_iu_j}$ is the Reynolds stress tensor and U_i is the mean flow. We will attempt to express (9) in a form consistent with (10) so that the Reynolds stresses and the rates of strain of the large-scale flow can be identified.

The following notation is introduced: $L_q=1/q$—a length scale of large eddies from the q band; $l_p=1/p$—a length scale of small eddies from the p band; $U_q^2=E(q)\Delta q$—energy of the large scales; $u_p^2=E(p)\Delta p$—energy of the small scales. Using this notation (9) can be rearranged as follows:

$$\Pi(p,q)\sim[E(p)\Delta p]\{[q^2E(q)\Delta q]^{1/2}[p^2E(q)\Delta q]^{1/2}\Theta\}$$

$$=u_p^2\left(\frac{U_q}{L_q}\frac{U_q}{l_p}\Theta\right). \tag{11}$$

The formula (11) has the same form as (10) if the following identification is made:

$$-\overline{u_iu_j}\sim u_p^2, \tag{12}$$

$$\frac{\partial U}{\partial x_j}\sim\frac{U_q}{L_q}\frac{U_q}{l_p}\Theta. \tag{13}$$

The estimate (12) of the Reynolds stress is consistent with the classical arguments (see Monin and Yaglom,[13] pp. 212–225), which, on the basis of the dimensional considerations, postulate proportionality between the Reynolds stresses and energy. Departure from the classical arguments occurs in the estimate of $\partial U_i/\partial x_j$. The estimate (13) is a composite expression that involves a product of the classical estimate U_q/L_q, time scale of turbulence Θ, and the rate of strain U_q/l_q. Since $U_q/l_q>U_q/L_q$ and $\Theta>U_q/L_q$, this product is much larger than the classical estimate U_q/L_q, and it suggests the existence of flow regions with the rates of strain determined by the velocity scale of the large eddies and the length scale of the small eddies. Such large strains may be induced by a mutual interaction of a few large scales occurring over long enough time. For instance, in boundary layer flows counter-rotating streamwise vortices with a length scale comparable to the boundary-layer thickness δ are known to generate, in about one large eddy turnover time, internal shear layers with much smaller length scales $l\ll\delta$ and the velocity scale comparable to the mean free-stream velocity, i.e., the velocity scale of the largest eddies. Secondary instabilities of these shear layers are responsible for the transition to turbulence and the generation of small scales, as demonstrated experimentally by Swearingen and Blackwelder[27] and numerically by Liu and Domaradzki.[28] In free shear layer flows similar strong internal shears have also been observed. Thus the existence of intermittent regions with strains much larger than postulated by the classical theories of turbulence is plausible, even though it has not been systematically investigated for isotropic turbulence. It is interesting to note that in the context of a passive scalar in the viscous-conductive range Kraichnan[15] observes that large intermittent rates of strain, if they exist in a flow, will determine the dissipation spectrum of the scalar. The above analysis of the scaling (7) provides a plausible physical mechanism of the energy transfer process, where the role of the large scales is to produce intermittent regions of relatively strong, internal shears characterized by smaller length scales, which serve as regions of efficient small-scale energy transfer. If one notes that Θ represents the inverse of a collective rate of strain of all scales from the energy-containing range then (13) is a fraction of the total strain U_q/l_q, which is attributable to the action of the large scales from the wave-number band $(q,q+\Delta q)$. The development of such intermittent regions is the result of an evolution of a flow over about one large eddy turnover time, and it is unlikely that any analysis that does not explicitly account for time evolution will be able to predict scaling (7). Note also that in this interpretation dependence of the transfer on rates of strain in the physical space is recovered, despite its formal dependence on the large-scale energy in the spectral representation.

To confirm (or reject) the interpretation of the energy transfer process proposed above a detailed analysis of turbulent fields should be made.

IV. CONSEQUENCES OF THE SCALING RELATION FOR LOW REYNOLDS NUMBER FLOWS

Since the classical closure hypotheses usually concern the energy flux through a given wave number, say k,

$$W(k)=\int_k^\infty T(k')dk'=-\int_0^k T(k')dk', \tag{14}$$

i.e., the energy transfer rate to all wave numbers $k'>k$ from all wave numbers $k'<k$, it is important to investigate the consequences of the scaling (11) on the flux (14).

The flux (14) is obtained from (11) by considering transfer from all $p<k$ and $q<k$. Because of the locality of the energy transfer only wave numbers p in the vicinity of k, for instance between $1/2k$ and k, will contribute. Therefore,

$$W(k)\sim\int_{(1/2)k}^k dp\int_0^k dq\,\Pi(p,q)$$

$$\sim\Theta\left(\int_{(1/2)k}^k pE(p)dp\right)\left(\int_0^k qE(q)dq\right). \tag{15}$$

For k beyond the energy-containing range the integrals in (15) can be estimated as follows:

$$\int_{(1/2)k}^k pE(p)dp\sim k^2E(k), \tag{16}$$

$$\int_0^k qE(q)dq\sim\frac{U^2}{L}\sim\frac{U}{\Theta}, \tag{17}$$

where U and L are the integral velocity and length scale, respectively. Note that, in general, these quantities depend on the wave number k, for instance $U=U(k)$. Using these formulas the estimate of the energy flux becomes

$$W(k)\sim k^2E(k)U(k). \tag{18}$$

The same result is obtained more directly by assuming that in (11) U_q and L_q are replaced by the integral scales U and L, and the rate of strain of small scales u_p^2 is approximated by Ellison's hypothesis:[13]

$$u_p^2\sim pE(p). \tag{19}$$

Note, however, that the derivation of Eq. (18) relies only on the scaling relation (7) and not on its physical interpretation given in the previous section. Therefore, the results of this and the next section are independent of the particular physical interpretation proposed in this work.

In summary, the formula (18) corresponds to the following closure assumption for the spectral energy flux:

$$W(k)\sim-\overline{u_iu_j}\frac{\partial U_i}{\partial x_j}\sim[kE(k)][kU(k)], \tag{20}$$

where the Reynolds stress of the small scales is represented by (19) and the rate of strain acting on these scales is given as a ratio of the integral velocity scale U and the length scale of the small eddies $1/k$. Note that in both Obukhov and Ellison theories this rate of strain is estimated by the following expression:

$$\frac{\partial U_i}{\partial x_j}\sim\left(\int_0^k k'^2E(k')dk'\right)^{1/2}\sim\frac{U}{L}. \tag{21}$$

The closure hypothesis (20) may be used to predict the form of the energy spectrum for the wave numbers beyond the energy-containing range, where it applies. The spectral energy equation is

$$\frac{\partial}{\partial t}\int_0^k E(k',t)dk'=-W(k,t)-2\nu\int_0^k k'^2E(k')dk'. \tag{22}$$

In turbulence at low Reynolds numbers the energy spectrum falls off rapidly for increasing wave numbers k and for the wave numbers beyond the energy-containing range,

$$\int_0^k E(k',t)dk'\simeq\int_0^\infty E(k',t)dk'=\frac{3}{2}u^2(t), \tag{23}$$

where u is the root mean square of turbulent velocity.

Using the velocity scale $U(k)=u$, Eq. (22) may be rewritten as

$$\epsilon=\beta k^2E(k)u+2\nu\int_0^k k'^2E(k')dk', \tag{24}$$

where ϵ is the energy dissipation rate, β is a constant, and the explicit time dependence is omitted. Differentiating (24) with respect to k we obtain the equation

$$\beta u\frac{d}{dk}[k^2E(k)]+2\nu k^2E(k)=0, \tag{25}$$

which has the following solution:

$$E(k)\sim\frac{1}{k^2}\exp(-ak), \tag{26}$$

where $a=(2\nu)/(\beta u)$. Equation (25) expresses an approximate balance between viscous dissipation and nonlinear transfer

$$T(k)=-\frac{\partial W}{\partial k}\sim\exp(-ak) \tag{27}$$

in the far dissipation range. Equations (26) and (27) are important conclusions derived from the scaling relation (7), which can be compared with experimental and numerical results for low Reynolds number turbulence.

In Fig. 2(a) we plot the energy spectrum for isotropic field K128 and in Fig. 2(b) the spectral energy balance for this field. At this low Reynolds number, $R_\lambda\simeq25$, all spectra are well resolved, with both the dissipation spectrum and the transfer spectrum vanishing for large wave numbers k and in the approximate balance outside the energy-containing range $0<k<10$, where the above derived expressions should be valid. Using the log–linear scales we plot in Fig. 3 the dissipation spectrum, i.e., the energy spectrum multiplied by k^2, and the transfer spectrum for this field with wave numbers k rescaled using the Kolmogorov length $\eta=0.0344$. It is seen that the functional forms Eqs. (26) and (27) are in an excellent agreement with the numerical results for the wave numbers $k>10$ ($\eta k>0.3$),

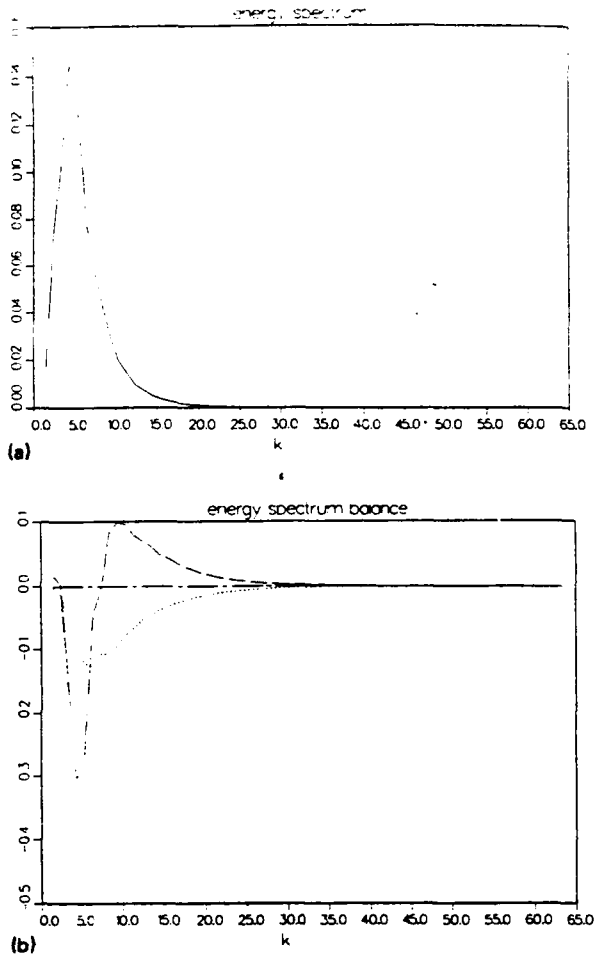

FIG. 2. (a) Energy spectrum for isotropic field K128 plotted using linear scales to accentuate the energy-containing range $0<k<10$. (b) Spectral energy balance for the field K128. Dashed line, dissipation spectrum $-2\nu k^2E(k)$; dash-dotted line, nonlinear energy transfer $T(k)$; dotted line, sum of dissipation and transfer, $T(k)-2\nu k^2E(k)=\partial E/\partial t$.

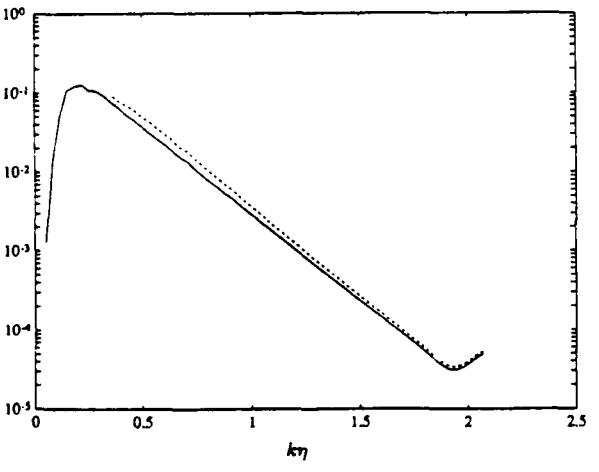

FIG. 3. Dissipation $2\nu k^2E(k)$ (solid line) and transfer spectrum $T(k)$ beyond the energy-containing range (broken line) for the field K128 plotted using log–linear scales and wave number k normalized by the Kolmogorov length scale η.

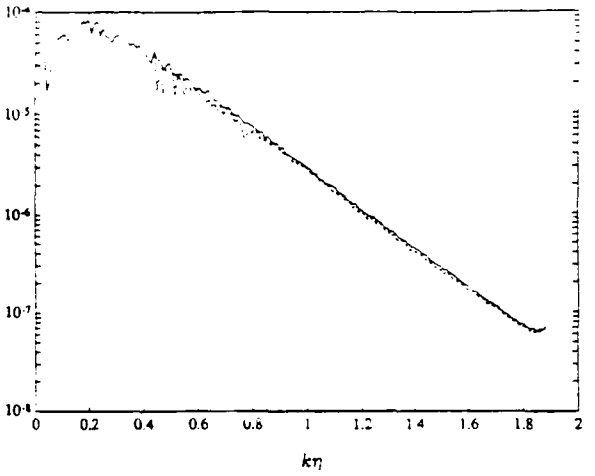

FIG. 4. Dissipation spectrum $2\nu k^2E(k)$ and transfer spectrum $T(k)$ beyond the energy-containing range for the turbulent Taylor–Green vortex field plotted using log–linear scales and wave number k normalized by the Kolmogorov length scale η.

i.e., for all wave numbers beyond the energy-containing range. The slope of the curves in Fig. 3 is $a/\eta\approx 2.19$.

In Fig. 4 we plot in the same manner the energy and transfer spectra for a flow at higher Reynolds number, $R_\lambda\approx 70$, obtained in numerical simulations of a decaying Taylor–Green vortex performed with an effective resolution 512^3 modes (Brachet[29]). For the wave numbers beyond the energy containing range Eqs. (26) and (27) provide a very good fit with the nondimensional constant $a/\eta\approx 2.08$.

Finally, in Fig. 5 the experimental results of Comte-Bellot and Corrsin[20] for the dissipation spectrum of grid turbulence at $R_\lambda=60.7$ and corresponding numerical results of Ruetsch and Maxey[30] for forced turbulence at $R_\lambda\approx 60$ are shown, again exhibiting good agreement (experimental and numerical data form a straight line on the

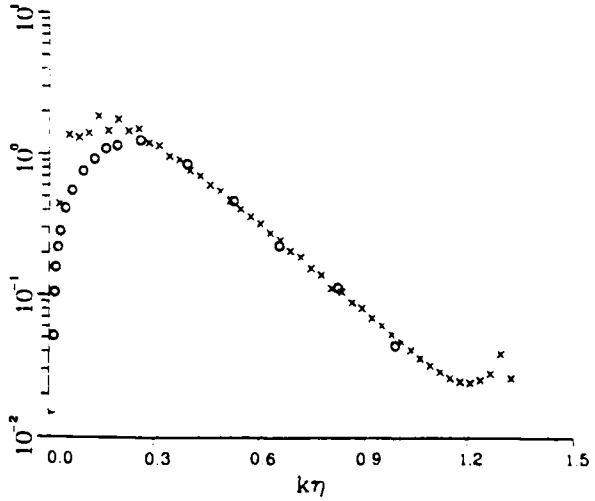

FIG. 5. The normalized dissipation spectrum $2\nu k^2E(k)$ in experiments of Comte-Bellot and Corrsin[19] (○) and numerical simulations of forced isotropic turbulence of Ruetsch and Maxey[29] (×).

log–linear plot with formula (26) beyond the energy-containing range. The nondimensional constant $a/\eta \simeq 2.12$ in this plot.

In view of the qualitative (scaling) character of the assumptions leading to the closure (18) the agreement between predictions (26) and (27) and the observed form of the energy and transfer spectra is surprisingly good. In a similar range of Reynolds numbers Kerr[21] fitted numerical energy spectra by a formula $E(k) \sim k^{-5/3} \exp(-ak)$, with the nondimensional constant $a/\eta \simeq 5.1$, and Kida and Murakami[22] obtained the best fit to the energy spectrum in the dissipation range as $k^{-1.6} \exp(-ak)$ with $a/\eta \simeq 4.9$. Sreenivasan[31] used as the best fit to the experimental energy spectra the formula $\exp(-ak)$ with $a/\eta = 12.7$ for $0.1 \leqslant k\eta \leqslant 0.5$ and $a/\eta = 8.8$ for $0.5 \leqslant k\eta \leqslant 1.5$. These results and Eq. (26) all predict the existence of the exponential factor in the formula for the dissipation range of low Reynolds number turbulence, but they differ in the form of the algebraic prefactor. At the present time the quality of the available data is probably not sufficient to distinguish between different prefactors. In any case, the exact value of the exponent m in the prefactor proportional to $(k\eta)^{-m}$ with positive m will influence the behavior of the energy spectrum only for $k\eta = O(1)$. Note, however, that the value of the exponent a/η will depend on the exact form of the prefactor, decreasing for increasing m, since for a given energy spectrum the exponential function must compensate for different fall-off rates associated with different prefactors.

At this point it is appropriate to briefly compare our approach to compute the energy flux with the recent results of Waleffe.[9] His analysis, performed for the inertial range spectrum, leads to the conclusion that two distinct classes of triad interactions operate in turbulent flows. Triads in class R (for reverse transfer) are characterized by the middle leg in the triad transferring large amounts of energy to the longest leg (small scale) and small amounts to the shortest leg (large scale). In triads belonging to the class F (for forward transfer) the shortest wave number is losing energy to the middle and the smallest wave numbers. The triads considered as dominant in the present work, which are nonlocal but result in the local energy transfer, belong to class R in Waleffe's nomenclature. An important result from his analysis is that the energy flux (14) is determined primarily by class F interactions and the weaker effect of class R interactions is the inverse energy flux, from small to large scales.

In view of this result our approach to compute the energy flux using Eq. (15), which takes into account only the class R triads, should be incorrect. To resolve this apparent contradiction between the present approach and Waleffe's[9] theory we have calculated for the isotropic field K128 the energy flux using Eq. (14) and the approximation analogous to (15), where the numerically computed $T(k'|p,q)$ is integrated over $0 < q < \frac{1}{2}k$, $\frac{1}{2}k < p < k$, and $k' > k$. The inequalities for p and q also imply that the length of the third leg of the triad does not exceed $\frac{3}{2}k$. Both results are compared in Fig. 6 for wave numbers $k > 20$ ($\eta k = 0.688$), i.e., outside the energy-containing range.

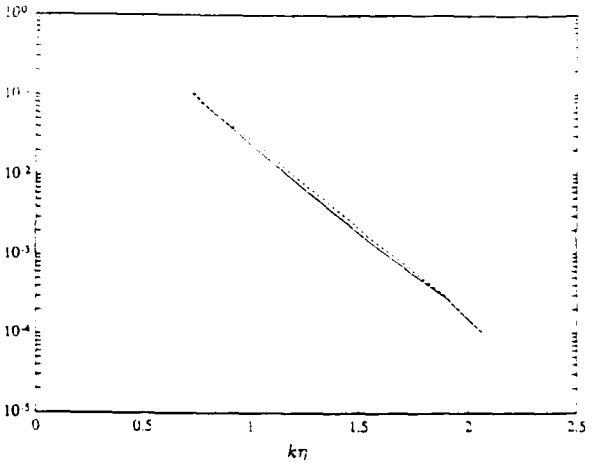

FIG. 6. Total energy flux $W(k)$ (solid line) and contribution to the flux from triads with wave numbers $0 < q < \frac{1}{2}k$, $\frac{1}{2}k < p < k$, and $k < k' < \frac{3}{2}k$ (broken line). The axes are scaled as in Fig. 3 to facilitate comparison of slopes in both figures.

Clearly, the approximation is in an excellent agreement with the exact energy flux, and we thus conclude that it is fully supported by the numerical data in the dissipation range. Moreover, formula (18) and the predicted form of the energy spectrum (26) imply that the energy flux should be proportional to $\exp(-ak)$. The numerical results plotted in Fig. 6 are in agreement with this conclusion.

It may also be noted that as seen in Fig. 6 these R-type interactions generally overestimate the total energy flux (but by no more than 10%). We may thus expect that the remaining triads, mostly of the F type, will result in the inverse energy transfer to counter the excess of the energy transferred to small scales by the R interactions. Therefore, the numerical results point to the energy transfer mechanism in the dissipation range, large forward transfer by the class R triads, and small inverse transfer by the F class interactions, which is in the diametrical opposition to the mechanism proposed by Waleffe[9] for the inertial range dynamics. Among other numerical works, which also do not agree with Waleffe's[9] theory are the results of Ohkitani and Kida.[6] Those authors found that in their simulations of a flow at $R_\lambda \simeq 180$, three types of interactions dominated. Among them, the class R triads constituted about 30% of all active triads, the class F about 15%, and more than 50% triads were characterized by both the largest and the middle scale losing energy to the smallest one, thus not adhering to Wallefe's classification. In view of the above disagreements it seems evident that the turbulence dynamics at these lower Reynolds numbers may be substantially different from the dynamics of turbulence in the inertial range.

V. CONSEQUENCES OF THE SCALING RELATION FOR HIGH REYNOLDS NUMBER FLOWS

Closure (20) is based on the phenomenological relation (7), which was obtained from the results of the direct numerical simulations of low Reynolds number turbulence.

However, relation (7) was also found to hold for the velocity field obtained in a large eddy simulation of turbulence at nominally infinite Reynolds number (LES128). It may therefore be useful to formally explore the consequences of this closure for high Reynolds number flows.

In the far dissipation range of high Reynolds number turbulence Eq. (22) still holds, but it is unlikely that the velocity scale will be given by the formula (23), which emphasizes scales from the energy-containing and inertial ranges. In this case we follow Batchelor,[14] Novikov,[16] and Saffmann,[17] who assumed that the far dissipation range eddies interact most strongly with the Kolmogorov eddies characterized by the velocity scale $v_k=(\nu\epsilon)^{1/4}$. With this velocity scale the formula (26) becomes

$$E(k)\sim\frac{1}{k^2}\exp\left(-\frac{2}{\beta}(\eta k)\right), \tag{28}$$

where η is the Kolmogorov length scale:

The exponential factor in (28) is in agreement with some other theories of the far dissipation range. For instance, Kraichnan predicts $E(k)\sim k^3\exp(-ak)$ in the framework of the direct interaction approximation theory and Foias *et al.*[23] obtain an exact sharp estimate $E(k)=o[\exp(-c\eta k)]$ using spectral properties of the Stokes operator. That work also suggests the prefactor k^{-4}, but this result is not considered mathematically exact by the authors. The faster falloff, proportional to $\exp(-bk^2)$, is suggested by a number of older theories (see Monin and Yaglom[13]) and the more recent work of Smith and Reynolds.[32] However, Manley[33] showed that the procedure employed by Smith and Reynolds,[32] after a reasonable modification, provides results in agreement with the $\exp(-ak)$ behavior. It seems that, at the present time, the experimental and numerical results favor the $\exp(-ak)$ behavior with a simple, algebraic prefactor, whose exact form remains to be determined.

In the inertial range the energy spectrum decays too slowly to use the approximation (23). We take instead

$$U=U(k,t)\sim\left(\int_0^k E(k',t)dk'\right)^{1/2}. \tag{29}$$

To avoid divergence of the integral at small k the inertial form of the energy spectrum cannot be continued to $k=0$ and the specific form of the energy spectrum, which vanishes at the low wave numbers, must be used.

Because of the limitation to the inertial range wave numbers the viscous term in Eq. (22) may be neglected, and using (29) one obtains the following equation:

$$\epsilon=\beta k^2E(k)\left(\int_0^k E(k',t)dk'\right)^{1/2}. \tag{30}$$

Introducing a variable $\theta(k)=\int_0^k E(k',t)dk'$, Eq. (30) is reduced to

$$\epsilon=\beta k^2\theta^{1/2}\frac{d\theta}{dk}. \tag{31}$$

The solution to (31) is

$$\theta(k)=\frac{3}{2}u^2\left[1-\left(\frac{2}{3}\right)^{1/2}\frac{\epsilon}{\beta u^3}\frac{1}{k}\right]^{2/3} \tag{32}$$

where $u=[\frac{2}{3}\int_0^\infty E(k',t)dk']^{1/2}$ is the mean turbulent velocity. For decaying turbulence $\epsilon\sim u^3/L$, where L is the integral length scale of turbulence. Then, if the constant β is of the order unity and $k\gg 1/L$ (inertial range), we may expand the expression (32) in Taylor series and keep only the lowest-order term in $1/k$. Differentiating this result with respect to k we obtain the energy spectrum for the wave numbers $1/L\ll k\ll 1/\eta$:

$$E(k)=\left(\frac{2}{3\beta^2}\right)^{1/3}\epsilon^{2/3}k^{-5/3}, \tag{33}$$

i.e., the classical Kolmogorov inertial range form. Assuming the value of the Kolmogorov constant $C_K\approx 1.5$–2.0, we obtain for the constant β a range of values 0.44–0.29.

The coefficient $a/\eta=2/\beta$ in the exponential law (28) for this range of values of the Kolmogorov constant is between 4.5 and 6.9. This value does not agree with the low Reynolds number result $a/\eta\approx 2$. The disagreement may reflect differences between low and high Reynolds number flows or, what is more plausible, an inadequacy of the assumption that the far dissipation range eddies interact most strongly with the eddies characterized by the velocity scale $u=v_k=(\nu\epsilon)^{1/4}$. Indeed,

$$\frac{a}{\eta}=\frac{2\nu}{\beta u}\frac{1}{\eta}=\frac{2}{\beta}\frac{v_k}{u}, \tag{34}$$

and if the velocity scale u is replaced by the physically more relevant velocity scale associated with the peak of the dissipation spectrum, $v_d>v_k$, the constant a/η will decrease. However, it does not seem that the value of the constant a/η for the far dissipation range can be uniquely determined in the framework of the above scaling arguments.

VI. CONCLUSIONS

Employing the phenomenological scaling relation for the detailed energy transfer functions $T(k|p,q)$ the physical interpretation of the observed local energy transfer caused by nonlocal triads is proposed. In this interpretation the large scales of turbulence, through their mutual interactions, create intermittent regions of relatively large rates of strain, where most of the small-scale energy transfer occurs. An important feature of this interpretation, suggested by the presence of the large eddy turnover time in the scaling relation, is an introduction of the time scale into the problem. This implies that any successful explanation of the observed energy transfer process must invoke the time evolution of turbulence. It may be an important observation in view of attempts to explain the transfer process by analyzing Navier–Stokes equations considered at a given instant of time. In such analyses valid assumptions about amplitudes of Fourier modes are made and conclusions about the dependence of energy transfer on the amplitudes are drawn. The transfer process, however, is determined by both the amplitudes and the phases of the

Fourier modes and the phase relationships are not known *a priori* and must be found by considering the time evolution of the system. This fact may explain why the scaling relation (7) is broadly consistent with the analytical theories of turbulence, which take into account the time evolution of turbulence, and why other approaches failed to predict this scaling. In this respect it must be stressed that the scaling relation (7) may be treated as being equivalent to an experimental result, and thus any theoretical explanation of the energy transfer process should be required to predict it.

Independently of its physical interpretation the scaling relation (7) was used to deduce the functional forms of the energy and transfer spectra in the far dissipation range of low Reynolds number turbulence. Considering an approximate character of the analysis, the predicted forms are in surprisingly good agreement with several numerical and experimental results for the range of nondimensional wave numbers $k\eta < 2$.

Assuming the validity of the scaling relation for high Reynolds number flows, the $k^{-5/3}$ behavior of the energy spectrum is predicted in the inertial range and the $k^{-2}\exp(-ak)$ form in the far dissipation range. These results are on a less firm ground than the results obtained for low Reynolds number flows. The reason is that the applicability of the scaling relation is confirmed only for large eddy simulation results of high Reynolds number turbulence, which are influenced by the additional assumptions made in this numerical methodology. Therefore, the more appropriate conclusion would be that the scaling relation (7) does not contradict the inertial range and the far dissipation range behavior of high Reynolds number turbulence.

ACKNOWLEDGMENTS

The numerical fields used in this work were made available to the author through the NASA Ames/Stanford University Center for Turbulence Research. The assistance of Dr. R. S. Rogallo and Dr. A. A. Wray in generating, accessing, and analyzing the velocity fields is greatfully acknowledged. The author also thanks Dr. M. Brachet for making available his numerical code used to generate results for Fig. 4 and Dr. G. R. Ruetsch for providing Fig. 5.

This research was supported by the AFOSR Contract No. 90-0300.

[1] M. Lesieur, *Turbulence in Fluids*, 2nd ed. (Martinus Nijhoff, Dordrecht, 1990).

[2] J. A. Domaradzki and R. S. Rogallo, "Energy transfer in isotropic turbulence at low Reynolds numbers," in *Proceedings of the 1988 Summer Program* (Center for Turbulence Research, NASA Ames/Stanford University, Stanford, CA, 1988), CTR-S88, p. 169.

[3] J. A. Domaradzki and R. S. Rogallo, "Local energy transfer and nonlocal interactions in homogeneous, isotropic turbulence," Phys. Fluids A **2**, 413 (1990).

[4] P. K. Yeung and J. G. Brasseur, "The response of isotropic turbulence to isotropic and anisotropic forcing at the large scales," Phys. Fluids A **3**, 413 (1991).

[5] J. A. Domaradzki, R. S. Rogallo, and A. A. Wray, "Interscale energy transfer in numerically simulated homogeneous turbulence," in *Proceedings of the 1990 Summer Program* (Center for Turbulence Research, NASA Ames/Stanford University, Stanford, CA, 1990), p. 319.

[6] K. Ohkitani and S. Kida, "Triad interactions in a forced turbulence," Phys. Fluids A **4**, 794 (1992).

[7] J. R. Chasnov, "Development and application of an improved subgrid model for homogeneous turbulence," Ph.D. thesis, Columbia University, 1990.

[8] J. G. Brasseur, "Comments on the Kolmogorov hypothesis of isotropy in the small scales," AIAA Paper No. AIAA-91-0230, 1991.

[9] F. Waleffe, "The nature of triad interactions in homogeneous turbulence," Phys. Fluids A **4**, 350 (1992).

[10] Y. Zhou and R. S. Rogallo, "Scale analysis of DNS energy transfer interactions," Bull. Am. Phys. Soc. **36**, 2627 (1991).

[11] M. M. Rogers, P. Moin, and W. C. Reynolds, "The structure and modeling of the hydrodynamic and passive scalar fields in homogenous turbulent shear flow," Report TF-25, Department of Mechanical Engineering, Stanford University, 1986.

[12] R. S. Rogallo (unpublished).

[13] A. S. Monin and A. M. Yaglom, *Statistical Fluid Mechanics* (MIT Press, Cambridge, MA, 1979).

[14] G. K. Batchelor, "Small-scale variation of convected quantities like temperature in turbulent fluid. Part 1," J. Fluid Mech. **5**, 113 (1958).

[15] R. H. Kraichnan, "Small-scale structure of a scalar field convected by turbulence," Phys. Fluids **11**, 945 (1968).

[16] E. A. Novikov, "Energy spectrum of turbulent flow of an incompressible fluid," Dokl. Akad. Nauk SSSR **139**, 331 (1961).

[17] P. G. Saffman, "On the fine-scale structure of vector fields convected by a turbulent fluid," J. Fluid Mech. **16**, 545 (1963).

[18] W. D. McComb, *The Physics of Fluid Turbulence* (Clarendon, Oxford, 1990).

[19] S. C. Ling and T. T. Huang, "Decay of weak turbulence," Phys. Fluids **13**, 2912 (1970).

[20] G. Comte-Bellot and S. Corrsin, "Simple Eulerian time correlation of full- and narrow-band velocity signals in grid-generated, 'isotropic' turbulence," J. Fluid Mech. **48**, 273 (1971).

[21] R. M. Kerr, "Velocity, scalar and transfer spectra in numerical turbulence," J. Fluid Mech. **211**, 309 (1990).

[22] S. Kida and Y. Murakami, "Kolmogorov similarity in freely decaying turbulence," Phys. Fluids **30**, 2030 (1987).

[23] C. Foias, O. Manley, and L. Sirovich, "Empirical and Stokes eigenfunctions and the far-dissipative turbulent spectrum," Phys. Fluids A **2**, 464 (1990).

[24] R. H. Kraichnan, "The structure of isotropic turbulence at very high Reynolds numbers," J. Fluid Mech. **5**, 497 (1959).

[25] A. M. Obukhov, "Spectral energy distribution in a turbulent flow," Dokl. Akad. Nauk SSSR **32**, 22 (1941).

[26] T. H. Ellison, "The universal small-scale spectrum of turbulence at high Reynolds numbers," in *Mecanique de la Turbulence*, Coll. Internationale du CNRS a Marseille, Paris, CNRS, 1962.

[27] J. D. Swearingen and R. F. Blackwelder, "The growth and breakdown of streamwise vortices in the presence of a wall," J. Fluid Mech. **182**, 255 (1987).

[28] W. Liu and J. A. Domaradzki, "Direct numerical simulation of transition to turbulence in Goertler flow," submitted to J. Fluid Mech.

[29] M. E. Brachet, "The geometry of small-scale structures of the Taylor–Green vortex," C. R. Acad. Sci. Paris **311**, 775 (1990).

[30] G. R. Ruetsch and M. R. Maxey, "Small-scale features of vorticity and passive scalar fields in homogeneous isotropic turbulence," Phys. Fluids A **3**, 1587 (1991).

[31] K. R. Sreenivasan, "On the fine-scale intermittency of turbulence," J. Fluid Mech. **151**, 81 (1985).

[32] L. M. Smith and W. C. Reynolds, "The dissipation range spectrum and the velocity-derivative skewness in turbulent flows," Phys. Fluids A **3**, 992 (1991).

[33] O. P. Manley, "The dissipation range spectrum," Phys. Fluids A **4**, 1320 (1992).

An analysis of subgrid-scale interactions in numerically simulated isotropic turbulence

by J. Andrzej Domaradzki, Wei Liu

Department of Aerospace Engineering, University of Southern California,

Los Angeles, CA 90089-1191, U.S.A.,

tel. 213-740-5357, FAX 213-740-7774

and

Marc E. Brachet

Laboratoire de Physique Statistique, École Normale Supérieure

75231 Paris CEDEX 05, France

August 13, 1992

Submitted to *The Physics of Fluids*

PACS 47.25.Cg

Abstract

Using a velocity field obtained in a direct numerical simulation of isotropic turbulence at a moderate Reynolds number we analyze the subgrid-scale energy transfer in the spectral and the physical space representation. The subgrid-scale transfer is found to be composed of a forward and an inverse transfer components, both being significant in dynamics of resolved scales. Energy exchanges between the resolved and unresolved scales from the vicinity of the cutoff wave number dominate the subgrid-scale processes and the energetics of the resolved scales are unaffected by the modes with wave numbers greater than twice the cutoff wave number. The dominance of nonlinear interactions among the largest scales in the subgrid-scale energy transfer process suggests that the resolved nonlinear term may serve as a basis of a new approach to the subgrid-scale modeling.

1 Introduction

Three approaches used in numerical predictions of turbulent flows are direct numerical simulations (DNS), large eddy simulations (LES), and Reynolds averaged Navier-Stokes (RANS) simulations. With currently available computer capabilities the applicability of the DNS methods is limited to low Reynolds number turbulence. In practical applications for high Reynolds number flows the RANS techniques are used most frequently. The main drawback of this method is the need for introduction of a number of phenomenological closure assumptions and empirical, flow dependent constants.

The LES techniques, reviewed by Rogallo and Moin [1] and more recently by Lesieur [2], are a compromise approach between DNS and RANS. In the LES large, resolved scales of a turbulent flow are simulated directly, akin to the DNS approach, and their interactions with the small, unresolved scales are modeled like in the RANS approach. However, contrary to the RANS, only a part of the nonlinear interactions is modeled in the LES, and since the modeled interactions involve small scales (usually in the inertial range of turbulence) which have more universal character than flow dependent large scales, the hope is that such modeling can be accomplished with less empiricism and with greater help from the theories of homogeneous turbulence than it is the case for the RANS approach. At the present time the most widely used subgrid-scale models are the Smagorinsky model [3] for the LES performed in the physical space representation and the Kraichnan [4] and the Cholet and Lesieur models [5] if the spectral representation is used. These, as well as other subgrid-scale models, despite exhibiting a number of desirable properties like accounting properly for the

global energy flux from the large to the small scales, are known to be deficient in some respects. For instance, the models are usually purely dissipative. However, the process of the subgrid-scale energy transfer is dissipative only in the mean and locally in the spectral or the physical space the effect of the subgrid-scale interactions may be to either decrease or increase the energy of the large, resolved scales. Various attempts were proposed in the past to account for the inverse energy transfer in the subgrid-scale modeling for homogeneous turbulence [6,7,8] and for inhomogeneous flows [9] but no generally accepted method exists.

The practical importance of the LES techniques and the deficiencies of the existing subgrid-scale models suggest that better understanding of subgrid-scale interactions is needed if improvements in the LES methods are to be made. To compute the effects of the subgrid-scale nonlinear interactions a full velocity field in three-space dimensions must be known; such detailed information cannot be obtained using current experimental techniques. Required information, however, is available in the direct numerical simulations of turbulent flows and has been used in the past to investigate the subgrid-scale interactions and to assess directly the validity of the models. Such an approach was pioneered by Clark *et al.* [10] for the physical space modeling and by Domaradzki *et al.* [11] for the spectral space modeling. A major limitation of this approach is that only low Reynolds number flows can be simulated numerically and thus it is unclear to what extent conclusions from such analyses are applicable to more important case of high Reynolds number turbulence.

In this work we investigate the properties of the subgrid-scale nonlinear interactions using both the physical and the spectral space representation for numerically simulated, decaying homogeneous turbulence. The simulated flow is the Taylor-Green vortex and using

its symmetries [12] it is possible to increase Reynolds number by a factor 2 as compared with the general nonsymmetric flows simulated with the same number of computational modes. It is hoped that the higher Reynolds number and the existence of a short inertial subrange for this flow can make results of such an investigation applicable to high Reynolds number turbulence.

2 Numerical simulations

The Taylor-Green vortex flow [13] develops from the following initial condition:

$$\begin{aligned} u &= \sin(x)\cos(y)\cos(z) \\ v &= -\cos(x)\sin(y)\cos(z) \\ w &= 0 \end{aligned} \tag{1}$$

At time $t = 0$ the flow is two-dimensional but becomes three-dimensional for all times $t > 0$ when it develops into initially well organized, laminar structures in the form of vortex sheets which subsequently become unstable resulting eventually in a fully turbulent flow. It was noted by Orszag [12] that the initial condition (1) has a number of symmetries which are consistent with symmetries of the Navier-Stokes equations and are thus preserved in time as flow evolves. In the context of spectral simulations the symmetries of the flow may then be used to reduce number of computational modes needed to describe the flow for a prescribed range of resolved scales. This idea was implemented by Brachet et al. [14] who were able to simulate the Taylor-Green vortex flow with an effective spatial resolution of

256^3 modes at a computer cost equivalent to simulating a general, non-symmetric flow with the resolution of 64^3 modes. More recently Brachet [15] reported results of simulations of the Taylor-Green flow performed with an effective resolution of up to 864^3 modes and Reynolds number $R_\lambda \approx 140$. A similar approach to increase range of scales and Reynolds numbers in numerical simulations of turbulence by employing symmetries of Navier-Stokes equations was pursued by Kida and his collaborators in a number of papers[16,17,18], employing a flow with even greater number of symmetries than the Taylor-Green vortex. At the present time these highly symmetric flows are the most computationally efficient means of numerically simulating isotropic turbulence with Reynolds number R_λ on the order 100.

Using the numerical code developed by Brachet [15] we have performed direct numerical simulations of the Taylor-Green vortex flow in order to generate a turbulent velocity field for the purpose of an analysis of the subgrid-scale nonlinear interactions. Since the details of such simulations were extensively described by Brachet *et al.* [14] and Brachet [15] we report here only a few main features of the time evolution of the flow and its properties at the end of the run. The velocity field at the end of the run is used in the subsequent sections for the analysis of the subgrid-scale interactions.

The flow is contained in a cube with a side length 2π resulting in wave numbers $\mathbf{k} = (k_1, k_2, k_3)$ in the spectral space with integer components k_i. In the physical space the flow is periodic with the period 2π in each coordinate direction x, y, and z. Because of the symmetries the flow never crosses the boundaries x, y, and $z = \pi$ and in the subsequent discussion it will be visualized in the so-called impermeable box [14] $0 \leq x, y, z \leq \pi$. The effective spatial resolution in the simulations was 512^3 modes, which, after dealiasing by the

2/3 rule, provides the maximum wave number $k_m = 170$ in each coordinate direction. Since the velocity and the length scale of the initial flow are order unity the large eddy turnover time is also order unity and Reynolds number is equal to the inverse of molecular viscosity $1/\nu$ (3000 in the simulations). The simulations were run until maximum time $t_m = 18$, i.e. for several large eddy turnover times, with the time step $\Delta t = 0.0025$.

In Figs. 1(a) - 1(d) we plot the time evolution of the total turbulent energy, the total dissipation rate ϵ, skewness S, and microscale Reynolds number R_λ, respectively. Until time $t \approx 5$ the evolution of the flow is essentially inviscid with the total energy nearly constant. During this period small scales are generated from the initial condition (1) resulting in a subsequent rapid rise of the dissipation rate which peaks at $t \approx 10$ and later decays because of the decrease in the intensity of turbulence caused by the viscous damping. The skewness, after fairly chaotic behavior until $t \approx 10$, at the end of the run approaches -0.5, which is the generally accepted value for this quantity in fully developed isotropic turbulence. The initial value of R_λ exceeds 1000, decays rapidly becoming an order of magnitude less at the time of the peak in the dissipation rate $t \approx 10$, and slowly approaches the final value $R_\lambda \approx 70$ at the end of the run.

The unnormalized energy and dissipation spectra at the end of the run are plotted in Fig. 2(a). Small number of modes in the low wave number shells causes relatively large fluctuations in these quantities at low wave numbers. In the range of wave numbers $k < 20$ the energy spectrum conforms to the inertial $k^{-5/3}$ law with the Kolmogoroff constant in the range 2.2 to 2.7. The dissipation spectrum peaks at $k \approx 20$ which, for the calculated Kolmogoroff length scale $\eta = 0.011$ in the units used, corresponds to $\eta k \approx 0.2$. This value

agrees with experimental findings [19] locating the dissipation peak in high Reynolds number turbulence at a wave number order of magnitude less than $1/\eta$. Because of a significant overlap of the energy containing range and the dissipation range it is unclear if the observed inertial range spectrum for $k < 20$ is the result of the same dynamical processes that operate at very high Reynolds numbers where there exists wide separation between the energy and the dissipation range. Also unusually high value of the Kolmogoroff constant in the simulations casts doubt on the significance of the observed inertial subrange as being indicative of high Reynolds number turbulence dynamics. We may claim at best that the Reynolds number in the simulations is high enough to capture the beginnings of the inertial range dynamics but too low to separate it from the effects of the dissipation range dynamics. In the far dissipation range for $k > 20$ the dissipation and the nonlinear transfer spectra balance each other and have the functional form proportional to $k^{-2}\exp(-ak)$ as seen in Fig. 2(b). This form was derived by Domaradzki [20] using scaling properties of the detailed energy transfer observed in low Reynolds number turbulence.

3 Basic quantities

For homogeneous turbulence incompressible Navier-Stokes equations in spectral (Fourier) representation are:

$$\frac{\partial}{\partial t}u_n(\mathbf{k}) = -\nu k^2 u_n(\mathbf{k}) + N_n(\mathbf{k}). \tag{2}$$

Here, $u_n(\mathbf{k})$ is the velocity field in spectral space, with the explicit dependence on time omitted, ν is the kinematic viscosity, and $N_n(\mathbf{k})$ is the nonlinear term

$$N_n(\mathbf{k}) = -\frac{i}{2} P_{nlm}(\mathbf{k}) \int d^3p u_l(\mathbf{p}) u_m(\mathbf{k}-\mathbf{p}) \,, \tag{3}$$

where tensor $P_{nlm}(\mathbf{k})$ accounts for the pressure and incompressibility effects. The summation convention is assumed throughout.

Let's assume that the wave number space is divided into two non-overlapping regions, $\mathcal{L}$ ($|\mathbf{k}| \leq k_c$) signifying large scales, and $\mathcal{S}$ ($|\mathbf{k}| > k_c$) signifying small scales. In the LES terminology these scales are also referred to as the resolved and unresolved scales, respectively. In the LES an evolution equation for the velocity field $u_n(\mathbf{k})$ truncated to the region $\mathcal{L}$

$$u_n^{\mathcal{L}}(\mathbf{k}) = \begin{cases} u_n(\mathbf{k}) & \text{if } \mathbf{k}\epsilon\mathcal{L} \\ 0 & \text{otherwise} \end{cases} \tag{4}$$

is sought. The truncation operation is trivially applied to the linear terms in Eq. (2). The nonlinear term (3) is decomposed as follows. First, it is computed with one of the contributing velocity fields truncated to $\mathcal{U}$ and the other to $\mathcal{V}$, where $\mathcal{U}$ and $\mathcal{V}$ may be any of the two previously prescribed regions. Details of such calculations are provided by Domaradzki and Rogallo [21,22]. Resulting quantity, denoted by $N_n{}^{\mathcal{U}\mathcal{V}}(\mathbf{k})$, describes the modification of the mode $\mathbf{k}$ caused by all triad interactions involving $\mathbf{k}$ and two other scales, one belonging to $\mathcal{U}$ and the other to $\mathcal{V}$. Second, to retain the effect of such nonlinear interactions on the large scales only, the quantity $N_n{}^{\mathcal{U}\mathcal{V}}(\mathbf{k})$ is truncated to the region $\mathcal{L}$, with the result denoted by $N_n{}^{\mathcal{L}\mathcal{U}\mathcal{V}}(\mathbf{k})$. The evolution equation for the large scales $\mathcal{L}$ becomes:

$$\frac{\partial}{\partial t} u_n{}^{\mathcal{L}}(\mathbf{k}) = -\nu k^2 u_n{}^{\mathcal{L}}(\mathbf{k}) + N_n(\mathbf{k}|k_c) + N_n{}^{s}(\mathbf{k}|k_c), \tag{5}$$

where the resolved nonlinear term is

$$N_n(\mathbf{k}|k_c) = N_n{}^{\mathcal{LLL}}(\mathbf{k}), \tag{6}$$

and the subgrid-scale nonlinear term $N_n{}^s(\mathbf{k}|k_c)$ is

$$N_n{}^s(\mathbf{k}|k_c) = N_n{}^{\mathcal{LLS}}(\mathbf{k}) + N_n{}^{\mathcal{LSS}}(\mathbf{k}). \tag{7}$$

In practice, the most straightforward way to compute (6) and (7) is to first use (3) with the full velocity fields $u_l(\mathbf{p})$ and $u_m(\mathbf{k}-\mathbf{p})$ and truncate the result to the region $\mathcal{L}$ to obtain the total nonlinear term

$$N_n{}^{tot}(\mathbf{k}|k_c) = N_n(\mathbf{k}|k_c) + N_n{}^s(\mathbf{k}|k_c) \tag{8}$$

Next, Eq. (3) is used again with the truncated velocity fields $u_l^{\mathcal{L}}(\mathbf{p})$ and $u_m^{\mathcal{L}}(\mathbf{k}-\mathbf{p})$ and the result is truncated to the region $\mathcal{L}$ giving the resolved nonlinear term $N_n(\mathbf{k}|k_c)$ (Eq. (6)). The subgrid-scale nonlinear term (7) is obtained as the difference between the total nonlinear term (8) and the resolved nonlinear term (6).

The above described procedure has its exact counterpart in the physical space representation. Inverse Fourier transform, signified by tilde, of $N_n(\mathbf{k})$ (Eq. (3)) is the sum of the convective and pressure terms in the Navier-Stokes equation in the physical space coordinates

$$\tilde{N}_n(\mathbf{x}) = -\tilde{u}_i(\mathbf{x})\frac{\partial \tilde{u}_n(\mathbf{x})}{\partial x_i} - \frac{\partial p(\mathbf{x})}{\partial x_n}. \tag{9}$$

Similarly, using $N_n{}^{uv}(\mathbf{k})$ we can define its physical space counterpart $\tilde{N}_n^{uv}(\mathbf{x})$ as well as

$\tilde{N}_n^{\mathcal{K}\mathcal{U}\mathcal{V}}(\mathbf{x})$ which is the inverse Fourier transform of $N_n{}^{\mathcal{U}\mathcal{V}}(\mathbf{k})$ truncated to the region $\mathcal{K}$ (which is either $\mathcal{L}$ or $\mathcal{S}$). $\tilde{N}_n^{\mathcal{U}\mathcal{V}}(\mathbf{x})$ can be interpreted as the contribution to the rate of change of the velocity field $\tilde{u}_n(\mathbf{x})$ at a point $\mathbf{x}$ made by the nonlinear interactions involving modes from the spectral regions $\mathcal{U}$ and $\mathcal{V}$. Note that these interactions influence all modes $\mathbf{k}$ which can form a triangle with two other modes such that one is in $\mathcal{U}$ and the other in $\mathcal{V}$. $\tilde{N}_n^{\mathcal{K}\mathcal{U}\mathcal{V}}(\mathbf{x})$ represents a contribution to the rate of change of $\tilde{u}_n(\mathbf{x})$ which is made by all modes from $\mathcal{K}$ interacting nonlinearly with modes in $\mathcal{U}$ and $\mathcal{V}$. Finally, the inverse Fourier transform of (5) is

$$\frac{\partial}{\partial t}\tilde{u}_n^{\mathcal{L}}(\mathbf{x}) = \nu\nabla^2\tilde{u}_n^{\mathcal{L}}(\mathbf{x}) + \tilde{N}_n(\mathbf{x}|k_c) + \tilde{N}_n^s(\mathbf{x}|k_c), \tag{10}$$

where the resolved nonlinear term $\tilde{N}_n(\mathbf{x}|k_c)$ and the subgrid-scale term $\tilde{N}_n^s(\mathbf{x}|k_c)$ in the physical space are obtained Fourier transforming (6) and (7), respectively.

In the LES the most fundamental requirement is that the models employed properly approximate effects of subgrid-scale interactions on the energetics of the resolved scales. Thus, in assessing the models, energy equations rather than momentum equations are usually considered. In the spectral space the equation for the energy amplitude $\frac{1}{2}|u(\mathbf{k})|^2 = \frac{1}{2}u_n(\mathbf{k})u_n^*(\mathbf{k})$ of mode $\mathbf{k}$ obtained from (2) is:

$$\frac{\partial}{\partial t}\frac{1}{2}|u(\mathbf{k})|^2 = -2\nu k^2\frac{1}{2}|u(\mathbf{k})|^2 + T(\mathbf{k}), \tag{11}$$

where $T(\mathbf{k})$ is the nonlinear energy transfer

$$T(\mathbf{k}) = Re[u_n^*(\mathbf{k})N_n(\mathbf{k})]. \tag{12}$$

For homogeneous turbulence the above equations are usually considered after summing up contributions from all modes with a prescribed wavelength $|\mathbf{k}| = k$, giving:

$$\frac{\partial}{\partial t}E(k) = -2\nu k^2 E(k) + T(k), \tag{13}$$

where $E(k)$ and $T(k)$ are the classical energy and transfer spectra, respectively, for homogeneous turbulence.

Similarly, the detailed energy transfer to/from mode $\mathbf{k}$ caused by its interactions with wave numbers $\mathbf{p}$ in a prescribed region $\mathcal{P}$ of the wave number space and $\mathbf{q} = \mathbf{k} - \mathbf{p}$ in another region $\mathcal{Q}$ is

$$T^{\mathcal{PQ}}(\mathbf{k}) = Re[u_n^*(\mathbf{k}) N_n{}^{\mathcal{PQ}}(\mathbf{k})]. \tag{14}$$

Truncating $T^{\mathcal{PQ}}(\mathbf{k})$ to another region $\mathcal{K}$ results in the quantity $T^{\mathcal{KPQ}}(\mathbf{k})$ which is interpreted as the energy transfer to the region $\mathcal{K}$ resulting from nonlinear interactions of scales in $\mathcal{K}$ with scales in $\mathcal{P}$ and $\mathcal{Q}$. For homogeneous turbulence the regions $\mathcal{P}$ and $\mathcal{Q}$ are usually chosen as spherical wave number bands centered at wave numbers p and q, respectively. In this case quantity $T^{\mathcal{PQ}}(\mathbf{k})$ will be denoted by $T(\mathbf{k}|p,q)$. Summing quantity $T(\mathbf{k}|p,q)$ over spherical shells with thickness $\Delta k = 1$ centered at wave number k gives a function denoted by either $T^{\mathcal{KPQ}}(k)$ or $T(k|p,q)$

$$T^{\mathcal{KPQ}}(k) = T(k|p,q) = \sum_{k-\frac{1}{2}\Delta k<|\mathbf{k}|<k+\frac{1}{2}\Delta k} T(\mathbf{k}|p,q). \tag{15}$$

Total nonlinear energy transfer $T(k)$ to the wave number band k is obtained by summing

contributions $T(k|p,q)$ from all possible bands p and q:

$$T(k) = \sum_p \sum_q T(k|p,q) = \sum_p P(k|p). \tag{16}$$

Here, the function $P(k|p)$ is a result of summation of $T(k|p,q)$ over all q-bands and is interpreted as the energy transfer between wave number bands k and p.

With this notation, the energy equation for the energy spectrum $E^{\mathcal{L}}(k)$ of resolved scales, obtained from Eq. (5), is

$$\frac{\partial}{\partial t} E^{\mathcal{L}}(k) = -2\nu k^2 E^{\mathcal{L}}(k) + T(k|k_c) + T^s(k|k_c), \tag{17}$$

where

$$T(k|k_c) = T^{\mathcal{LLL}}(k), \tag{18}$$

and

$$T^s(k|k_c) = T^{\mathcal{LLS}}(k) + T^{\mathcal{LSS}}(k). \tag{19}$$

Equivalent expressions in the physical space are obtained by considering an equation for the rate of change of the turbulent energy of the resolved scales $e^{\mathcal{L}}(\mathbf{x}) = \frac{1}{2}\tilde{u}_n^{\mathcal{L}}(\mathbf{x})\tilde{u}_n^{\mathcal{L}}(\mathbf{x})$:

$$\frac{\partial e^{\mathcal{L}}(\mathbf{x})}{\partial t} = \nu \tilde{u}_n^{\mathcal{L}}(\mathbf{x}) \nabla^2 \tilde{u}_n^{\mathcal{L}}(\mathbf{x}) + \tilde{T}(\mathbf{x}|k_c) + \tilde{T}^s(\mathbf{x}|k_c), \tag{20}$$

where

$$\tilde{T}(\mathbf{x}|k_c) = \tilde{u}_n^{\mathcal{L}}(\mathbf{x})\tilde{N}_n(\mathbf{x}|k_c), \tag{21}$$

is the resolved energy transfer and

$$\tilde{T}^s(\mathbf{x}|k_c) = \tilde{u}_n^{\mathcal{L}}(\mathbf{x})\tilde{N}_n^s(\mathbf{x}|k_c) \tag{22}$$

is the subgrid-scale energy transfer in the physical space representation.

4 Results

Using the methodology described in the previous section and employing the numerically simulated velocity fields it is possible to compute directly the subgrid-scale energy transfer for any prescribed cutoff wave number $k_c < k_m$. It is customary to represent spectral subgrid-scale energy transfer in terms of the subgrid-scale eddy viscosity

$$\nu_e(k|k_c) = -\frac{T^s(k|k_c)}{2k^2 E^{\mathcal{L}}(k)}, \quad k < k_c, \tag{23}$$

which, following Kraichnan [4], is usually normalized by the factor equal to the product of the velocity scale $[E(k_c)k_c]^{1/2}$ and the length scale $1/k_c$ at the cutoff k_c

$$\nu_e{}^K(k|k_c) = \frac{\nu_e(k|k_c)}{[E(k_c)/k_c]^{1/2}}. \tag{24}$$

In order to compute the function $T^s(k|k_c)$, which depends on the length of the wave number k, according to Eq. (15) summation over all wavevectors $\mathbf{k}$ in a thin spherical shell centered at k must be performed. The components of such a sum are in general of both

signs implying that a particular mode k may be either losing energy (forward transfer) or gaining energy (inverse transfer) because of the subgrid-scale nonlinear interactions. To assess the relative importance of these two processes we have performed partial summations over components of same sign, effectively splitting the subgrid-scale energy transfer to/from scales k into the forward and the inverse transfer contributions. This procedure is equivalent to decomposing the total eddy viscosity into two parts, a positive one associated with the forward energy transfer, and a negative one associated with the inverse energy transfer. In Fig. 3 we plot the total eddy viscosity and its positive and negative components computed for three different cutoff wave numbers: one, $k_c = 20$, at the end of the (nominal) inertial subrange; the next, $k_c = 40$, at the beginning of the dissipation range; and the last one, $k_c = 80$, deep in the dissipation range. For $k_c = 20$ the total eddy viscosity is predominantly positive, with the absolute values of the negative component about 30-50% of the values of the positive component for $k/k_c < 0.6$. For $k/k_c > 0.6$ the ratio of the negative to the positive component decreases to about 20%. For $k_c = 40$ in the range $k/k_c < 0.6$ the positive and negative components nearly balance each other with the resulting total eddy viscosity close to zero. For $k/k_c > 0.6$ both components exhibit cusp-like behavior with the cusp for the positive component much stronger than for the negative one. Nevertheless, even close to the cutoff the ratio of the negative to the positive component is about 15%. For the case $k_c = 80$ in the range $k/k_c < 0.6$ the positive component is practically zero and the negative one is slightly less than zero, resulting in small negative values of the total eddy viscosity. Beyond that range, for k approaching the cutoff, the positive component increases very rapidly, reaching at the cutoff k_c values by factor 20 greater than the values of the negative

component. In the last figure we also plot the subgrid-scale eddy viscosity calculated by Kraichnan [4] and Cholet and Lesieur [5] from the analytical theories of turbulence under the assumption of the infinite inertial range. This function is essentially constant (equal to 0.267) for $k/k_c < 0.6$, and exhibits the cusp-like behavior for $k/k_c > 0.6$. We conclude from this analysis that the spectral inverse energy transfer may be quite significant, in some cases comparable to the forward transfer for given scales k. However, in all cases the forward transfer dominates as the cutoff wave number is approached. Since the transfer is obtained by multiplying the eddy viscosity by k^2, the cusp in the eddy viscosity for $k/k_c > 0.6$ is actually even more significant for the subgrid-scale transfer.

Using Eq. (22) we have computed the subgrid-scale energy transfer in the physical space $\tilde{T}^s(\mathbf{x}|k_c)$ for several spectral cutoff wave numbers. In Fig. 4 we plot a cross-section of this quantity for $k_c = 20$ and $k_c = 40$ for a plane in the impermeable box located at $y = \pi/4$. The larger spectral cutoff wave number results in presence of smaller scales in the physical space. Regions of the forward transfer (broken contours) and the inverse transfer (solid contours) are clearly visible. Even though the overall subgrid-scale transfer integrated over the computational box is negative, the forward and inverse transfer regions in these plots are roughly in balance. This indicates that both effects may be equally important in the dynamics of the flow. This conclusion agrees with the corresponding conclusion reached in the analysis of the spectral subgrid-scale transfer. It should be noted, however, that there is no direct relation between sets of spectral modes characterized by positive/negative transfer and the physical space regions with the same characteristics. Assuming that in the large scale momentum equation (5) the subgrid-scale nonlinear term $N_n^s(\mathbf{k}|k_c)$ is represented using

the classical spectral eddy viscosity model $\nu_e(k|k_c)$ of Kraichnan [4] and Cholet and Lesieur [5]

$$N_n^s(\mathbf{k}|k_c) = -\nu_e(k|k_c)k^2 u_n^{\mathcal{L}}(\mathbf{k}), \tag{25}$$

we have calculated the physical space subgrid-scale energy transfer for this model from (22). The results of the calculations are plotted in Fig. 5 for $k_c = 20$ and the same cross-plane as in Fig. 4. The modeled transfer is predominantly of the forward type as expected from the use of the strictly positive eddy viscosity but the appearance of weak inverse transfer regions may seem surprising. However, it should be noted that the molecular viscosity term in the incompressible Navier-Stokes equations results in two distinct effects in the energy equation: the kinetic energy dissipation, which is negative everywhere, and the change in the kinetic energy caused by work done by viscous stresses, which locally in space may be either positive or negative. Therefore any model which approximates the subgrid-scale nonlinear term N_n^s by a viscous-like term in the Navier-Stokes equations may contain regions of the increasing kinetic energy caused by work done by the modeled stresses. In practice, however, as seen in Fig. 5, these positive regions are quite insignificant since they occupy much less space than the negative regions and have also much lower maximum values. Obviously, such models give poor representation of the actual subgrid-scale energy transfer as seen comparing the actual and modeled transfers shown in Fig. 4(a) and Fig. 5, respectively. The conclusions from the physical space analysis of the subgrid-scale energy transfer parallel those drawn from the spectral space analysis: a relative importance of the inverse energy transfer process and an inability of the classical subgrid-scale models to properly account for it.

Cusps observed in spectral eddy viscosities in the vicinity of the cutoff wave number

suggest that the total energy transfer across this wave number is dominated by energy exchanges among resolved and unresolved scales from the vicinity of the cutoff. Indeed, it has been established in a number of papers [18,21,22,23] that in numerically simulated turbulence at low Reynolds numbers the energy transfer beyond the energy containing range is local, occuring between scales of similar size, even though the nonlocal wave number triads with one scale in the energy containing range are responsible for this local transfer. One would thus expect that the subgrid-scale nonlinear interactions between the resolved scales ($k < k_c$) and the unresolved scales characterized by wave numbers slightly greater than the cutoff wave number k_c will dominate the subgrid-scale energy transfer process. To evaluate this hypothesis in more detail we have calculated, for several values of the cutoff wave number k_c, the subgrid-scale energy transfer for the truncated velocity fields obtained from the original field by setting to zero all modes with wave numbers $k > ck_c$, where c was equal to 3/2 and 2. In this way the effect of all modes $k > ck_c$ on the subgrid-scale energy transfer is eliminated. In Fig. 6 we plot the resulting spectral subgrid-scale eddy viscosities (24) for $k_c = 20$ and $k_c = 40$ and compare them with the eddy viscosities computed using the full velocity field, i.e. with all modes $k < k_m$ being non-zero. It is seen that the value of the eddy viscosity computed for $c = 3/2$ provides a very good approximation to the total eddy viscosity while for $c = 2$ both quantities are practically indistinguishable on the plots. The similarly calculated subgrid-scale transfer in the physical space (22) is shown in Fig. 7 for the cutoff wave number $k_c = 20$ and two values of the parameter c, 3/2 and 2. The plane shown is the same as in Fig. 4. The spatial structure of the subgrid-scale energy transfer in Fig. 7 and Fig. 4(a) is the same, with differences seen only in the values of the

transfer at particular locations. For $c = 3/2$ the peak values of the approximated transfer (Fig. 7(a)) may depart by about 10% from the exact values (Fig. 4(a)) with the departures decreasing to about 5% for $c = 2$ (Fig. 7(b)). Therefore, both in the spectral and the physical space representation the subgrid-scale energy transfer for the resolved modes $k < k_c$ can be determined with high accuracy by considering their interactions with a limited range of unresolved modes $k_c < k \leq 2k_c$. It may be instructive to note that that for $k_c = 20$ and $k_m = 170$ the resolved modes constitute about 0.0016 of all modes, and modes with $k \leq 2k_c$ about 0.013 of all modes. Thus the dynamics of the largest 0.16% modes is determined almost entirely by their nonlinear interactions with about 1% of all modes, the remaining 99% modes not affecting visibly the largest scales. Moreover, the lack of direct influence of small scales $k > 2k_c$ on the energetics of the large resolved scales $k < k_c$ implies that the direct nonlocal energy transfer, inherent in the classical eddy viscosity theories [19], is not present in our simulations. The dynamics of the largest modes observed in the simulations is quite similar to the classical picture of the dynamics of the energy containing range in high Reynolds number turbulence. Quoting Batchelor [24]: "It seems that the energy-containing eddies determine the rate of energy transfer by their mutual interactions, and the larger wave-numbers adjust themselves, according to the Reynolds number, in order to convert this energy into heat at the required rate."

For the purpose of subgrid-scale modeling it is important to investigate relations between observed subgrid-scale energy transfer and various features of the resolved velocity field (4). In Figs. 8, 9, and 10 we plot in the physical space representation the kinetic energy $\frac{1}{2}\mathbf{u}(\mathbf{x}) \cdot \mathbf{u}(\mathbf{x})$, the enstrophy $\frac{1}{2}\omega(\mathbf{x}) \cdot \omega(\mathbf{x})$, where $\omega(\mathbf{x})$ is the vorticity, and the dissipation

rate $\frac{1}{2}\nu(\partial u_i/\partial x_k + \partial u_k/\partial x_i)^2$, respectively. All these quantities are computed using both the full velocity field (all modes $k < k_m$ are nonzero) and the velocity field (4) truncated at $k_c = 20$. One cross-sectional plane at the location $y = (3/4)\pi$ in the impermeable box is plotted and for comparison we also plot in Fig. 11 the subgrid-scale energy transfer in the same plane. Spatial structure of energy fields for the full and truncated fields is nearly the same. This feature is expected since the modes $k < k_c$ contain most of the total energy. The peak values of the energy for the full field may exceed by 30% the peak values for the truncated field. The maximum values for the dissipation and the enstrophy fields computed using the full velocity fields are by a factor 5 greater than for the truncated fields, indicating fairly large contributions coming from higher wave numbers $k > k_c$. The importance of these wave numbers is also reflected in the spatial structure of these quantities, with the full fields showing the presence of much smaller scales than the truncated fields. Despite these differences between the full and the truncated fields, for the enstrophy the spatial structure of the large scale component (Fig. 9(b)) is remarkably similar to the structure of the total enstrophy (Fig. 9(a)). In particular the regions of large values of the total enstrophy are very well correlated with the regions where the truncated field also gives large values. This result is somewhat surprising since the large scale enstrophy field is determined using only 0.16% of all modes. It suggests that these largest scales contain most of phase information required to determine spatial structure of the enstrophy field, and the role of higher wave number modes is to merely reflect the fact that the velocity gradients are steeper than can be resolved by the low wave number modes. In other words, larger wave numbers in the spectral space are needed to resolve steep velocity gradients rather than small eddies thought

of as small, individual flow structures like localized vortices. The level of correlation between the full and truncated fields for the dissipation is lower. The regions of the most intense dissipation for the truncated field (located along diagonals, half way between the center and the corners of the plotted plane in Fig. 10(b)) correlate well with the full dissipation field in the same region (Fig. 10(a)) but some equally strong regions in the full field farther away from the center do not have clear counterparts in the truncated field. Finally, all three quantitites computed using the truncated velocity field were compared with the subgrid-scale energy transfer plotted in Fig. 11. There is some level of spatial correlation between the subgrid-scale transfer and the enstrophy and the dissipation fields, with the regions of significant transfer in the vicinity (but not on the top of) regions of large enstrophy and dissipation. Also, the regions of intense large scale dissipation are usually located on the peripheries of the regions of intense large scale enstrophy. Interestingly, the regions of large subgrid-scale transfer seem to correlate best with the regions of large scale energy (Fig. 9(b)). Such correlations were observed previously [25] for different velocity fields but no convincing physical explanation of this observation is known. The above observations are based on visual inspection of countour plots and thus have a very qualitative character. A more quantitative procedure would have to be used to evaluate correlations in a systematic way. Nevertheless, this qualitative analysis clearly illustrates a fairly complex character of inter-relations among different physical quantities and gives no indications that any simple expression for the subgrid-scale transfer in terms of the resolved energy, enstrophy, or dissipation exists. We conclude from the analysis of the truncated fields that the the subgrid-scale energy transfer is at best marginally correlated with the large scale energy, enstrophy, and dissipation. This

analysis also reveals that the turbulent activity is spatially intermittent and its physical locations are determined by the mutual interactions of the largest scales. The high wave number modes in this flow cannot be interpreted as individual, small scale turbulent eddies, but reflect the presence of steep gradients at the spatial locations determined by the large scales.

The observed importance of the large scales, which constitute only a minute fraction of all spectral modes, in the dynamics of turbulence is encouraging since it suggests that their dynamics may be almost self-contained and thus the accurate subgrid-scale models based on the large scale velocity information should be possible. The term "almost self-contained dynamics" is not very precise but can be illustrated by the following example. In Fig. 12(a) we plot one plane from the resolved nonlinear transfer field (Eq. (21)) and in Fig. 12(b) the corresponding result for the total nonlinear transfer, i.e. the sum of (21) and (22). It is seen that the spatial structure of the resolved nonlinear transfer is highly correlated with the structure of the total nonlinear transfer. In that sense the dynamics of the large resolved scales, which involves interactions with all modes in the system (the total transfer) is "almost" the same as the internal nonlinear dynamics of the large scales only (the resolved transfer). The difference between both quantities is of course the subgrid-scale nonlinear transfer (22), which when viewed this way, is a small correction to the resolved transfer needed to get the total transfer and to account for the non-conservative character of the entire system. The large degree of correlation between the resolved and the total transfers suggests that in the subgrid-scale modeling a good strategy may be to model the total (unknown) transfer using the resolved (known) transfer rather than to model their

difference, the subgrid-scale transfer, as is always done.

5 Conclusions

We have performed a detailed analysis of the effects of the subgrid-scale nonlinear interactions on the energetics of isotropic turbulence. The analyzed turbulent velocity field was obtained from a direct numerical simulation of the Taylor-Green vortex flow. Symmetries of the flow allowed to reach the spatial resolution in the simulation equivalent to 512^3 mesh points and the Reynolds number $R_\lambda \approx 70$. At this Reynolds number the flow exhibits a beginning of the inertial range dynamics at the lowest wave numbers. However, even these low as well as all higher wave numbers are still dominated by dissipative processes. Therefore, while our conclusions are certainly valid for the disspation range dynamics it is less certain that they are applicable to the inertial range dynamics.

An important feature of the computed subgrid-scale energy transfer, in both spectral and physical space representation, is the presence of significant inverse energy transfers, from the unresolved to the resolved scales. The inverse subgrid-scale transfer was predicted and observed before in the context of spectral dynamics of homogeneous turbulence [4,6,11,8] and in the physical space for homogeneous and wall-bounded turbulent flows [7,25,9,26]. The observed significance of the inverse transfer in the energetics of the resolved scales implies that successful subgrid-scale models should properly account for such effects. At the present time these effects are rarely taken into account in the subgrid-scale modeling procedures. If accounted for they are modeled by either adding a random force to the subgrid-scale equations [7,8] or extrapolating from the dynamics of the resolved scales [9]. Since most of the

subgrid-scale transfer observed in this work is caused by interactions among highly correlated modes on both sides of the cutoff wave number, approximating effects of such interactions by random forces is debatable. An approach used in the dynamic subgrid-scale model [9] seems more appropriate but it suffers from modeling the inverse transfer by a diffusion type term with a negative diffusion coefficient, mathematically an inherently unstable situation. It appears that alternate ways of the subgrid-scale modeling which overcome these conceptual and mathematical difficulties should be explored.

Our analysis also reveals that the nonlinar dynamics of the resolved modes with wave numbers $k < k_c$ is governed almost exclusively by their interactions with a limited range of modes with wave numbers not exceeding $2k_c$ and nonlocal, eddy-viscosity type energy transfer is not observed. Thus, in agreement with the classical picture of the turbulence dynamics [24], the large scales of a turbulent flow determine the energy flux down the spectrum and the small scales play entirely passive role by adjusting themselves in such a way as to accomodate this energy flux prescribed by the large scales.

The physical space energy, enstrophy, and dissipation have been computed for the full and truncated velocity fields and compared with the subgrid-scale energy transfer for the same truncation wave number. Surprisingly, these physical quantities computed for both full and truncated fields show many similar spatial features despite the fact that the truncated field contains only 0.16% of all modes present in the system. This result reinforces our conclusion about the dominant role played by the very largest scales in the dynamics of the flow. The level of correlation between these quantities and the subgrid-scale transfer varies from weak for the enstrophy and dissipation, to moderate for the energy.

Finally, using the observed importance of the nonlinear interactions among the largest scales in the overall dynamics of the resolved scales it is suggested that the resolved nonlinear term may possibly serve as a basis of a new approach to the subgrid-scale modeling.

ACKNOWLEDGMENTS

This research was supported by the AFOSR Contract No. 90-0300. The numerical simulations were performed at the Air Force Supercomputer Center - Kirtland.

[1]R.S. Rogallo and P. Moin, "Numerical simulation of turbulent flows", Ann. Rev. Fluid Mech. **16**, 99 (1984).

[2]M. Lesieur, "Turbulence in Fluids", Second Edition, (Martinus Nijhoff Publishers, Dordrecht, 1990).

[3]J. Smagorinsky, "General circulation experiments with the primitive equations", Mon. Weath. Rev. **93**, 99 (1963).

[4]R.H. Kraichnan, "Eddy viscosity in two and three dimensions", J. Atmos. Sci. **33**, 1521 (1976).

[5]J. Chollet and M. Lesieur, "Parametrization of small scales of three-dimensional isotropic turbulence utilizing spectral closures", J. Atmos. Sci. **38**, 2767 (1981).

[6]D.C. Leslie and G.L. Quarini, "The application of turbulence theory to the formulation of subgrid modelling procedures", J. Fluid Mech. **91**, 65 (1979).

[7]C.E. Leith, "Stochastic backscatter in a subgrid-scale model: plane shear mixing layer", submitted to Phys. Fluids A (1989).

[8]J.R. Chasnov, "Development and Application of an Improved Subgrid Model for Homogeneous Turbulence", Ph.D. thesis, Columbia University, 1990.

[9]M. Germano, U. Piomelli, P. Moin, and W.H. Cabot, "A dynamic subgrid-scale eddy viscosity model", Phys. Fluids A**3**, 1760 (1991).

[10]R.A. Clark, J.H. Ferziger, and W.C. Reynolds, "Evaluation of subgrid-scale models using an accurately simulated turbulent flow", J. Fluid Mech. **91**, 1 (1979).

[11]J.A. Domaradzki, R.W. Metcalfe, R.S. Rogallo, and J.J. Riley, "Analysis of subgrid-scale eddy viscosity with use of results from direct numerical simulations", Phys. Rev. Lett. **58**, 547 (1987).

[12]S.A. Orszag, "Numerical simulation of incompressible flows within simple boundaries. I. Galerkin (spectral) representations", Stud. Appl. Math. **50**, 293 (1971).

[13]G.I. Taylor and A.E. Green, "Mechanism of the production of small eddies from large ones", Proc. Roy. Soc. A **158**,499 (1937).

[14]M.E. Brachet, D.I. Meiron, S.A. Orszag, B.G. Nickel, R.H. Morf, and U. Frisch, "Small-scale structure of the Taylor-Green vortex", J. Fluid Mech. **130**, 411 (1983).

[15]M.E. Brachet, "The geometry of small-scale structures of the Taylor-Green vortex", C. R. Acad. Sci. Paris **311**, 775 (1990).

[16]S. Kida, "Three-dimensional periodic flows with high-symmetry", J. Phys. Soc. Jap. **54**, 2132 (1985).

[17]S. Kida and Y. Murakami, "Kolmogorov similarity in freely decaying turbulence", Phys. Fluids **30**, 2030 (1987).

[18]K. Ohkitani and S. Kida, "Triad interactions in a forced turbulence", Phys. Fluids A **4** 794 (1992).

[19]A.S. Monin and A.M. Yaglom, *Statistical Fluid Mechanics* (The MIT Press,Cambridge, 1979).

[20]J.A. Domaradzki, " Nonlocal triad interactions and the dissipation range of isotropic turbulence", to appear in Phys. Fluids (1992).

[21]J.A. Domaradzki and R.S. Rogallo, "Energy transfer in isotropic turbulence at low Reynolds numbers", in *Proceedings of the 1988 Summer Program* (Center for Turbulence Research, CTR-S88, NASA Ames/Stanford University, 1988), p. 169.

[22]J.A. Domaradzki and R.S. Rogallo, "Local energy transfer and nonlocal interactions in homogeneous, isotropic turbulence", Phys. Fluids A **2**, 413 (1990).

[23]P.K. Yeung and J.G. Brasseur, "The response of isotropic turbulence to isotropic and anisotropic forcing at the large scales", Phys. Fluids A**3**, 413 (1991).

[24]G.K. Batchelor, "The theory of homogeneous turbulence", (Cambridge University Press, Cambridge, 1953), p. 113.

[25]J.A. Domaradzki, R.S. Rogallo, and A.A. Wray, "Interscale energy transfer in numerically simulated homogeneous turbulence", in *Proceedings of the 1990 Summer Program* (Center for Turbulence Research, NASA Ames/Stanford University, 1990), p. 319.

[26]U. Piomelli, W.H. Cabot, P. Moin, and S. Lee, Phys. Fluids A**3**, 1766 (1991).

Figure Captions

Figure 1. Time evolution of flow quantities: (a) total kinetic energy; (b) total dissipation; (c) skewness; (d) microscale Reynolds number.

Figure 2. Spectral quantities at the end ot the run ($t = 18$): (a) unnormalized spectra of the energy (solid line) and the dissipation (broken line); (b) the dissipation spectrum (solid line) and the transfer spectrum (broken line) outside the energy containing range. Both quantities plotted using a log-linear scale to accentuate their exponential behavior.

Figure 3. The spectral subgrid-scale eddy viscosity (solid line) and its negative (broken line) and positive (dotted line) components: (a) $k_c = 20$; (b) $k_c = 40$; (c) $k_c = 80$.

Figure 4. The subgrid-scale energy transfer in the physical space representation: (a) $k_c = 20$; (b) $k_c = 40$. Plane $y = \pi/4$ in the impermeable box is shown. Here and in all subsequent contour plots the solid lines represent positive values and the broken lines represent negative values.

Figure 5. The subgrid-scale energy transfer in the physical space computed using the spectral eddy viscosity model of Kraichnan [4] and Chollet and Lesieur [5].

Figure 6. The spectral subgrid-scale eddy viscosity: (a) $k_c = 20$; (b) $k_c = 40$. The velocity fields used to compute this quantity were the full field (solid line), the full field truncated at $(3/2)k_c$ (broken line), and the full field truncated at $2k_c$ (dotted line).

Figure 7. The physical space subgrid-scale energy transfer computed for $k_c = 20$ and the full fields truncated at (a) $(3/2)k_c$ and (b) $2k_c$.

Figure 8. The kinetic energy field in a plane $y = (3/4)\pi$ in the impermeable box: (a) computed using the full velocity field; (b) computed using the resolved velocity field with

the truncation wave number $k_c = 20$.

Figure 9. The enstrophy field in a plane $y = (3/4)\pi$ in the impermeable box: (a) computed using the full velocity field; (b) computed using the resolved velocity field with the truncation wave number $k_c = 20$.

Figure 10. The dissipation field in a plane $y = (3/4)\pi$ in the impermeable box: (a) computed using the full velocity field; (b) computed using the resolved velocity field with the truncation wave number $k_c = 20$.

Figure 11. The subgrid-scale energy transfer in the physical space representation computed for the cutoff wavenumber $k_c = 20$ and shown in a plane $y = (3/4)\pi$ in the impermeable box.

Figure 12. The nonlinear energy transfer to/from the resolved modes $k < 20$ represented in the physical space: (a) caused by interactions with the resolved modes only; (b) caused by interactions with the resolved and unresolved modes.

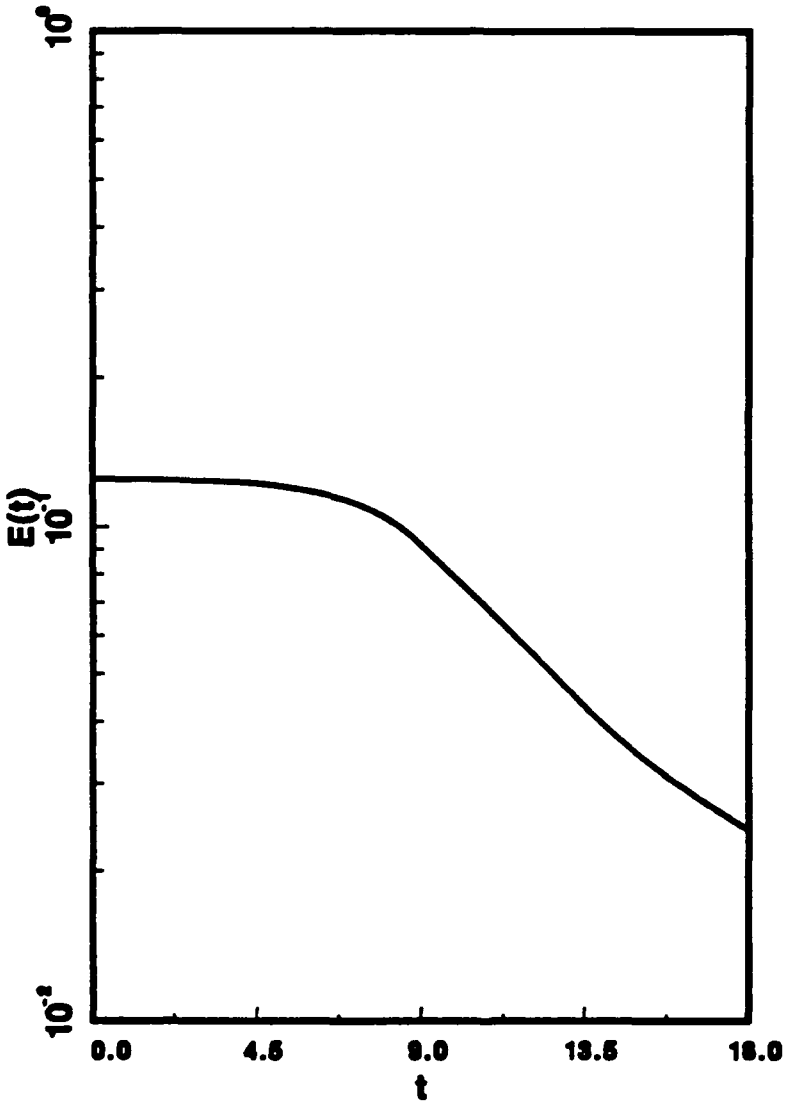

Fig. 1(a)

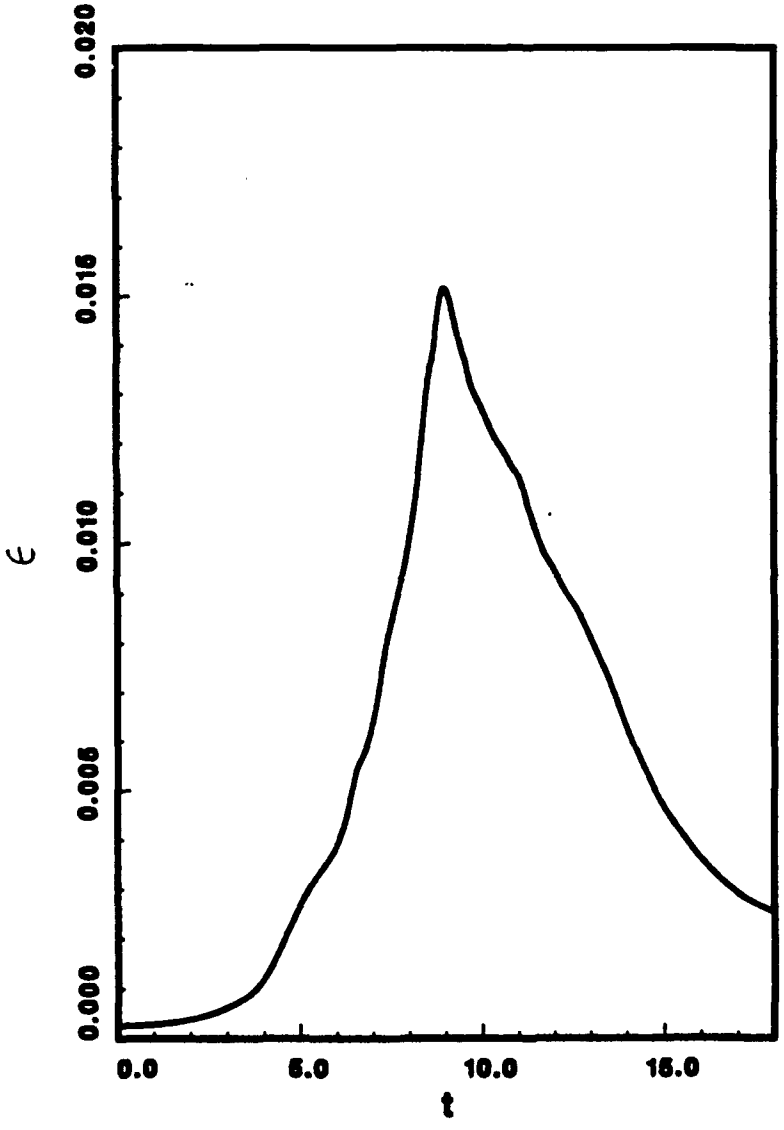

Fig. 1(b).

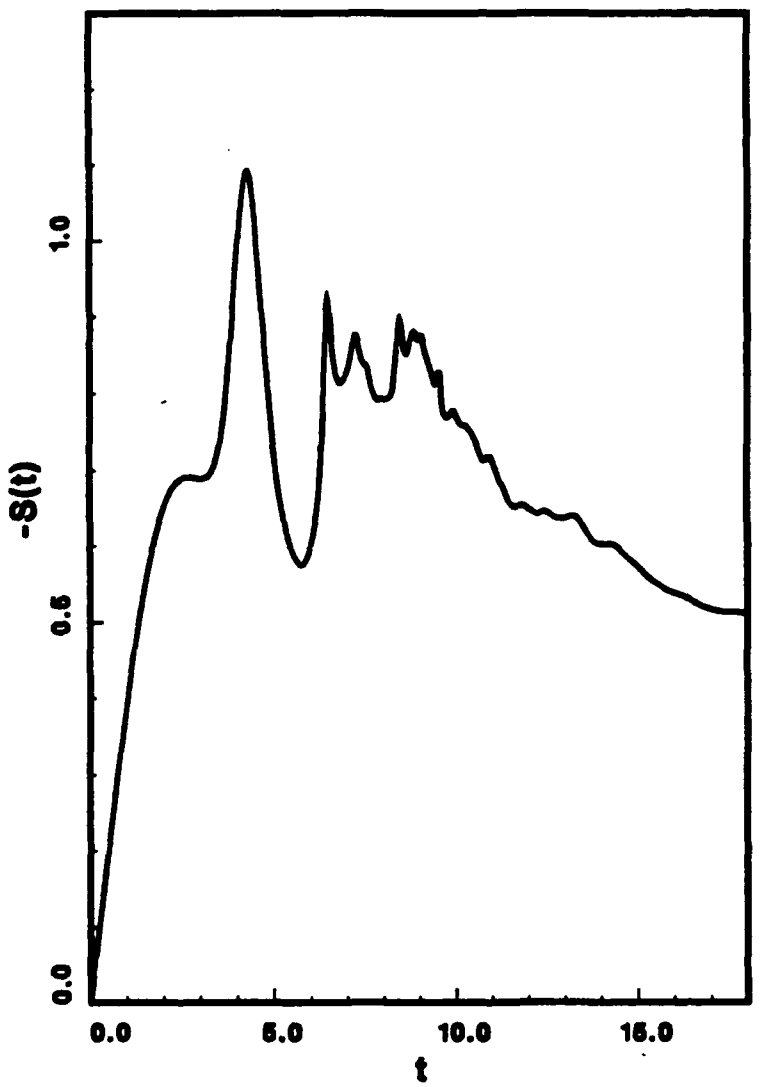

Fig. 1(c)

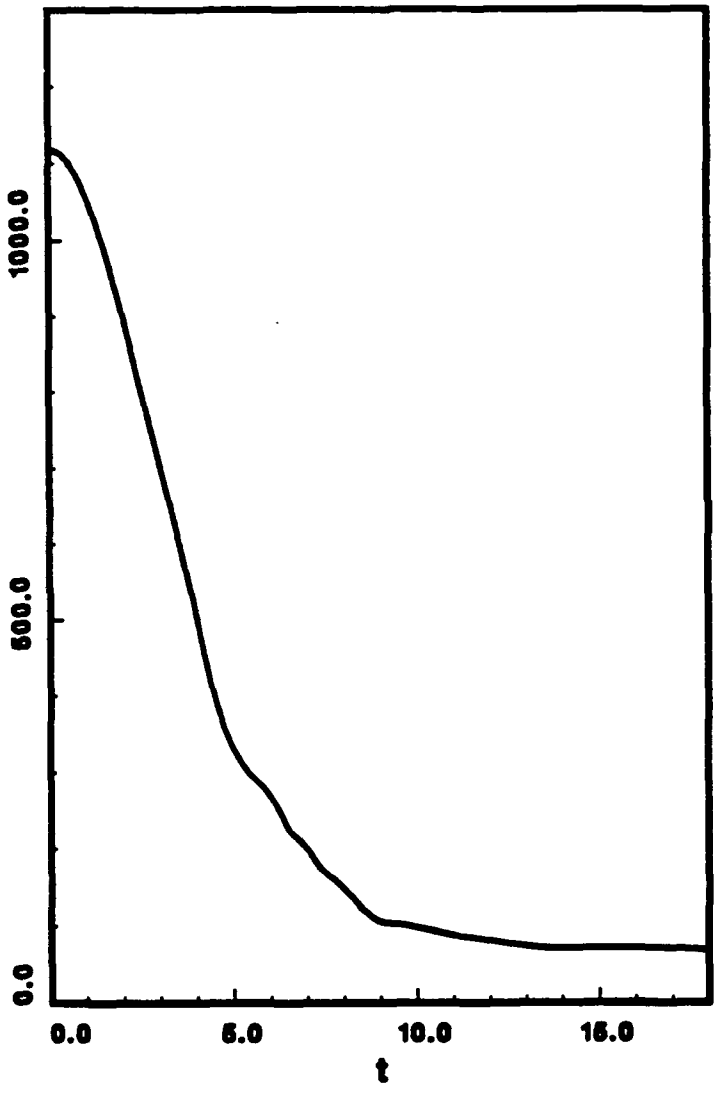

Fig 1(a)

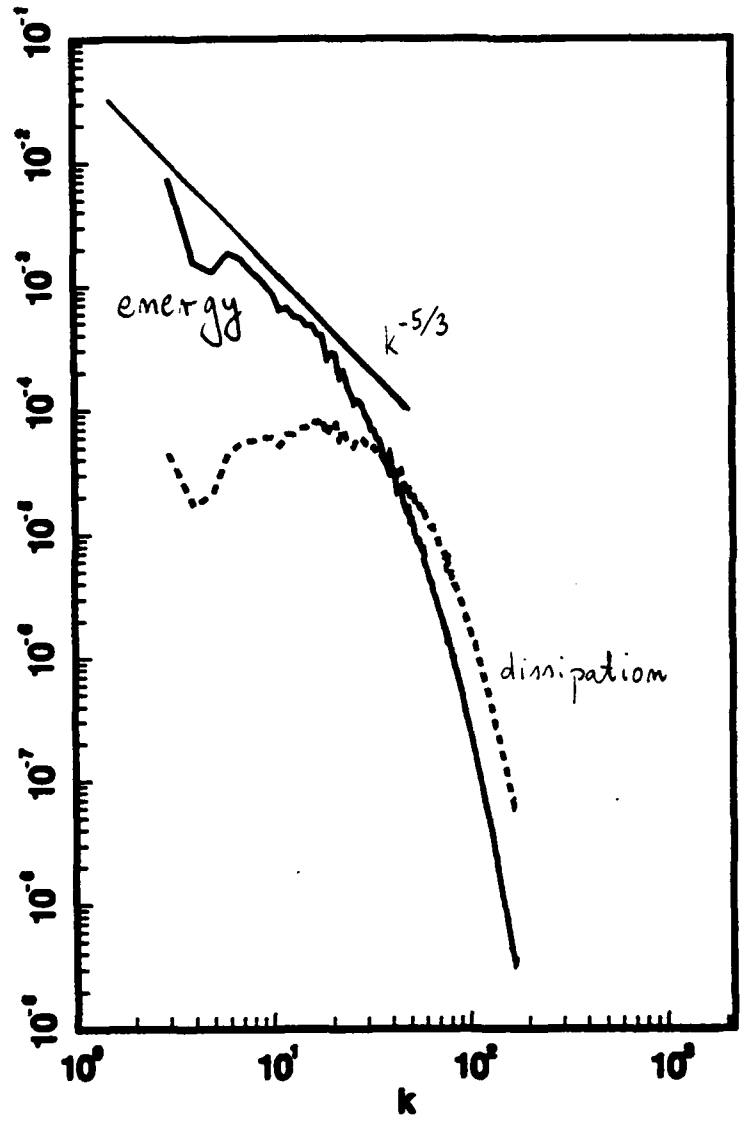

Fig. 2 (a)

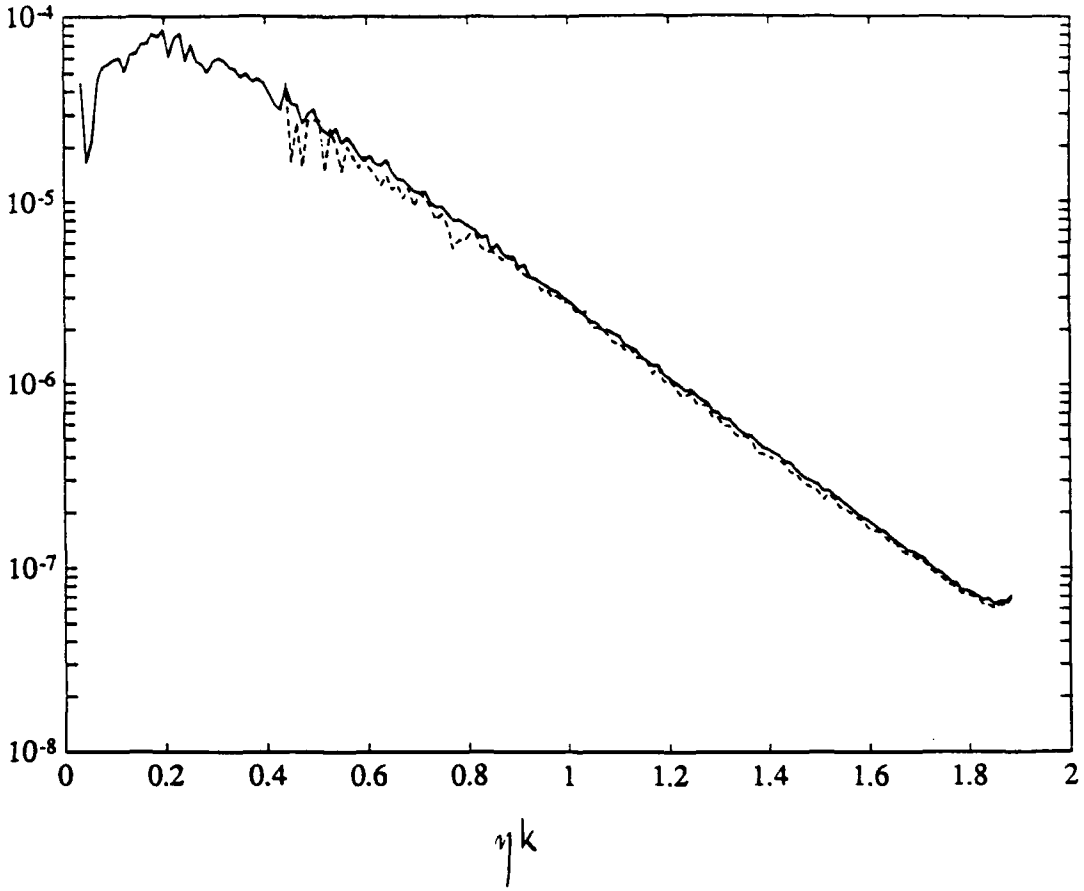

Fig 2(b)

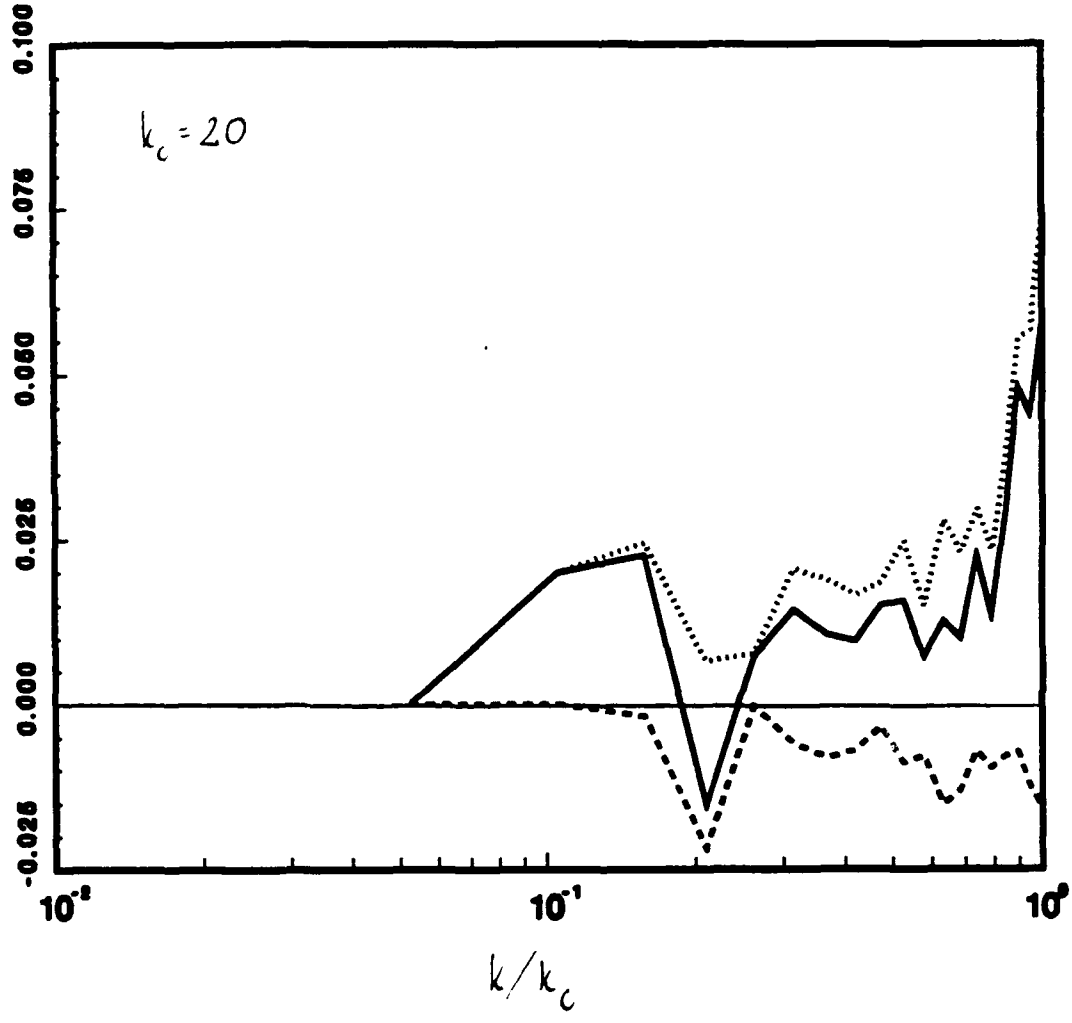

Fig. 3(a)

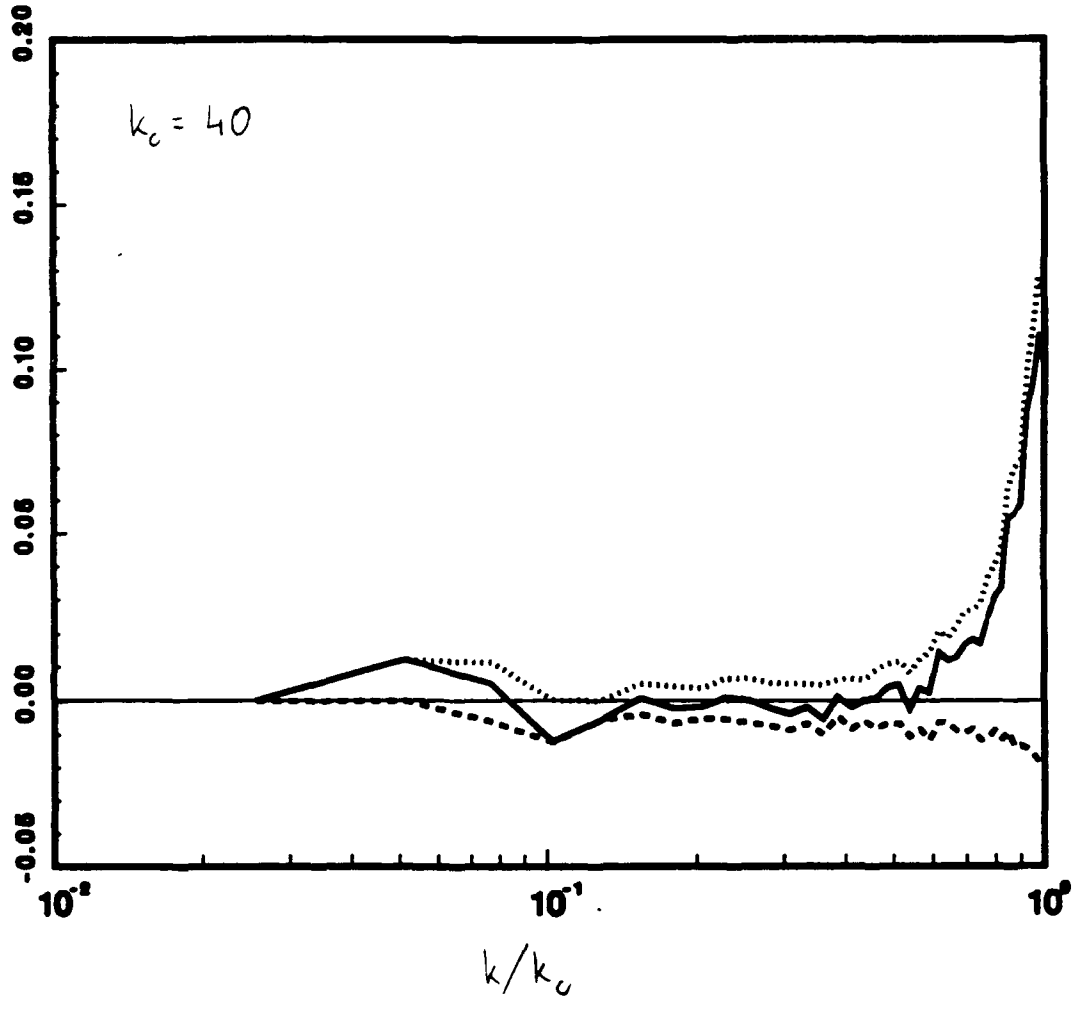

Fig. 3(b)

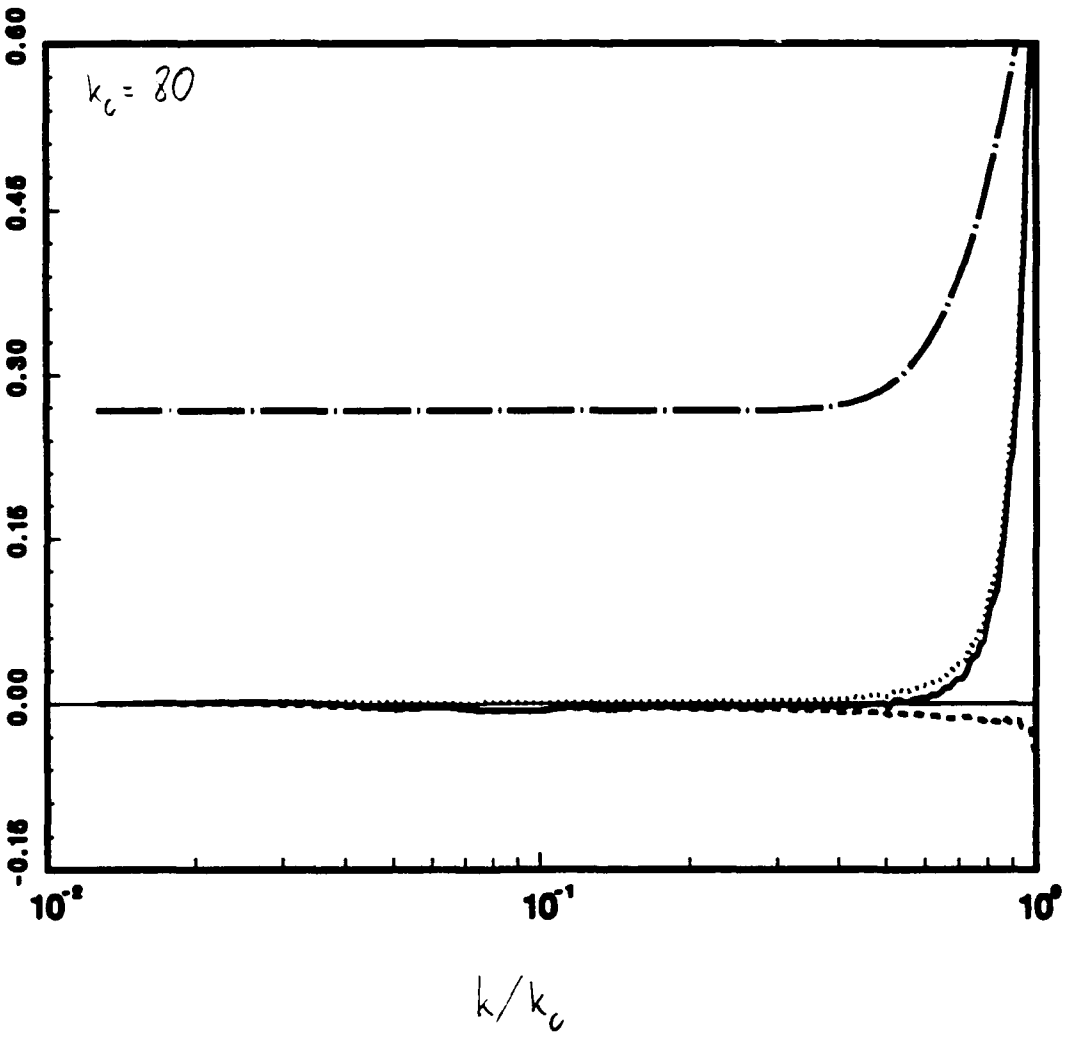

Fig. 3(c)

SUBGRID SCALE

ISO-CONTOURS IN X-Z PLANE AT JCUT = 65

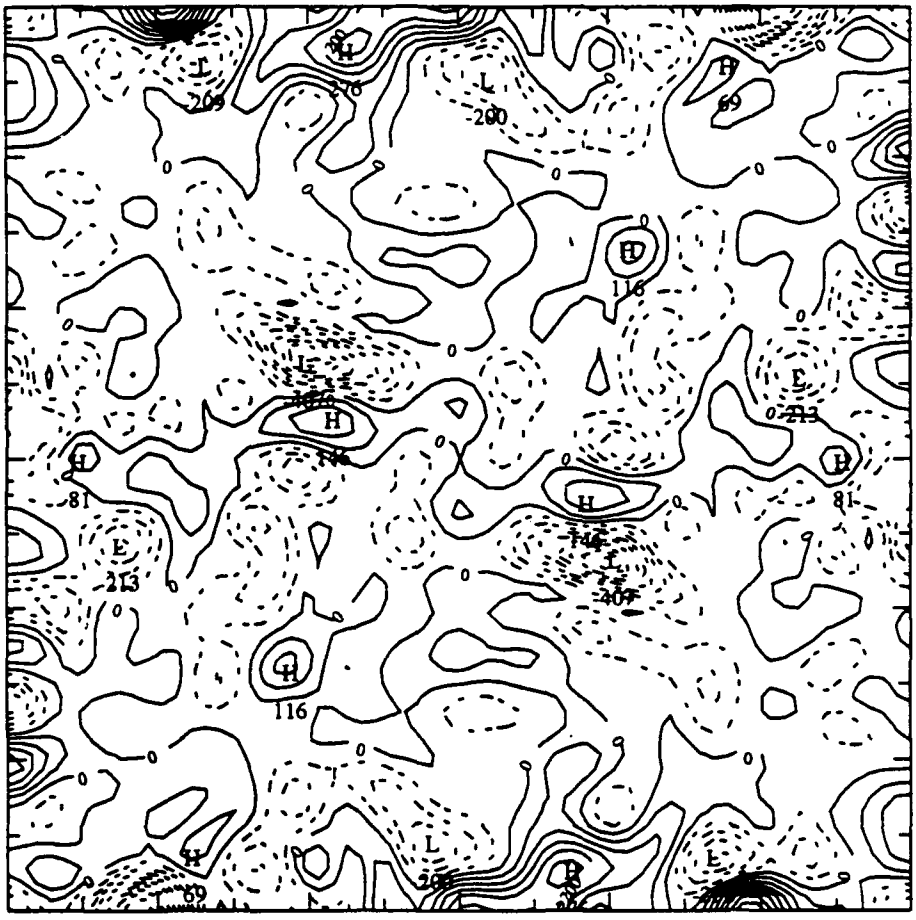

$k_c = 20$

CONTOUR FROM -0.XXXXE-XX TO 0.XXXXE-XX CONTOUR INTERVAL OF 0.XXXXE-XX PT(1,3)= 0.XXXXE-XX LABELS SCALED BY XXXX

Fig. 4(a)

SUBGRID SCALE CUT WAVE NUMBER = 40

ISO-CONTOURS IN X-Z PLANE AT JCUT = 65

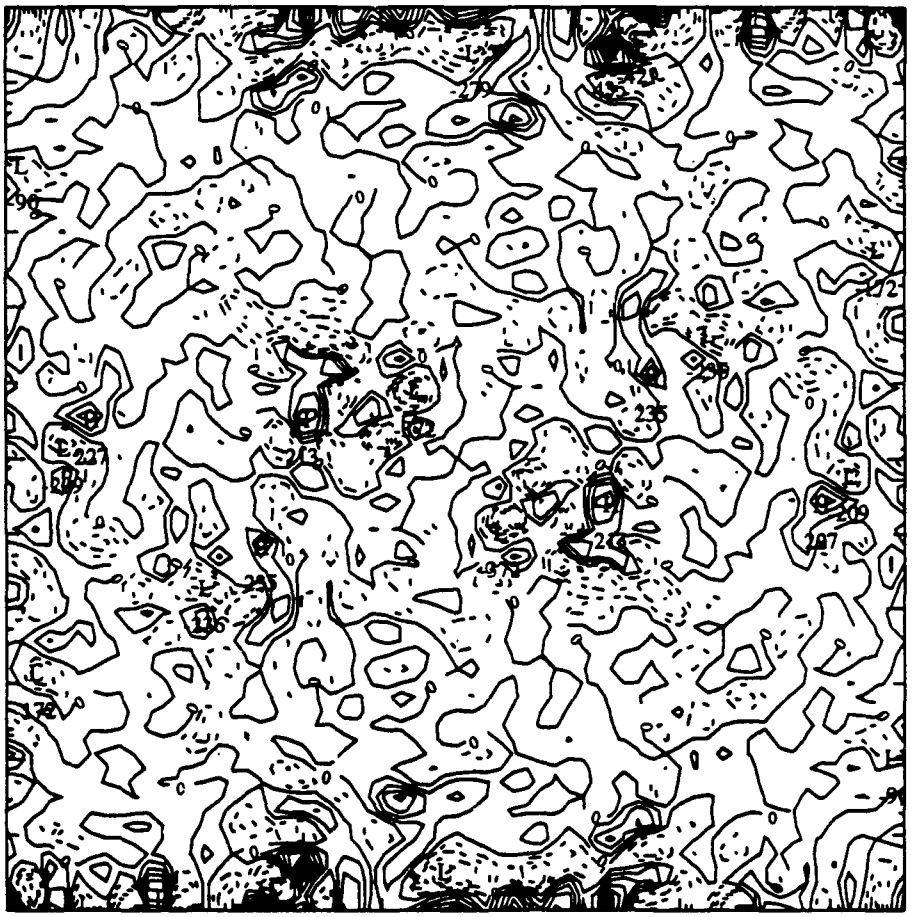

z from 0 to π

x from 0 to π

$k_c = 40$

CONTOUR FROM -0.46E-01 TO 0.46E-01 CONTOUR INTERVAL OF 0.46E-02 PT(2,3)= -0.25E-01 LABELS SCALED BY 1E+00

Fig 4(b)

SUBGRID SCALE OF THEORETICAL RESULT (CUT=20)

ISO-CONTOURS IN X-Z PLANE AT JCUT = 65

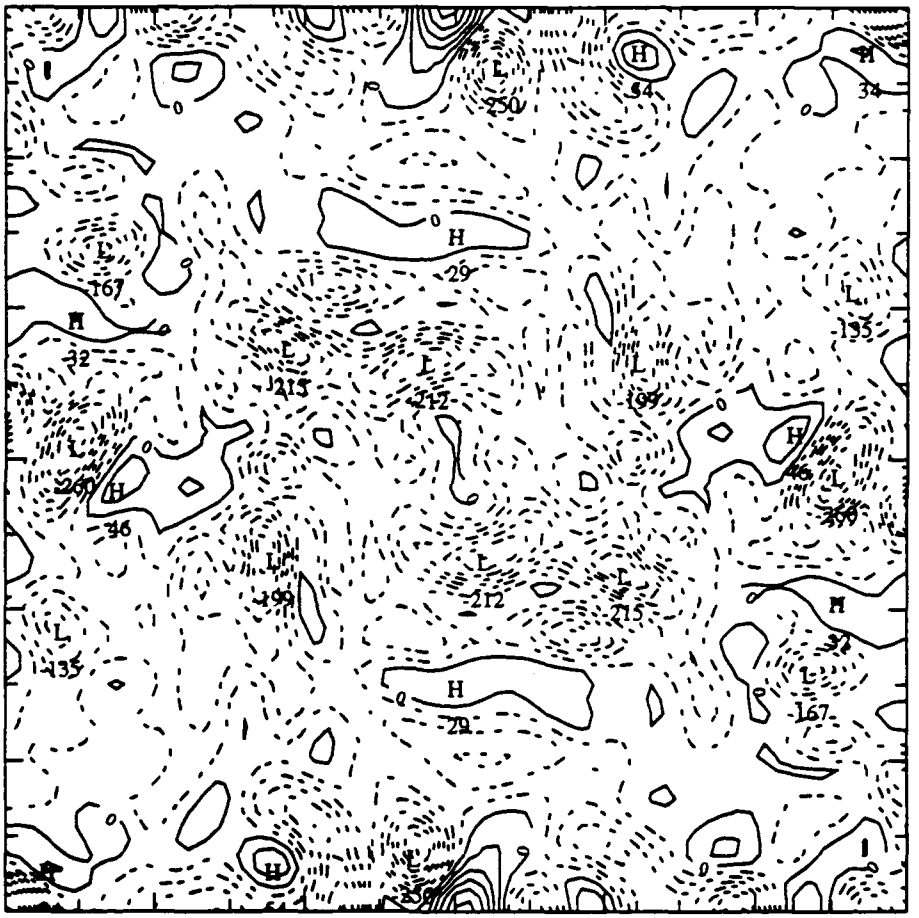

z from 0 to π

x from 0 to π

$k_c = 20$

CONTOUR FROM -0.3[illegible] TO 0.1[illegible] CONTOUR INTERVAL OF 0.3[illegible] FT(3,3)= -0.72[illegible] LABELS SCALED BY [illegible]

Fig. 5

DISTRIBUTION OF EDDY VISCOSITY (KC=20)

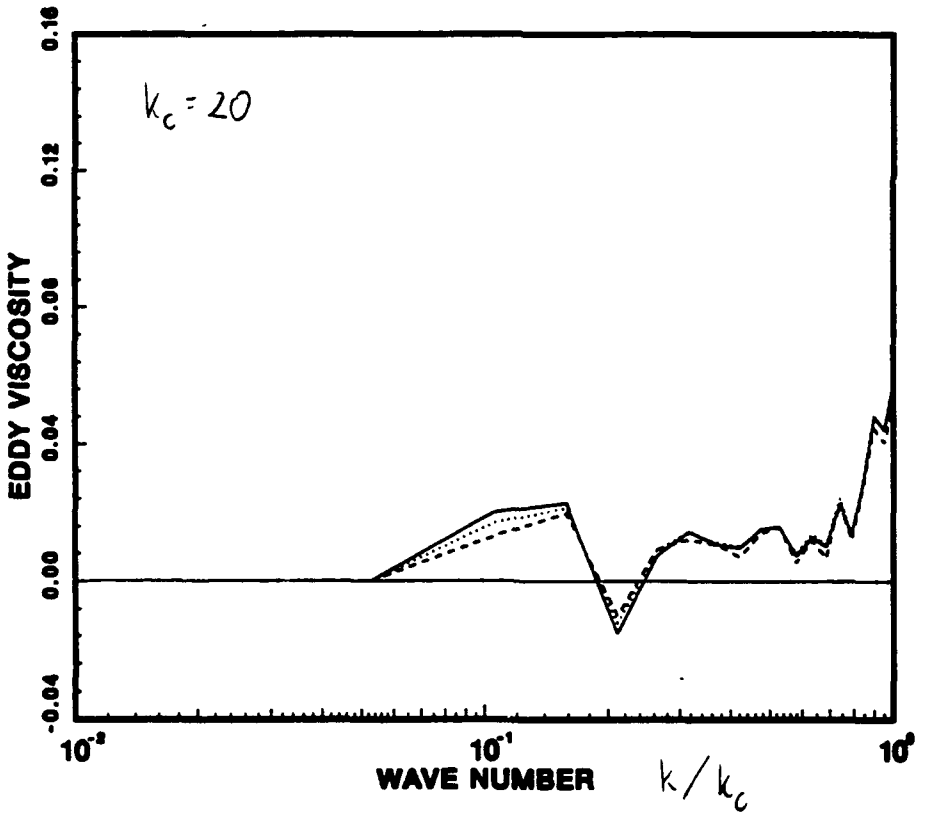

Fig 6(a)

DISTRIBUTION OF EDDY VISCOSITY (KC=40)

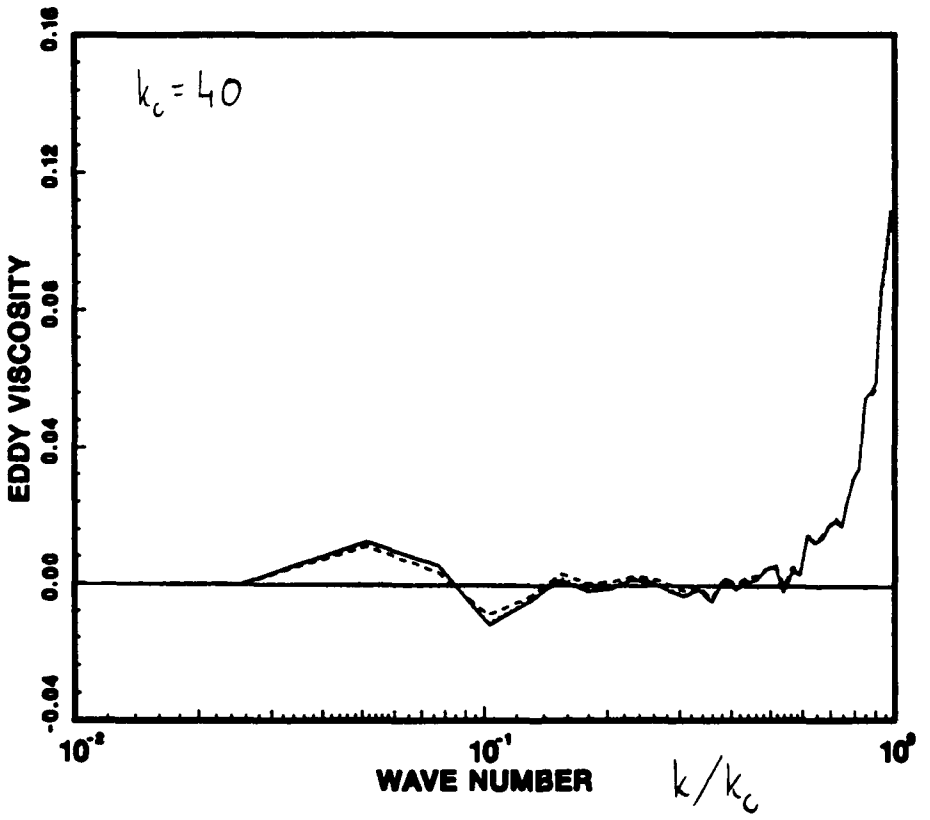

Fig. 6(b)

SUBGRID SCALE CUT WAVE NUMBER = 20

THE LARGEST WAVE NUMBER = 30

ISO-CONTOURS IN X-Z PLANE AT JCUT = 65

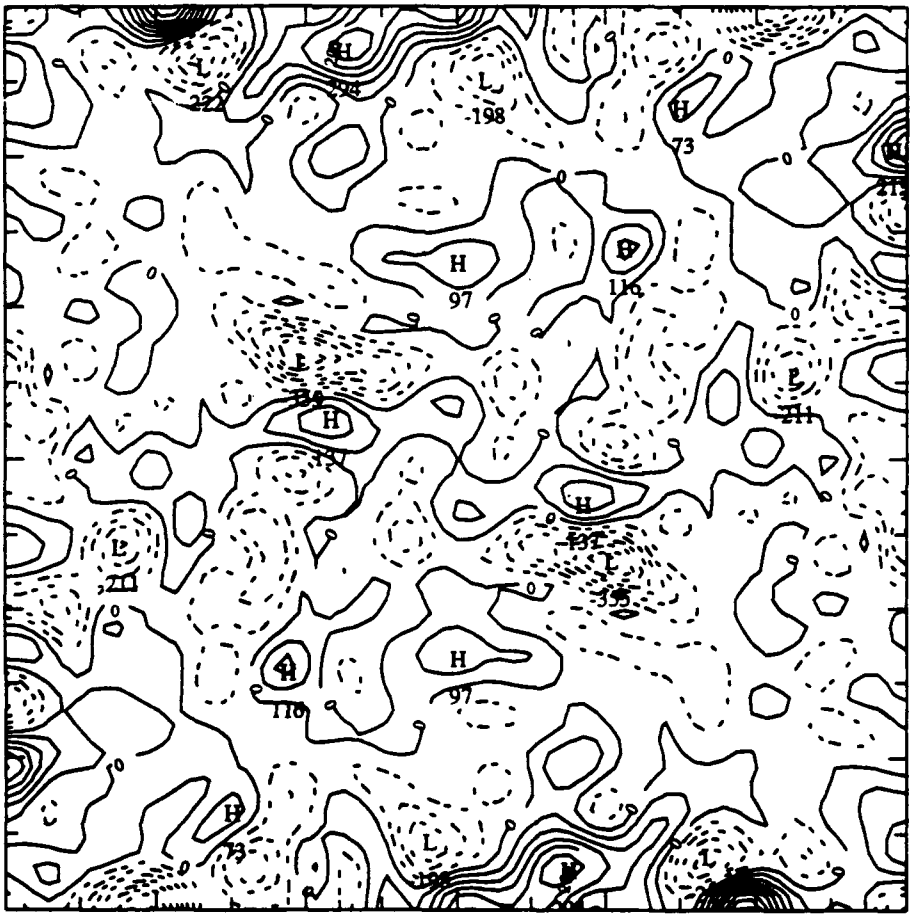

Fig. 7(a)

SUBGRID SCALE CUT WAVE NUMBER = 20

THE LARGEST WAVE NUMBER = 40

ISO-CONTOURS IN X-Z PLANE AT JCUT = 65

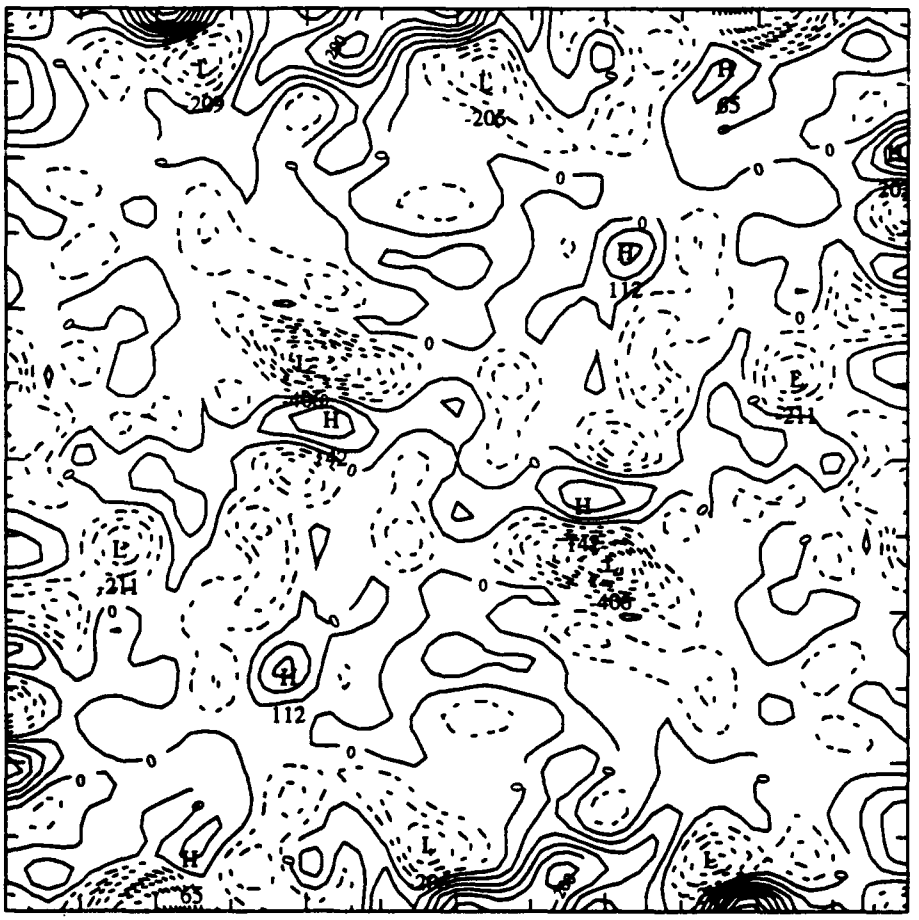

z from 0 to π

x from 0 to π

Fig 7(b)

ENERGY OF WHOLE WAVE NUMBER

ISO-CONTOURS IN X-Z PLANE AT JCUT = 193

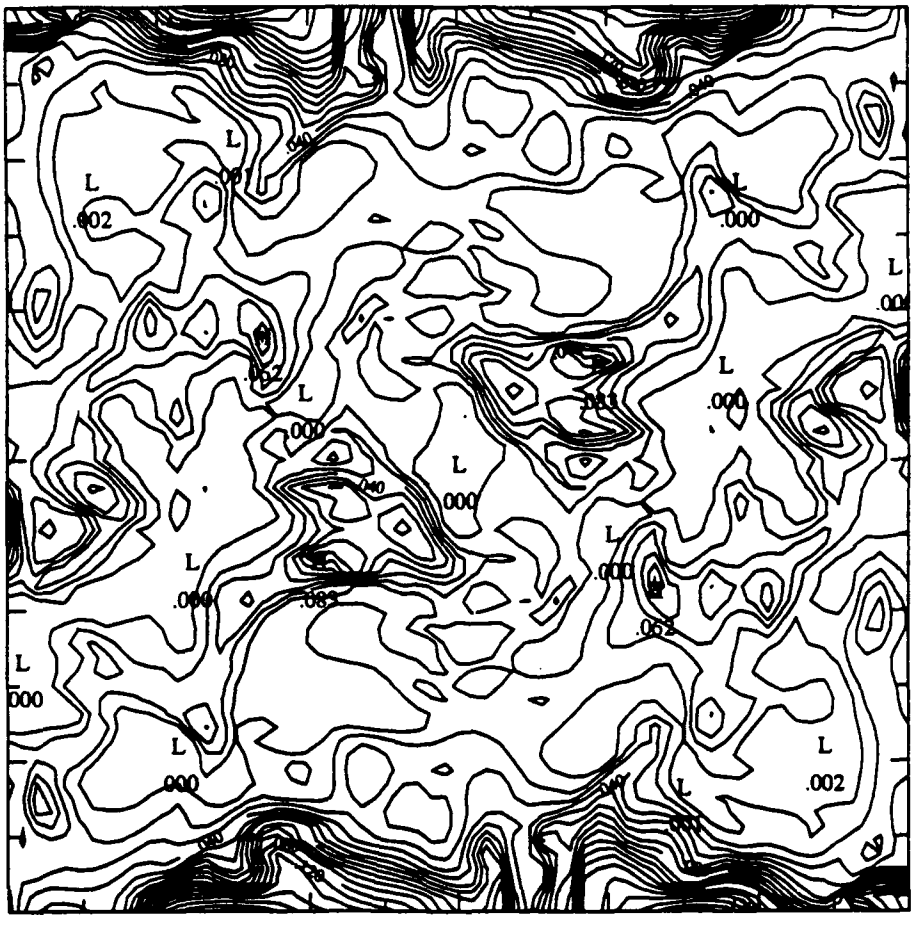

CONTOUR FROM [illegible] TO [illegible] CONTOUR INTERVAL OF [illegible]

Fig. 8(a)

ENERGY OF LOW WAVE NUMBER
ISO-CONTOURS IN X-Z PLANE AT JCUT = 193

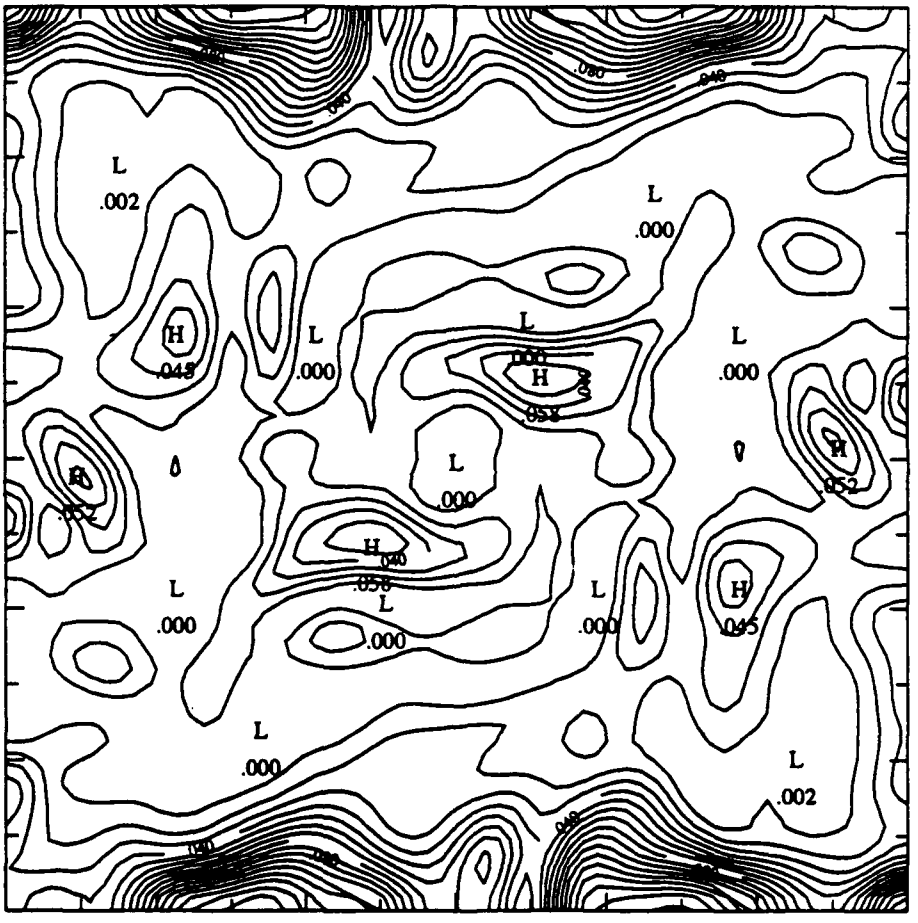

z from 0 to π

x from 0 to π

CONTOUR FROM [illegible] TO [illegible] CONTOUR INTERVAL OF [illegible] FT(1,1)= [illegible]

Fig. 8(b)

ω^2 OF WHOLE WAVE NUMBER

ISO-CONTOURS IN X-Z PLANE AT JCUT = 193

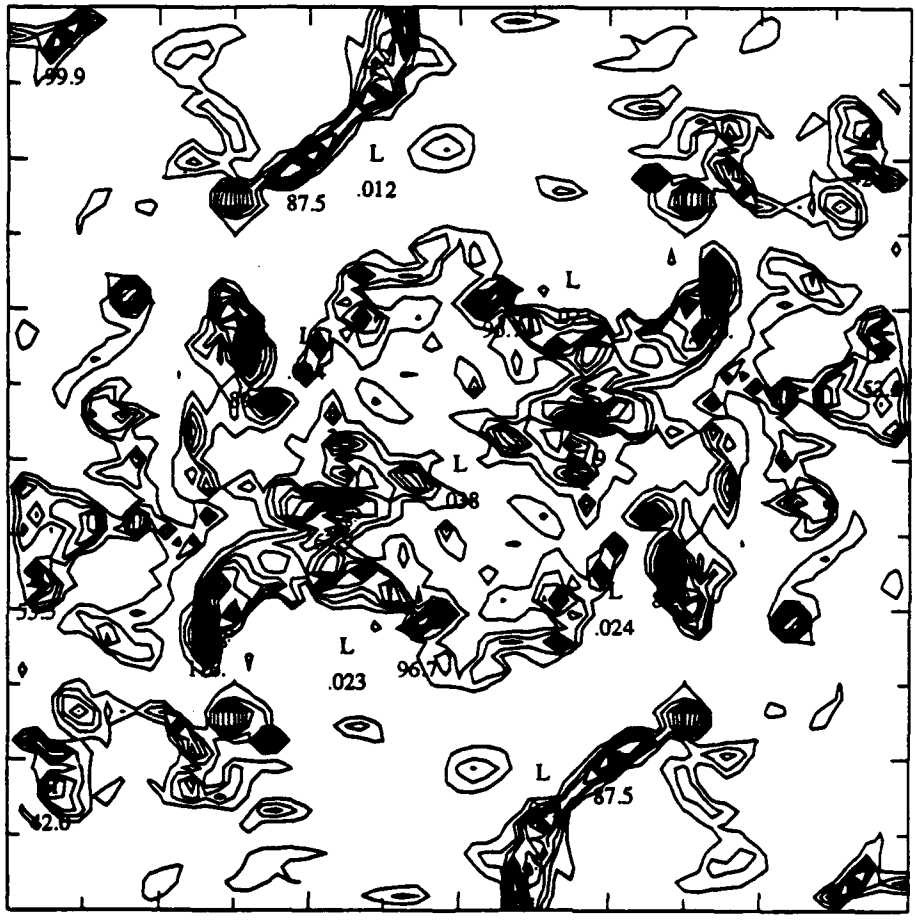

z from 0 to π

x from 0 to π

CONTOUR FROM 0.000000E+00 TO 113.00 CONTOUR INTERVAL OF 7.0000 FF(3,3)= 3.2000

Fig. 3(a)

ω^2 OF LOW WAVE NUMBER

ISO-CONTOURS IN X-Z PLANE AT JCUT = 193

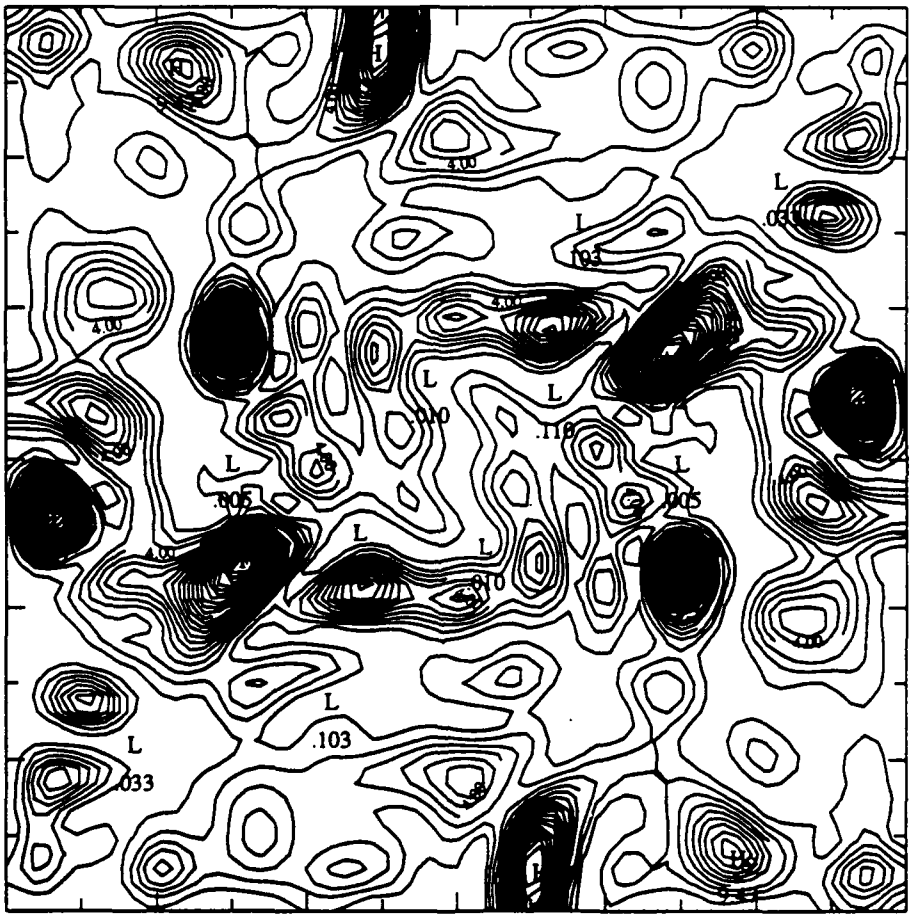

z from 0 to π

x from 0 to π

CONTOUR FROM 0.000000E+00 TO 25.600 CONTOUR INTERVAL OF 1.0000 FT(3,3)= 2.0510

Fig. 9(b)

DISSIPATION OF WHOLE WAVE NUMBER
ISO-CONTOURS IN X-Z PLANE AT JCUT = 193

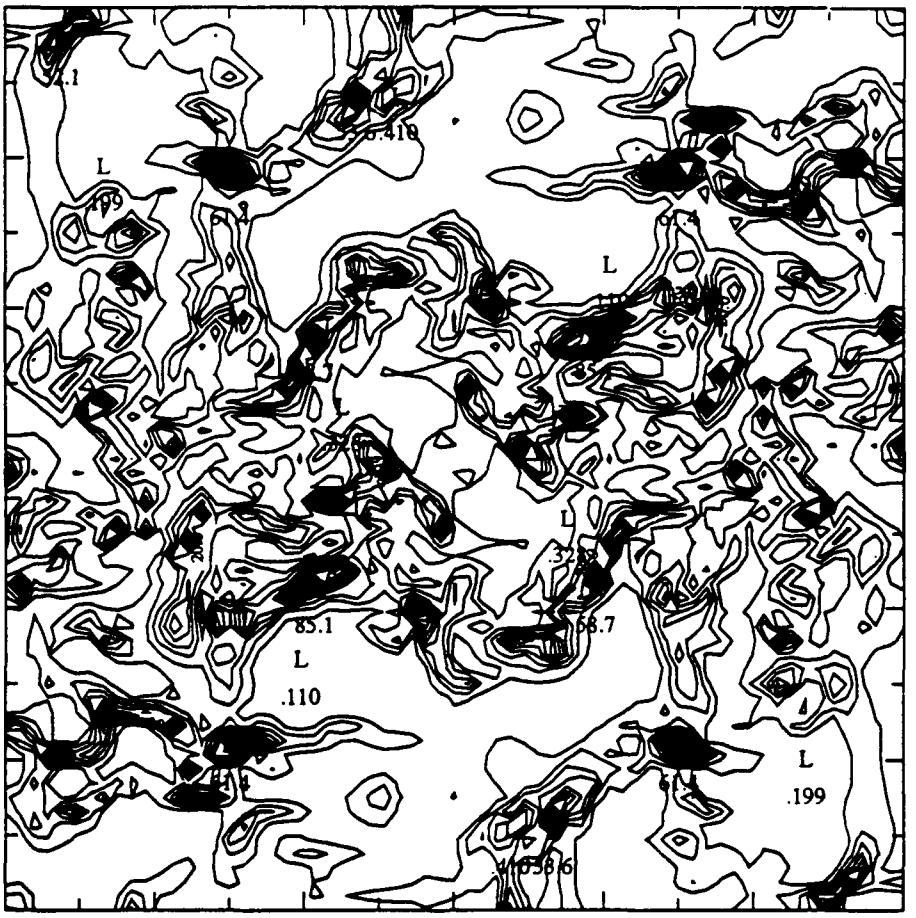

z from 0 to π

x from 0 to π

CONTOUR FROM 0.000000E+00 TO 15.600 CONTOUR INTERVAL OF 1.0000 FT(3,3)= 4.1250

Fig. 10 (a)

DISSIPATION OF LOW WAVE NUMBER
ISO-CONTOURS IN X-Z PLANE AT JCUT = 193

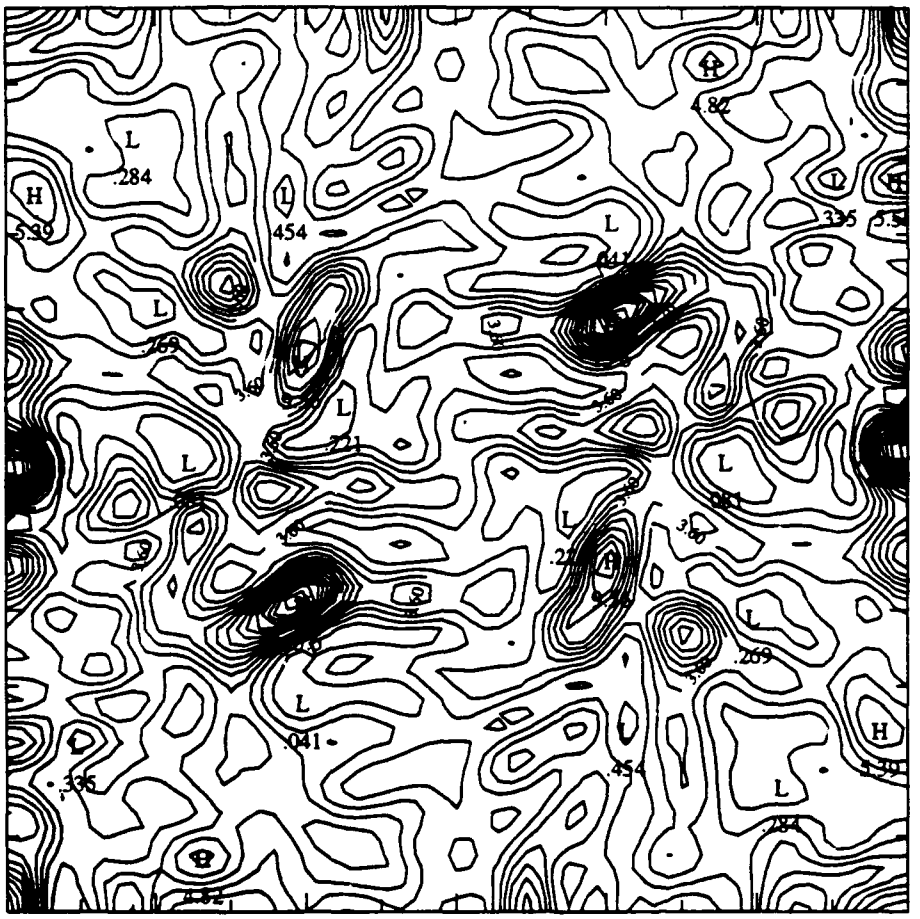

CONTOUR FROM [illegible] TO 1.300 CONTOUR INTERVAL OF [illegible] PT(3.3)= 3.8730

Fig. 10(b)

SUBGRID SCALE

ISO-CONTOURS IN X-Z PLANE AT JCUT = 193

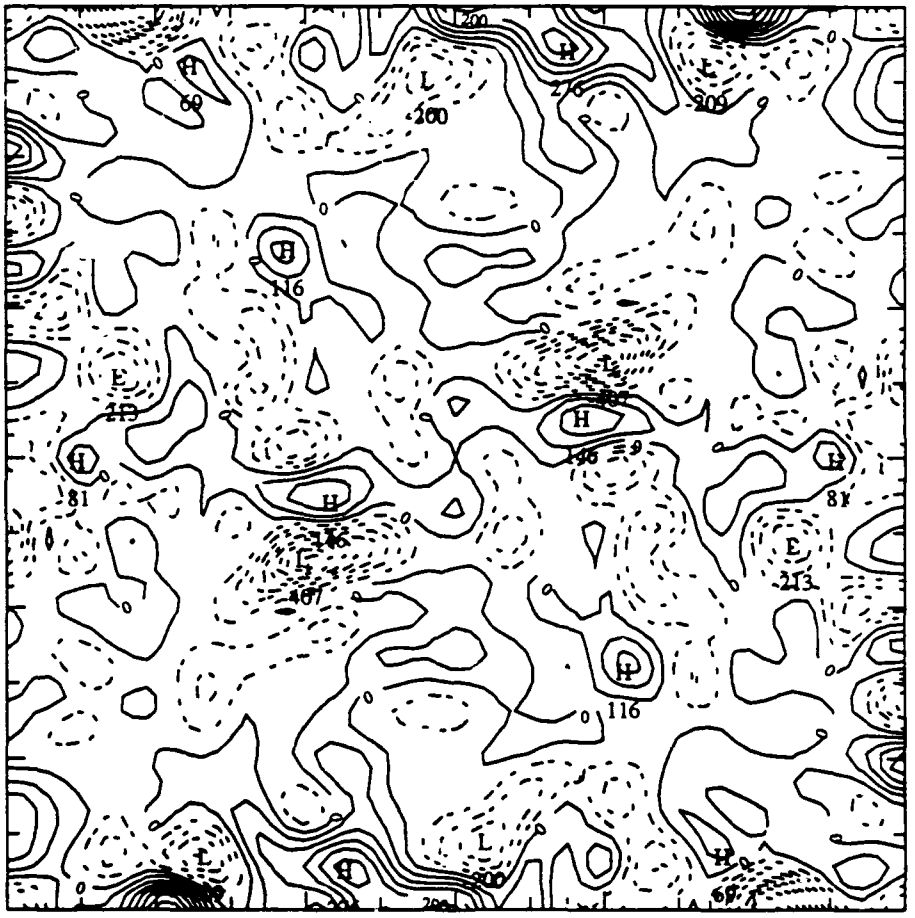

CONTOUR FROM -0.XXXXE-01 TO 0.XXXXE-01 CONTOUR INTERVAL OF 0.XXXXE-02 FT(3.3)= -0.XXX MIN=XX LABELS SCALED BY XXXX

Fig. 11

LARGE SCALE

ISO-CONTOURS IN X-Z PLANE AT JCUT = 1

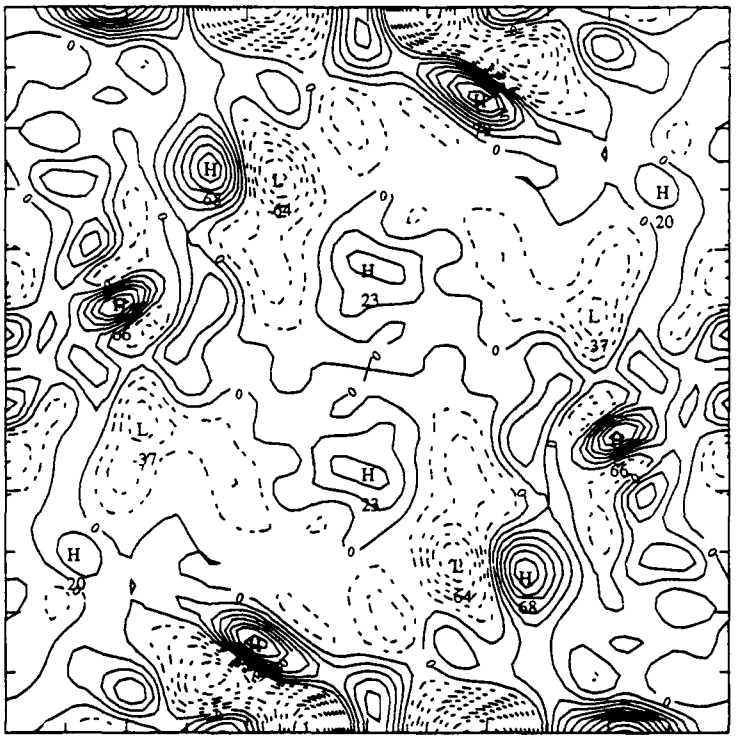

CONTOUR FROM 0.0000 TO 0.0000 CONTOUR INTERVAL OF 0.0000E+00 IS 0.0% OF 0.0000E+00 LABELS SCALED BY 0.0e0

Fig. 12(a)

T OF ALL WAVE NUMBER

ISO-CONTOURS IN X-Z PLANE AT JCUT = 1

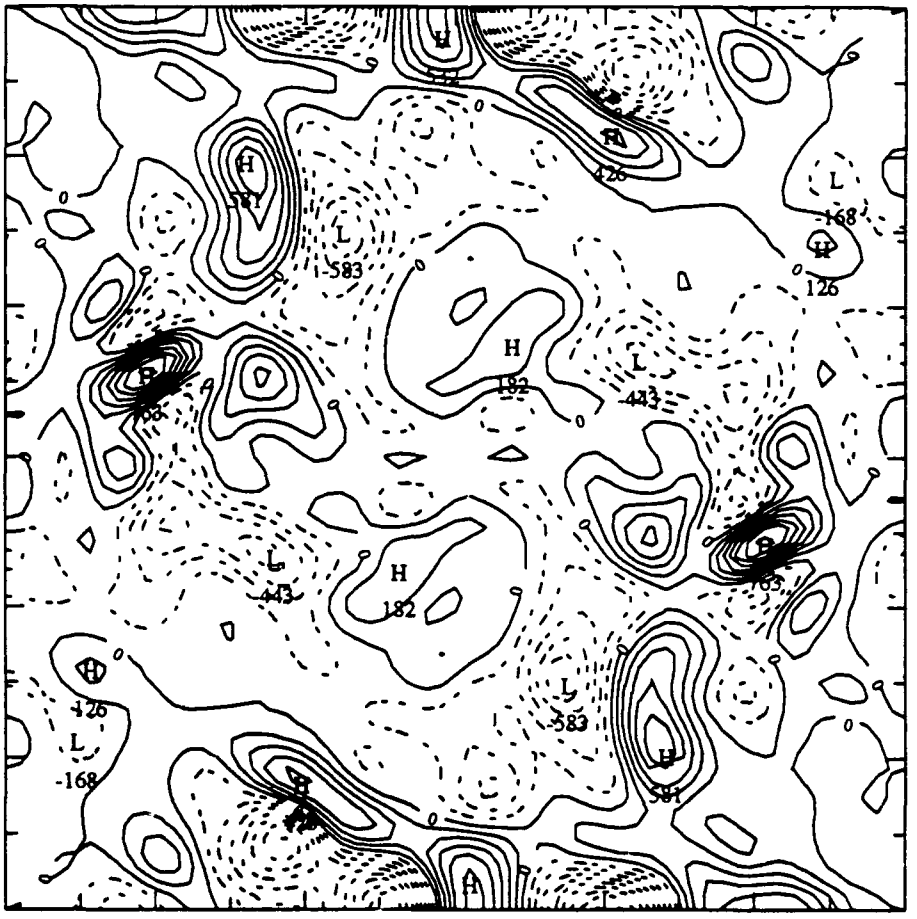

CONTOUR FROM -6.[illegible] TO 6.[illegible] CONTOUR INTERVAL OF 6.[illegible] F(1,1)= -6.[illegible] LABELS SCALED BY [illegible]

Fig. 12(b)

Subgrid-scale energy transfer and large scales of motion in isotropic turbulence

by J. Andrzej Domaradzki

Department of Aerospace Engineering, University of Southern California,

Los Angeles, CA 90089-1191, U.S.A.,

tel. 213-740-5357, FAX 213-740-7774

and

Robert M. Kerr

Geophysical Turbulence Program

National Center for Atmospheric Research

Boulder, CO 80307-3000, U.S.A.

tel. 303-497-8991

September 14, 1992

First Draft

To be submitted to *The Physics of Fluids*

PACS 47.25.Cg

Abstract

Using results of direct numerical simulations of isotropic turbulence the subgrid-scale energy transfer in the physical space is calculated exactly employing a spectral decomposition of the velocity field into large and small scales. Both the forward and the inverse subgrid-scale transfer components are found to be significant. The spatial structure of the exact subgrid-scale transfer is qualitatively compared with the spatial structure of a number of physical quantities which are considered to govern the dynamics of the large scales of turbulence. We find that all quantities determined by the first derivatives of the velocity field correlate poorly with the transfer which is largest at the peripheries of regions characterized by large values of these quantities. The spatial structure of the transfer correlates much better with the large scale energy and the Smagorinsky's subgrid-scale energy transfer which is determined by the second derivatives of the velocity field. None of the considered quantities is capable of predicting sign of the subgrid-scale transfer.

1 Introduction

It is generally recognized that in the forseeable future numerical predictions of turbulent flows at high Reynolds numbers will have to rely on models accounting for the effects of nonlinear interactions between resolved (large) and unresolved (small) scales of motion. Commonly used models, either for Reynolds averaged Navier-Stokes (RANS) equations or for large eddy simulations (LES), are known to be deficient in many respects and the improvements in the models will be difficult to achieve in the absence of underlying, generally accepted theory of turbulence. This gives impetus to fundamental investigations of nonlinear interactions in turbulent flows which may eventually provide better models. In such investigations [1,2,3] the nonlinear interactions between prescribed scales of motion are analyzed using accurately resolved velocity fields obtained in direct numerical simulations. In the context of large eddy simulations a class of subgrid-scale nonlinear interactions is of prime importance. Clark *et al.* [4] pioneered use of exactly computed subgrid-scale interactions to assess phenomenological subgrid-scale eddy viscosity models in the physical space representation. Later, Domaradzki *et al.* [5] applied similar methodology to compare the exactly computed spectral subgrid-scale eddy viscosity with eddy viscosities predicted by the analytical theories of turbulence. More recently Domaradzki *et al.* [6] used the same approach in investigating the inverse subgrid-scale energy transfer in both spectral and physical space representation and the degree of localness of the subgrid-scale transfer.

Apart from the usefulness of this approach in assessing existing subgrid-scale models we believe that it may also be very useful in investigation of coherent structures. Indeed, despite years of research devoted to coherent structures in turbulent flows controversies persist as to their dy-

namical significance in evolution of turbulence with the resulting lack of progress in developing turbulence models that would explicitly include information about coherent structures. Since the nonlinear energy transfer is a principal physical process influencing the evolution of turbulent fields the dynamical significance of the coherent structures may be established if it is shown that they are associated with significant transfer. More generally, one may argue that the existence of a noticable correlation between a given physical quantity and the transfer implies the dynamical significance of this quantity. Along these lines Domaradzki *et al.* [6] investigated qualitative correlations between subgrid-scale energy transfer and the energy, vorticity, and dissipation fields for the symmetric Taylor-Green vortex flow.

In this paper the same approach is used to investigate the subgrid-scale energy transfer in regular, non-symmetric flows, and its spatial correlations with several physical quantities which customarily are considered as being dynamically important in turbulent flows.

2 Numerical simulations

Description of field A - 128^3.

Description of field B - 256^3.

3 Basic quantities

Details of calculations of the subgrid-scale interactions from the results of direct numerical simulations of isotropic turbulence are described by Domaradzki *et al.* [6]. Here we quote only the main formulas. For homogeneous turbulence incompressible Navier-Stokes equations in spectral (Fourier) representation are:

$$\frac{\partial}{\partial t}u_n(\mathbf{k}) = -\nu k^2 u_n(\mathbf{k}) + N_n(\mathbf{k}). \tag{1}$$

Here, $u_n(\mathbf{k})$ is the velocity field in spectral space, with the explicit dependence on time omitted, ν is the kinematic viscosity, and $N_n(\mathbf{k})$ is the nonlinear term

$$N_n(\mathbf{k}) = -\frac{i}{2}P_{nlm}(\mathbf{k})\int d^3p u_l(\mathbf{p})u_m(\mathbf{k}-\mathbf{p})\ , \tag{2}$$

where tensor $P_{nlm}(\mathbf{k})$ accounts for the pressure and incompressibility effects. The summation convention is assumed throughout.

The wave number space is divided into two non-overlapping regions, $\mathcal{L}$ ($|\mathbf{k}| \leq k_c$) signifying large, resolved scales, and $\mathcal{S}$ ($|\mathbf{k}| > k_c$) signifying small, unresolved scales. An evolution equation for the resolved scales i.e. the velocity field $u_n(\mathbf{k})$ truncated to the region $\mathcal{L}$

$$u_n^{\mathcal{L}}(\mathbf{k}) = \begin{cases} u_n(\mathbf{k}) & \text{if } \mathbf{k}\epsilon\mathcal{L} \\ 0 & \text{otherwise} \end{cases} \tag{3}$$

is:

$$\frac{\partial}{\partial t}u_n{}^{\mathcal{L}}(\mathbf{k}) = -\nu k^2 u_n{}^{\mathcal{L}}(\mathbf{k}) + N_n(\mathbf{k}|k_c) + N_n{}^{s}(\mathbf{k}|k_c), \tag{4}$$

where $N_n(\mathbf{k}|k_c)$ is the resolved nonlinear term and $N_n{}^{s}(\mathbf{k}|k_c)$ is the subgrid-scale nonlinear term. These terms are computed as follows. First, Eq. (2) is used with the full (untruncated) velocity fields $u_l(\mathbf{p})$ and $u_m(\mathbf{k}-\mathbf{p})$ and the result is truncated to the region $\mathcal{L}$ to obtain the total nonlinear term

$$N_n{}^{tot}(\mathbf{k}|k_c) = N_n(\mathbf{k}|k_c) + N_n{}^s(\mathbf{k}|k_c) \tag{5}$$

Next, Eq. (2) is used again with the truncated velocity fields $u_l^{\mathcal{L}}(\mathbf{p})$ and $u_m^{\mathcal{L}}(\mathbf{k}-\mathbf{p})$ and the result is truncated to the region $\mathcal{L}$ giving the resolved nonlinear term $N_n(\mathbf{k}|k_c)$. The subgrid-scale nonlinear term is obtained as the difference between the total nonlinear term (5) and the resolved nonlinear term.

The above described procedure has its exact counterpart in the physical space representation. Inverse Fourier transform, signified by tilde, of $N_n(\mathbf{k})$ (Eq. (2)) is the sum of the convective and pressure terms in the Navier-Stokes equation in the physical space coordinates

$$\tilde{N}_n(\mathbf{x}) = -\tilde{u}_i(\mathbf{x})\frac{\partial \tilde{u}_n(\mathbf{x})}{\partial x_i} - \frac{\partial p(\mathbf{x})}{\partial x_n}. \tag{6}$$

Similarly, the inverse Fourier transform of (4) is

$$\frac{\partial}{\partial t}\tilde{u}_n^{\mathcal{L}}(\mathbf{x}) = \nu\nabla^2\tilde{u}_n^{\mathcal{L}}(\mathbf{x}) + \tilde{N}_n(\mathbf{x}|k_c) + \tilde{N}_n^s(\mathbf{x}|k_c), \tag{7}$$

where the resolved nonlinear term $\tilde{N}_n(\mathbf{x}|k_c)$ and the subgrid-scale term $\tilde{N}_n^s(\mathbf{x}|k_c)$ in the physical space are obtained Fourier transforming corresponding expressions in the spectral space. An equation for the rate of change of the turbulent energy of the resolved scales

$$E(\mathbf{x}) = \frac{1}{2}\tilde{u}_n^{\mathcal{L}}(\mathbf{x})\tilde{u}_n^{\mathcal{L}}(\mathbf{x}) \tag{8}$$

is obtained from (7) as

$$\frac{\partial E(\mathbf{x})}{\partial t} = \nu \tilde{u}_n^{\mathcal{L}}(\mathbf{x}) \nabla^2 \tilde{u}_n^{\mathcal{L}}(\mathbf{x}) + \tilde{T}(\mathbf{x}|k_c) + \tilde{T}^s(\mathbf{x}|k_c), \tag{9}$$

where

$$\tilde{T}(\mathbf{x}|k_c) = \tilde{u}_n^{\mathcal{L}}(\mathbf{x}) \tilde{N}_n(\mathbf{x}|k_c), \tag{10}$$

is the resolved energy transfer and

$$\tilde{T}^s(\mathbf{x}|k_c) = \tilde{u}_n^{\mathcal{L}}(\mathbf{x}) \tilde{N}_n^s(\mathbf{x}|k_c) \tag{11}$$

is the subgrid-scale energy transfer in the physical space representation.

The goal of the subgrid-scale modeling is to obtain as good as possible an approximation to the subgrid-scale nonlinear term $\tilde{N}_n^s(\mathbf{x}|k_c)$ using only information available in the resolved scales. Thus on the level of the energy equation we are interested in relations between observed subgrid-scale energy transfer (11) and various physical quantities computed for the resolved velocity field (3). In addition to the large scale energy (8) the following large scale quantities have also been considered: enstrophy, dissipation, vorticity production, enstrophy production, pressure, the second invariant, and Smagorinsky's subgrid-scale energy transfer. These quantities are defined as follows. The enstrophy is

$$O(\mathbf{x}) = \frac{1}{2} \Omega_i(\mathbf{x}) \Omega_i(\mathbf{x}) \,, \tag{12}$$

where Ω_i is the large scale vorticity. Introducing the large scale rate-of-strain tensor

$$S_{ij} = \frac{1}{2}(\partial u_i^{\mathcal{L}}/\partial x_j + \partial u_j^{\mathcal{L}}/\partial x_i) \tag{13}$$

and the large scale rotation tensor

$$R_{ij} = \frac{1}{2}(\partial u_i^{\mathcal{L}}/\partial x_j - \partial u_j^{\mathcal{L}}/\partial x_i), \tag{14}$$

we define dissipation

$$D(\mathbf{x}) = \frac{1}{2}\nu S_{ij}(\mathbf{x})S_{ij}(\mathbf{x}), \tag{15}$$

the square of the vorticity production (i.e. the square of the vortex stretching term in the vorticity equation)

$$P(\mathbf{x}) = \Omega_i(\mathbf{x})S_{ij}(\mathbf{x})S_{jk}(\mathbf{x})\Omega_k(\mathbf{x})\,, \tag{16}$$

enstrophy production

$$V(\mathbf{x}) = \Omega_i(\mathbf{x})S_{ij}(\mathbf{x})\Omega_j(\mathbf{x})\,, \tag{17}$$

the second invariant of the large scale velocity gradient tensor

$$R(\mathbf{x}) = \frac{1}{2}\left[R_{ij}R_{ij} - S_{ij}S_{ij}\right], \tag{18}$$

and the quantity proportional to the subgrid-scale energy transfer predicted by the Smagorinsky's model [12]

$$S(\mathbf{x}) = u_i^{\mathcal{L}}(\mathbf{x}) \frac{\partial}{\partial x_j} \left[(S_{ij} S_{ij})^{1/2} S_{ij} \right] . \tag{19}$$

4 Results

Structures in isotropic turbulence are often identified as regions of concentrated vorticity. Visualizations of numerically simulated isotropic turbulence [7,8,9,10] show existence of vortex tubes and vortex sheets in such flows with vortex tubes being predominant. In Fig. 1 we plot isocontours of enstrophy for the field A [vorticity level is ?]. The vorticity indeed forms elongated, tube-like structures, in accordance with other simulations of isotropic turbulence. In Figs. 2(a) and 2(b) we plot cross-sections through this enstrophy field taken in horizontal planes at distances from the lower plane equal to a quarter and a half of the periodicity length, respectively. In Fig. 2(a) two regions of intense vorticity are clearly visible. The elongated region in the lower left corner results from the cut of the vortex tube along its horizontally oriented axis and the more circular region to the right results from the cut of the vortex tube with its axis inclined with respect to the horizontal plane. In Fig. 2(b) several regions with large vorticity values have generally oval shapes and, after comparison with Fig. 1 is made, appear to result from cutting vortex tubes with axes in the directions not far from normal to the cutting plane.

In Figs. 3(a) and 3(b) we plot subgrid-scale energy transfer (11) in horizontal planes at the same locations as used in plotting the enstrophy. An important observation is that the calculated subgrid-scale transfer contains regions of large forward transfer (broken line contours) and regions of inverse transfer of comparable magnitude (solid line contours). This observation is consistent with results of Piomelli *et al.* [11] for turbulent channel flow and results of Domaradzki *et al.* [6] for the turbulent

Taylor-Green vortex flow. The presence of significant inverse transfer is in direct contradiction to the implicit assumptions made in turbulence models that the subgrid-scale interactions are of purely dissipative character i.e. transferring energy always in one direction, from the large to the small scales.

In this work we are mainly interested in how regions of the large transfer are located with respect to regions characterized by by large values of the other physical quantities. In order to investigate such spatial correlations between the computed subgrid-scale energy transfer and the dynamics of large scales we plot transfer superimposed on contour plots of the previously defined functions of the large scale velocity field. No attempt was made to make point-wise comparison between the exact values for the plotted quantities nor the point-wise correlation coefficient was computed. Our analysis is qualitative but in view of the complexity of the analyzed fields is necessary to establish guidelines for more quantitative analysis which should be attempted later. For instance, the presence of both positive and negative values for the computed transfer may imply negligible correlation coefficient between the transfer and a purely positive quantity, even though both may have a very similar spatial structure. The correlation coefficient will also be small if one quantity is concentrated in the vicinity of the other but not on top of it. Yet such relation may imply that both quantities are dynamically correlated even though the pointwise correlation coefficient is small. Therefore it appears that the qualitative analysis reported here is a reasonable first step in establishing approximate correlations between various fields and in suggesting directions for a more quantitative analysis.

In Fig. 4 large values of enstrophy (12) are usually accompanied by large positive/negative values of the subgrid-scale transfer but there is only partial overlap between these quantities. It

appears that maxima of both fields are shifted with respect to each other such that regions of large transfer are located on the edges of high enstrophy regions. Even though transfer seems to be associated with enstrophy the reverse is not necessarily true i.e. the regions of high transfer may be present without any significant enstrophy in their vicinity.

Higher degree of correlation is observed in Fig. 5 between the subgrid-scale transfer and the large scale energy (8). In this case the regions of the most intense subgrid-scale transfer lie almost directly on top of high energy regions. This is particularly clearly illustrated in Fig. 5(b) where a sequence of the subgrid-scale regions of alternating signs forms a pattern overlapping with the pattern formed by the large scale energy. The observed correlation is puzzling since it is expected that the energy transfer process is associated with gradients of the velocity field, not with the velocity field itself. This correlation may be explained if a significant fraction of the observed subgrid transfer in the physical space is a result of an advection of the small scales by the large ones. Even though such a process does not contribute to the change in the energy of the large scales integrated over entire domain, it affects their energy locally in the physical space and constitutes a legitimate part of the transfer in the physical space according to the definition (11). Obviously, such a process will be most pronounced at the locations where the advective velocity is large and these locations coincide with the regions of high large scale energy.

In Fig. 6 the subgrid-scale transfer is overlayed on the large scale dissipation field (15). As in the case of correlations with the enstrophy, the regions of the large transfer are generally found on peripheries of the regions with large dissipation. This is perhaps not surprising since both the enstrophy and the dissipation are determined by the strength of the velocity gradients. However, it should also be noted that the regions of the large enstrophy and the large dissipation are not in

the same locations, with the dissipation largest in the regions of small enstrophy values, and vice versa.

The vorticity and the enstrophy production terms, (16) and (17), respectively, were found to be fairly well correlated with the enstrophy field. This in turn implies that the subgrid-scale transfer will be largest at the peripheries of the regions with large values of these quantities, similarly to the case of the enstrophy. Plots of the transfer superimposed on the contour plots of the vorticity and the enstrophy production terms are shown in Figs. 7 and 8, respectively, and confirm this supposition. Finally, in Fig. 9 the comparison is made between the subgrid-scale transfer and the second invariant for a higher resolutions field, run B. Again, we find that the correlations between both fields is such that the most intense transfer is located around the edges of regions with significant values of the second invariant.

With the exception of the energy, all the above quantities are various combinations of the first order velocity derivatives. All these combinations correlate poorly with the computed subgrid-scale energy transfer in a sense that large values of these quantities are found in different spatial locations than large positive/negative values of the transfer. However, the transfer is usually most intense in the regions located on peripheries of the regions characterized by large values of these quantities. It may be expected that at these locations gradients of the above analyzed quantities will be large. It suggests that correlations between the subgrid-scale energy transfer and quantities involving second order derivatives of the velocity field may be better than for quantities based on the first derivatives. One possible quantity of this kind, which is of interest in the context of this work, is the classical expression of Smagorinsky [12] for the subgrid-scale energy transfer. In Fig. 10 we plot this quantity superimposed on the exact subgrid-scale energy transfer. The Smagorinsky's

model captures locations of the most intense transfer much better than the other investigated quantities, with the exception of the energy. The obvious drawback of this model is that it has a purely dissipative character predicting the energy transfer always from the large to the small scales whereas the exact transfer contains regions of the forward as well as inverse transfer, both being significant.

5 Conclusions

ACKNOWLEDGMENTS

One of the authors (JAD) was supported by the AFOSR Contract No. 90-0300.

[1]J.A. Domaradzki and R.S. Rogallo, "Local energy transfer and nonlocal interactions in homogeneous, isotropic turbulence", Phys. Fluids A **2**, 413 (1990).

[2]P.K. Yeung and J.G. Brasseur, "The response of isotropic turbulence to isotropic and anisotropic forcing at the large scales", Phys. Fluids A**3**, 413 (1991).

[3]K. Ohkitani and S. Kida, "Triad interactions in a forced turbulence", Phys. Fluids A **4**, 794 (1992).

[4]R.A. Clark, J.H. Ferziger, and W.C. Reynolds, "Evaluation of subgrid-scale models using an accurately simulated turbulent flow", J. Fluid Mech. **91**, 1 (1979).

[5]J.A. Domaradzki, R.W. Metcalfe, R.S. Rogallo, and J.J. Riley, "Analysis of subgrid-scale eddy viscosity with use of results from direct numerical simulations", Phys. Rev. Lett. **58**, 547 (1987).

[6]J.A. Domaradzki, W. Liu, and M.E. Brachet,"An analysis of subgrid-scale interactions in numerically simulated turbulence", submitted to Phys. Fluids (1992).

[7]E.D. Siggia, "Numerical study of small scale intermittency in three-dimensional turbulence", J. Fluid Mech. **107**, 385 (1981).

[8]R.M. Kerr, "Higher-order derivative correlations and the alignment of small-scale structures in isotropic turbulence", J. Fluid Mech. **153**, 31 (1985).

[9]Z.S. She, E. Jackson, and S.A. Orszag, Nature **344**, 226 (1990).

[10]A. Vincent and M. Meneguzzi, "The spatial structure and statistical properties of homogeneous turbulence", J. Fluid Mech. **225**, 1 (1991).

[11]U. Piomelli, W.H. Cabot, P. Moin, and S. Lee, Phys. Fluids A**3**, 1766 (1991).

[12]J. Smagorinsky, "General circulation experiments with the primitive equations", Mon. Weath. Rev. **93**, 99 (1963).

Figure Captions

Figure 1. Isosurface plot of the total enstrophy for the velocity field A.

Figure 2. Cut through the enstrophy field in a horizontal plane: (a) located at $z = L/4$; (b) located at $z = L/2$, where L is the periodicity length.

Figure 3. The subgrid-scale energy transfer in a horizontal plane: (a) located at $z = L/4$; (b) located at $z = L/2$, where L is the periodicity length.

Figure 4. The subgrid-scale energy transfer superimposed on the large scale enstrophy in a horizontal plane $z = L/4$.

Figure 5. The subgrid-scale energy transfer superimposed on the large scale energy in a horizontal plane: (a) $z = L/4$; (b) $z = L/2$.

Figure 6. The subgrid-scale energy transfer superimposed on the large scale dissipation in a horizontal plane $z = L/4$.

Figure 7. The subgrid-scale energy transfer superimposed on the large scale vorticity production in a horizontal plane $z = L/4$.

Figure 8. The subgrid-scale energy transfer superimposed on the large scale enstrophy production in a horizontal plane $z = L/4$.

Figure 9. The subgrid-scale energy transfer superimposed on the second invariant of the large scale velocity gradient tensor (the velocity field B).

Figure 10. The exact subgrid-scale energy transfer superimposed on the transfer obtained from the Smagorinsky's eddy-viscosity model in a horizontal plane $z = L/4$.

enstrophy

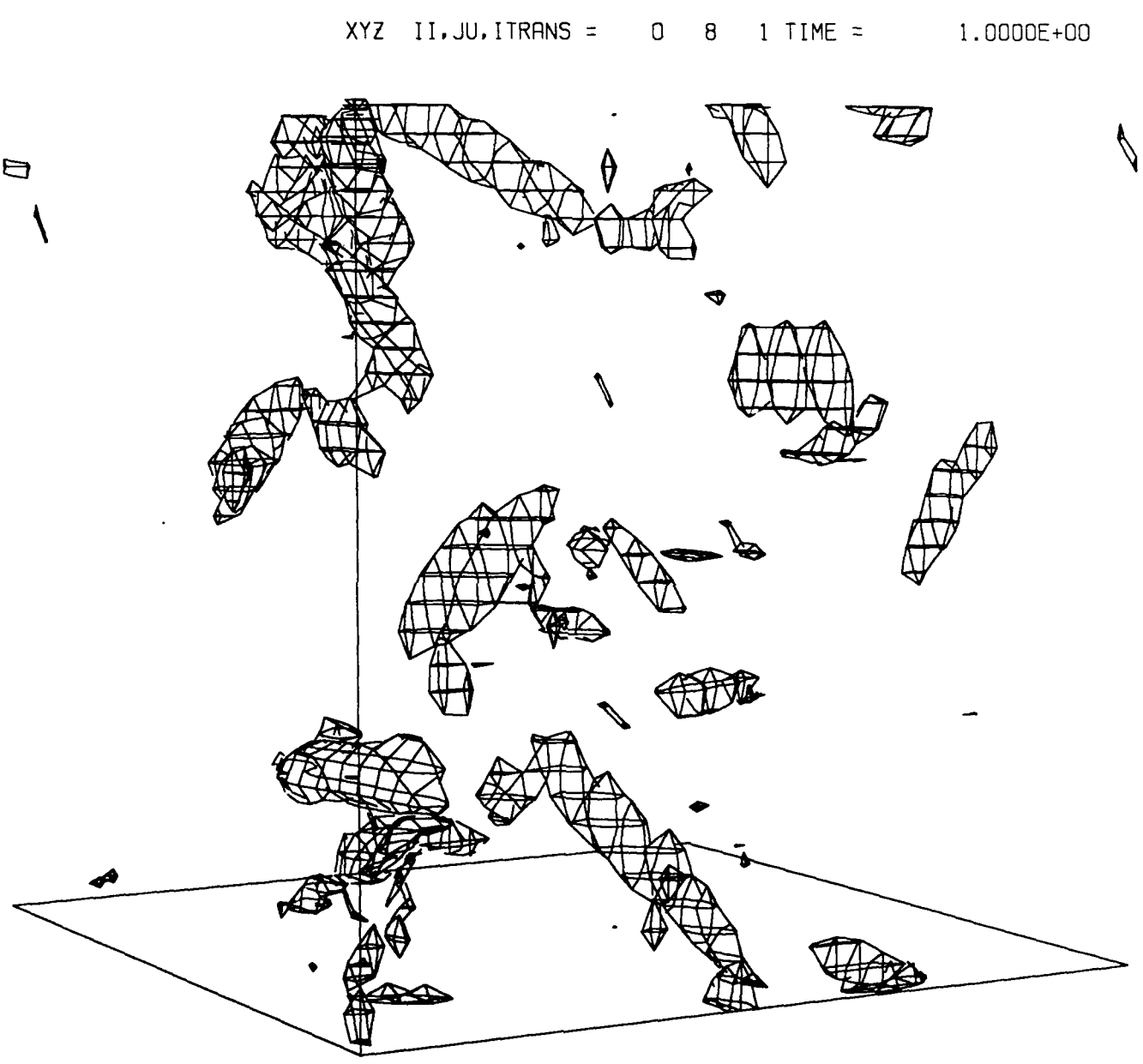

Fig. 1

NU24AG5

entropy

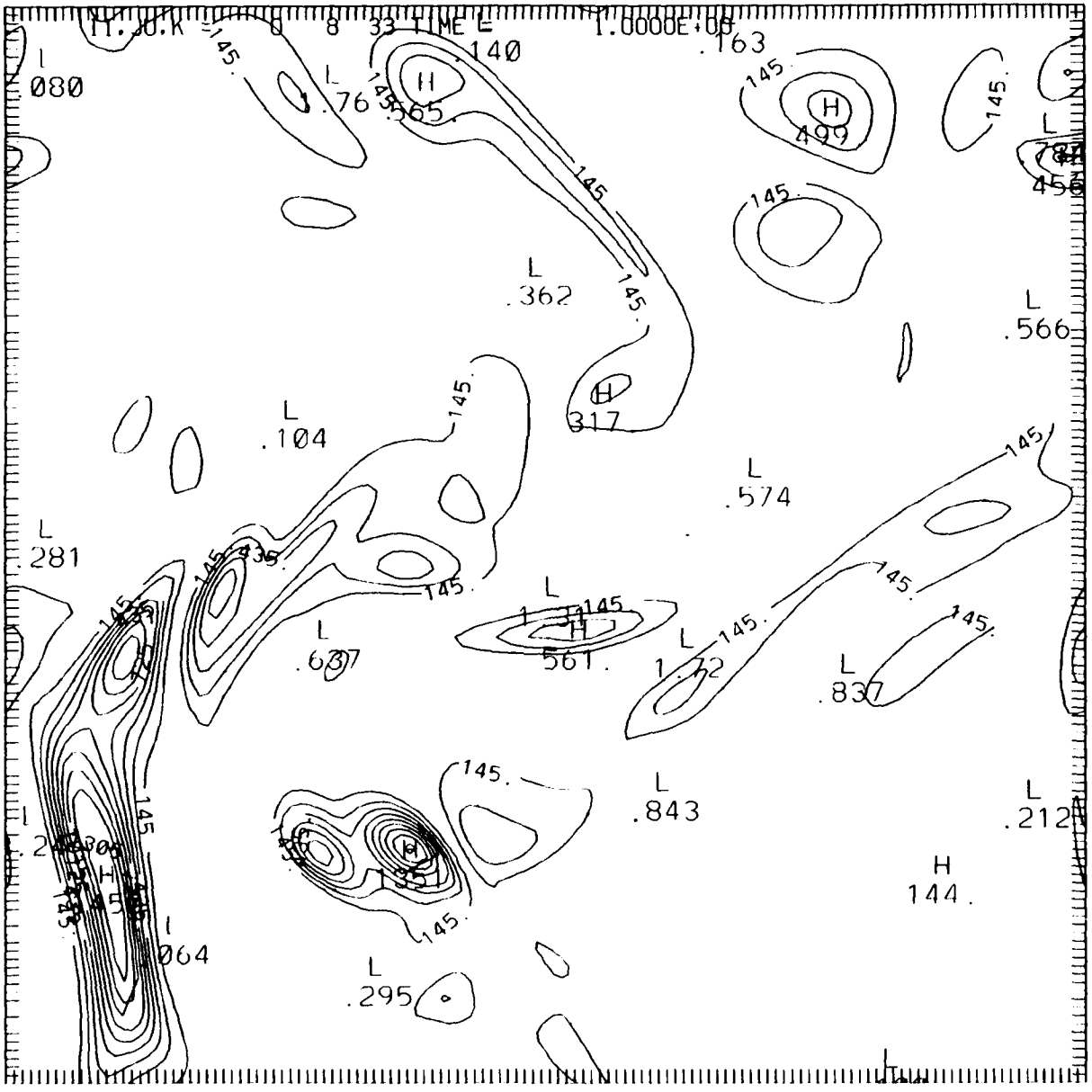

Fig. 2(a)

NU24AG5

enstrophy

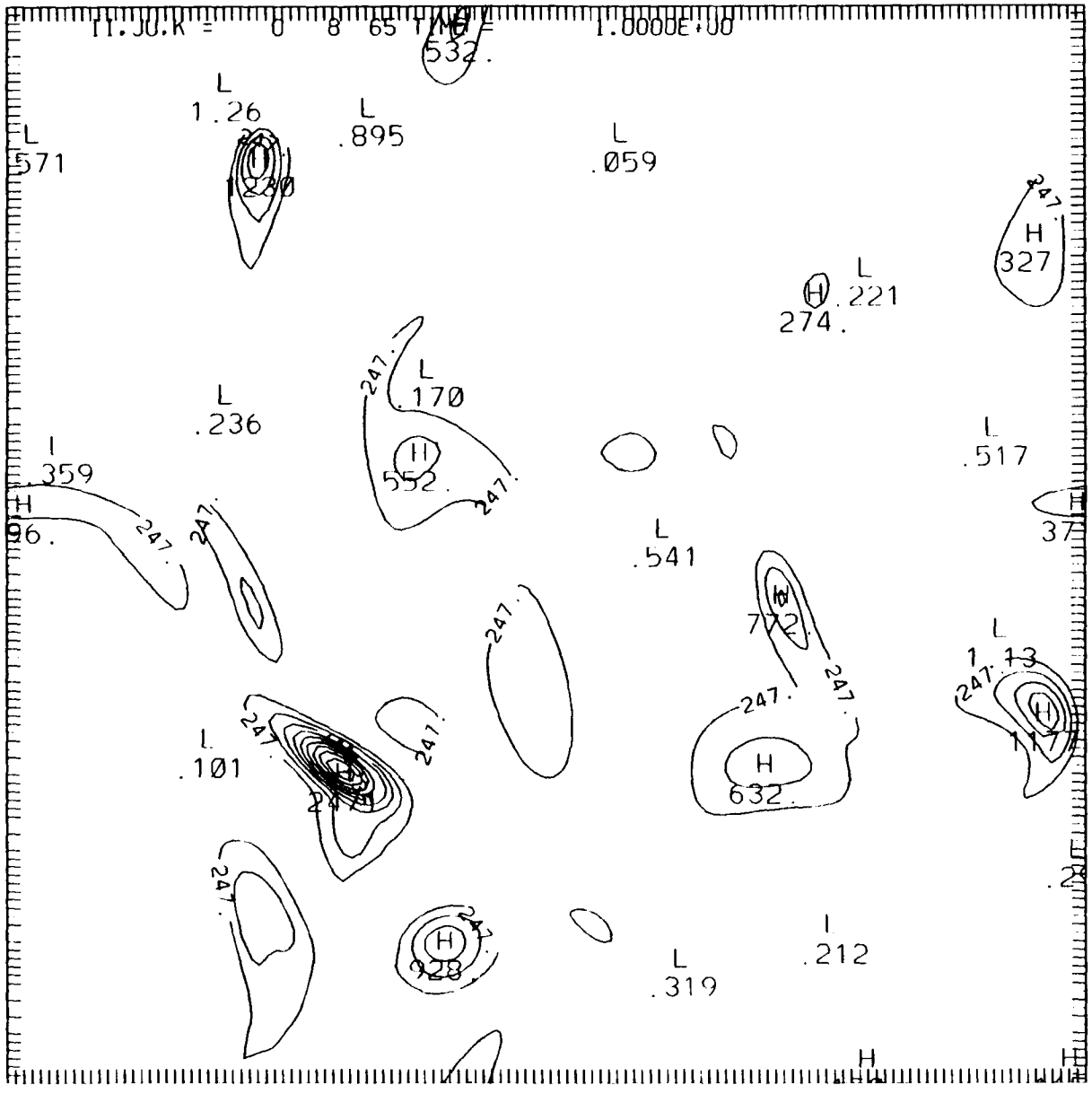

Fig 2.(b)

NU24AF5.PLT

SGS transfer

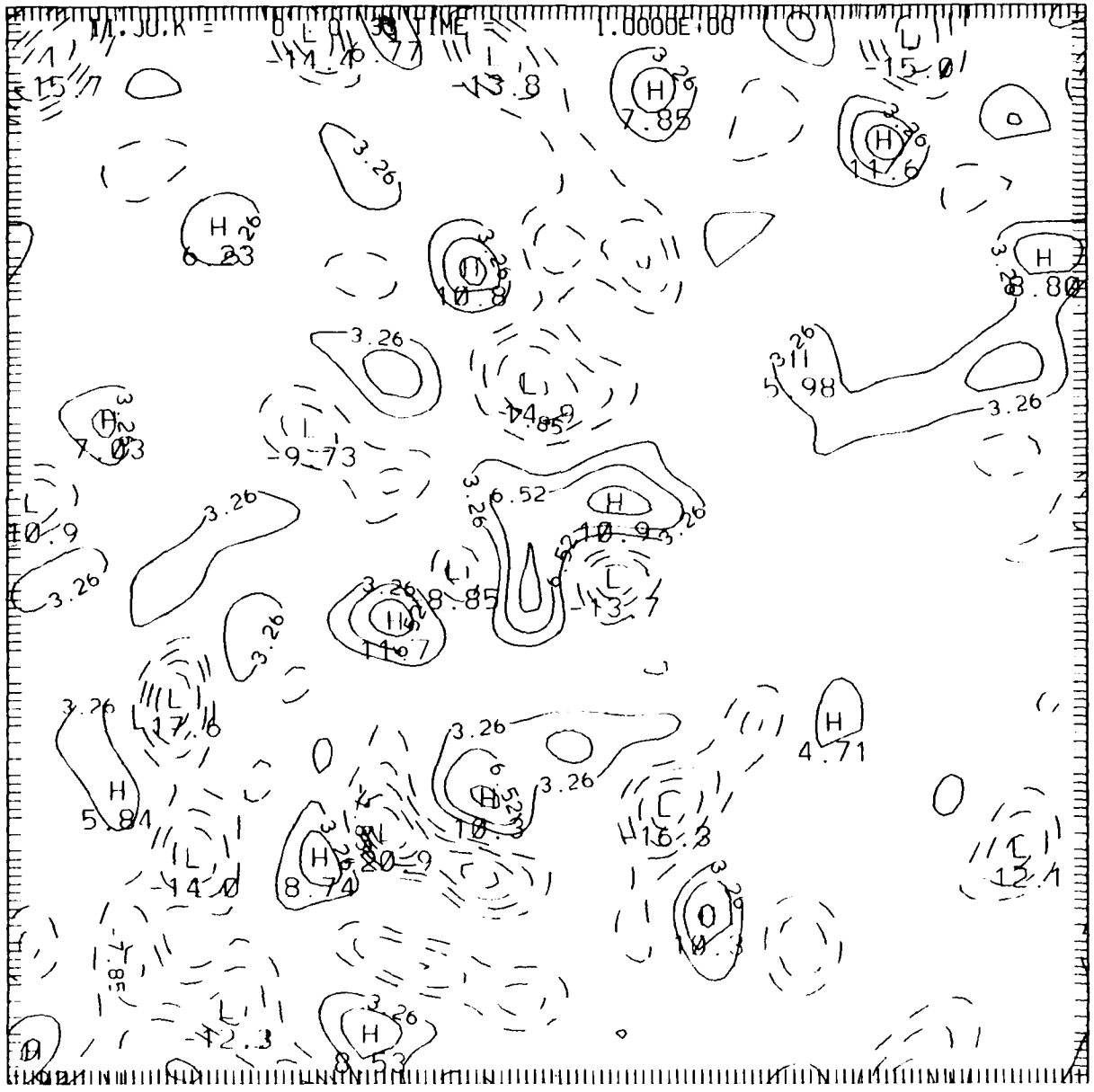

Fig. 3(a)

NU24AF5.PLT

SGS transfer

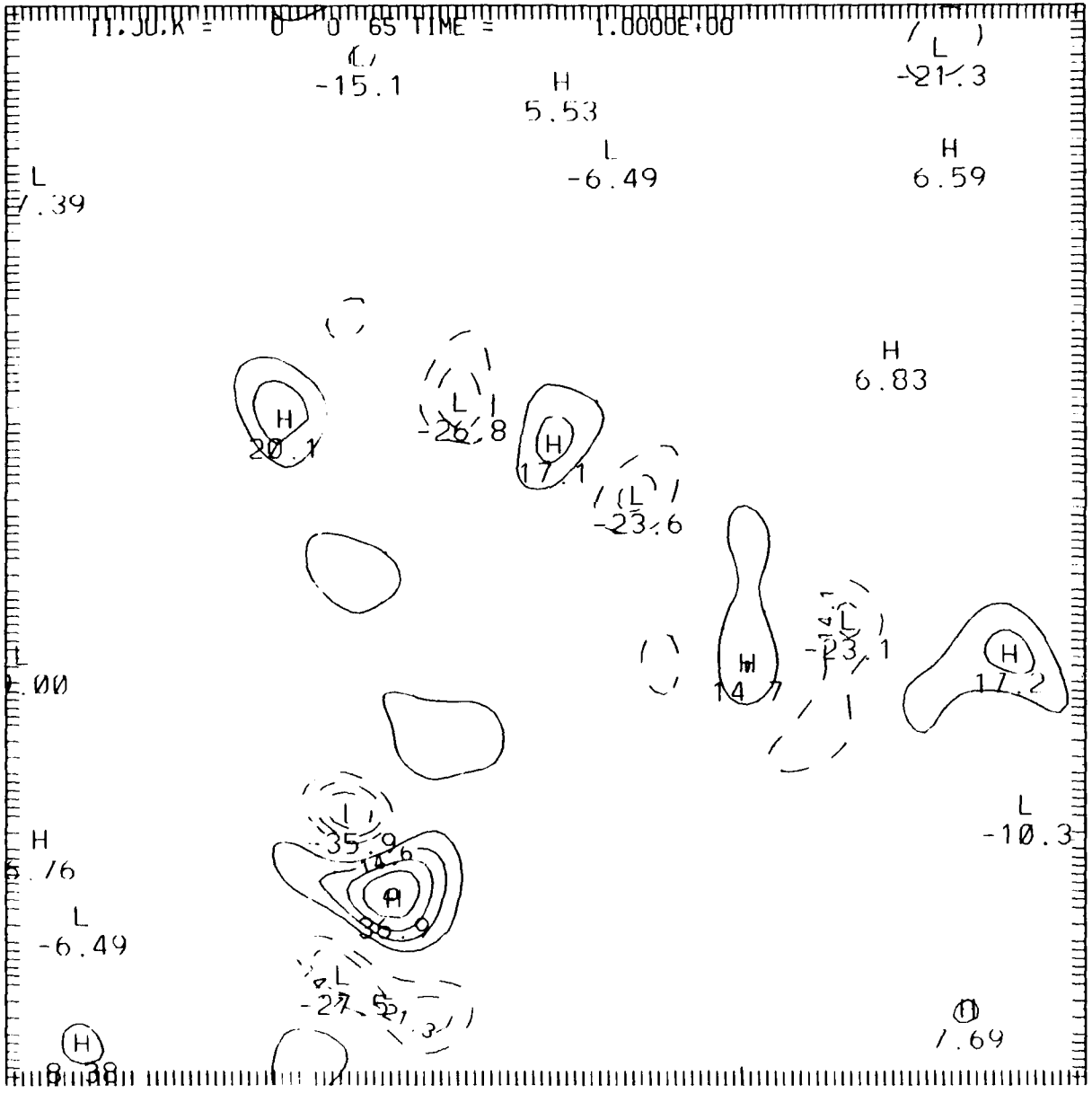

Fig. 3(b)

enstrophy

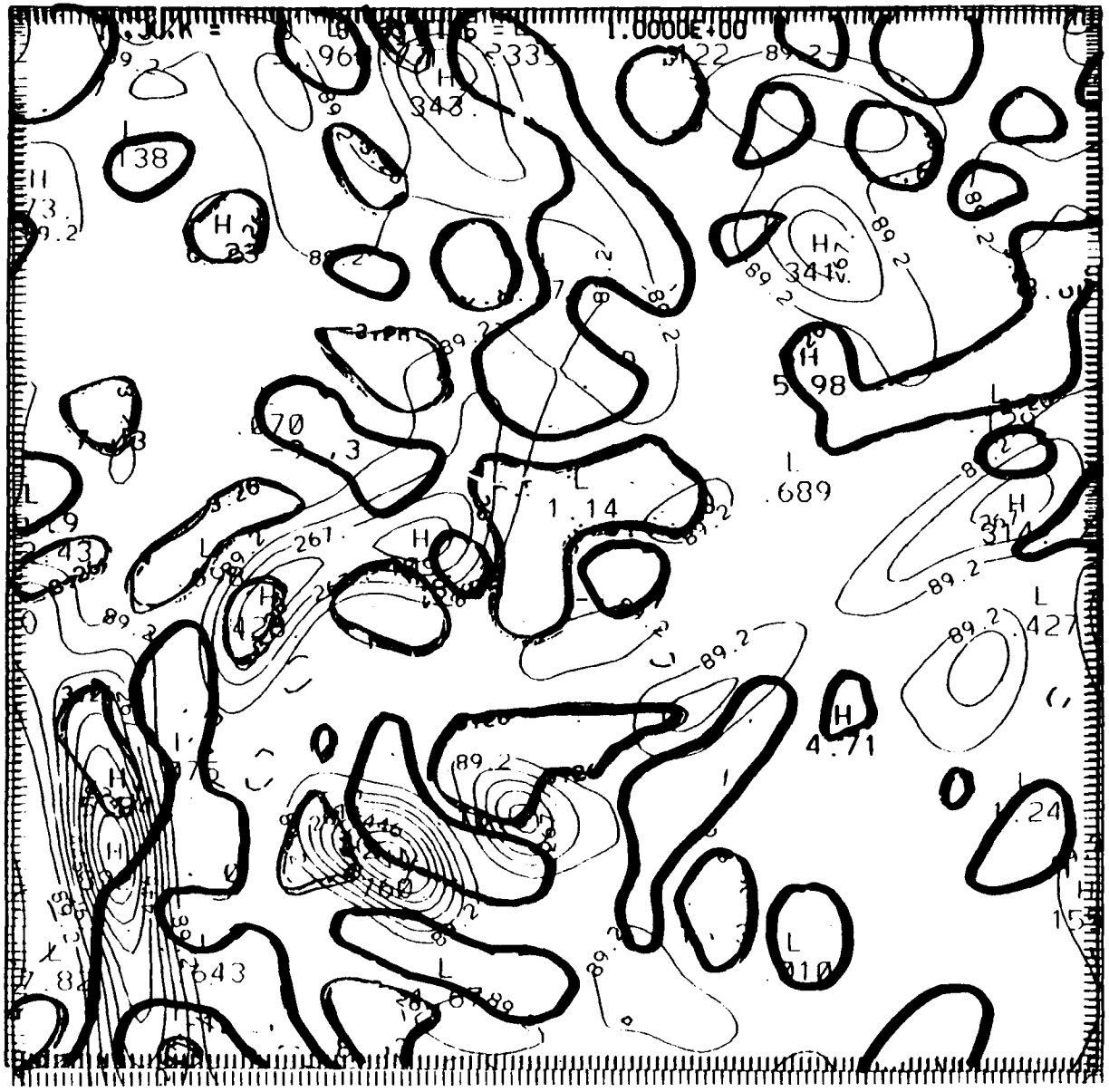

Fig. 4

emergy

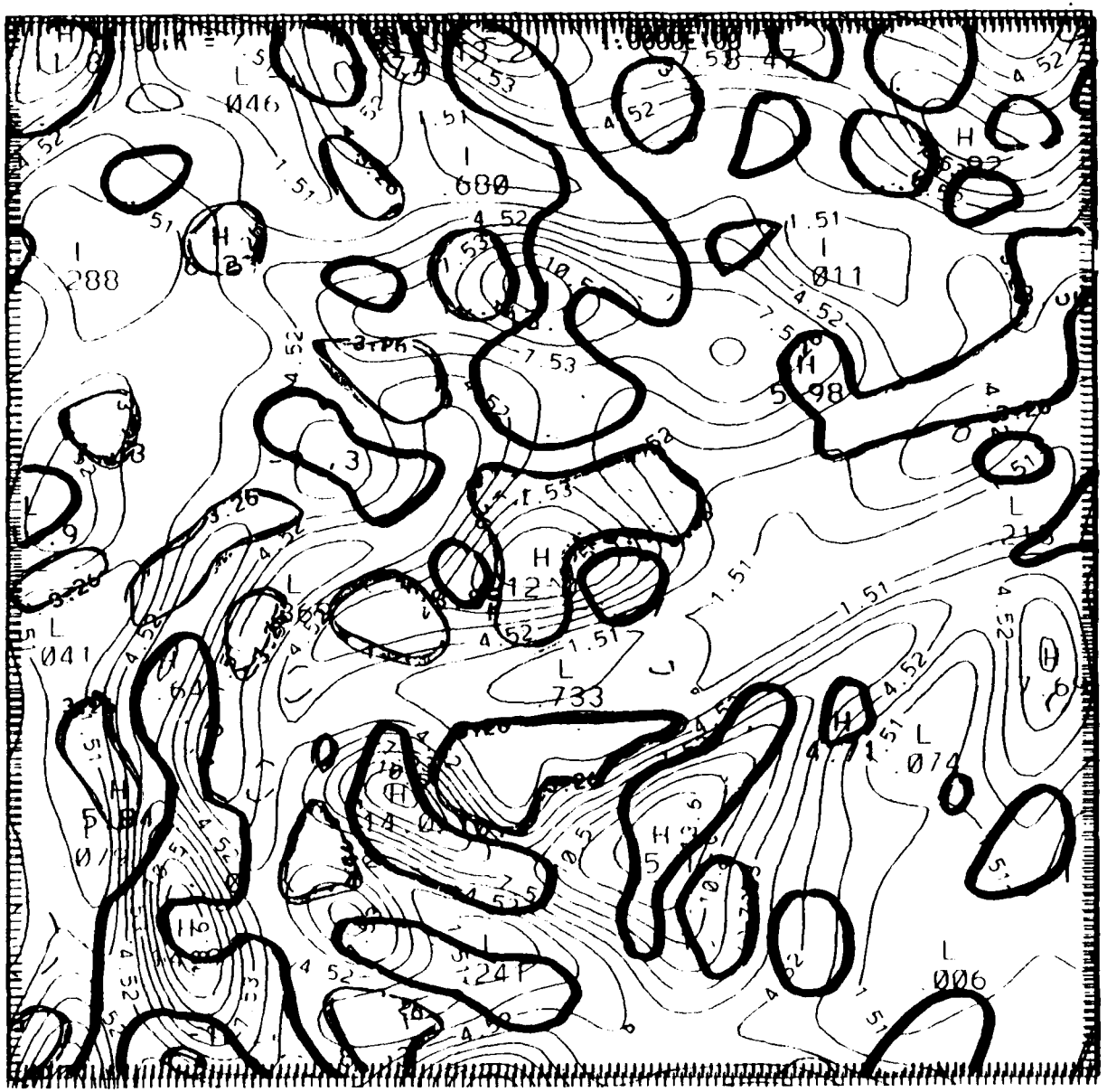

Fig. 5(a)

energy

Fig. 5(b)

dissipation

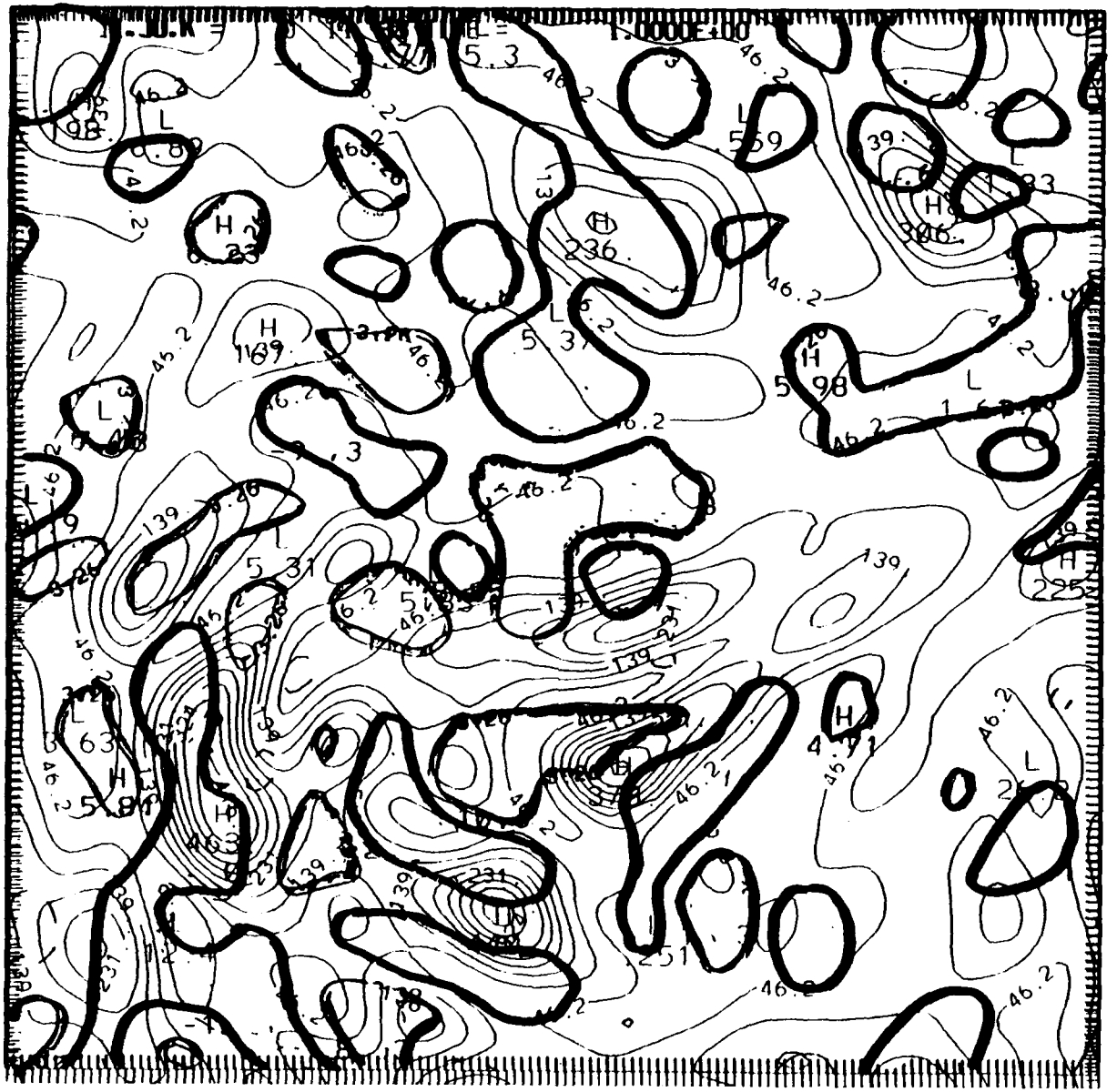

Fig. 6

vorticity production

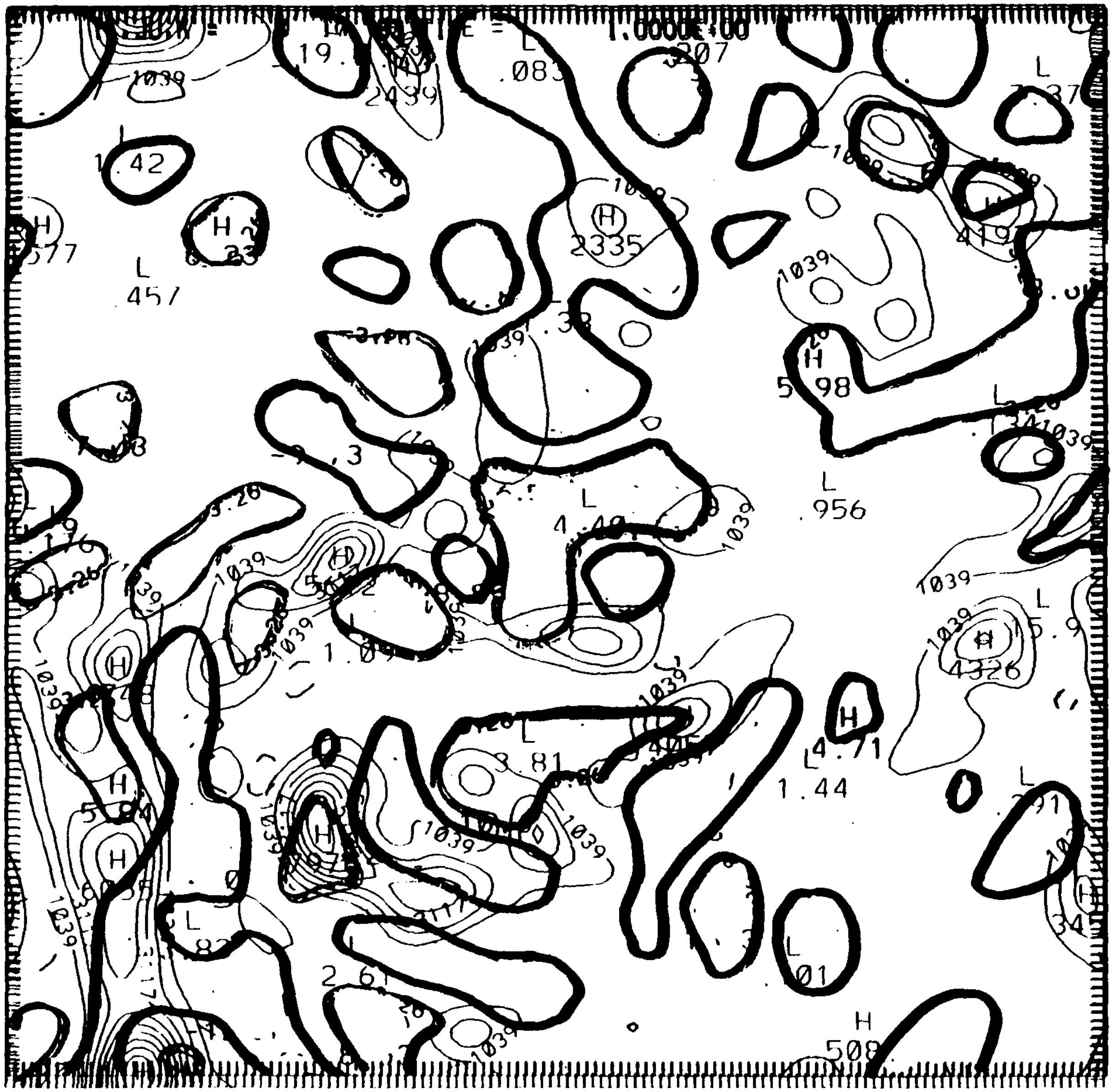

CONTOUR FROM -202009 10 -0.9000 CONTOUR INTERVAL OF 3.2609 PT(3,3)= 6.1190
CONTOUR FROM 1039.0 10 10390 CONTOUR INTERVAL OF 1039.0 PT(3,3)= 385.44

Fig. 7

enstrophy
production

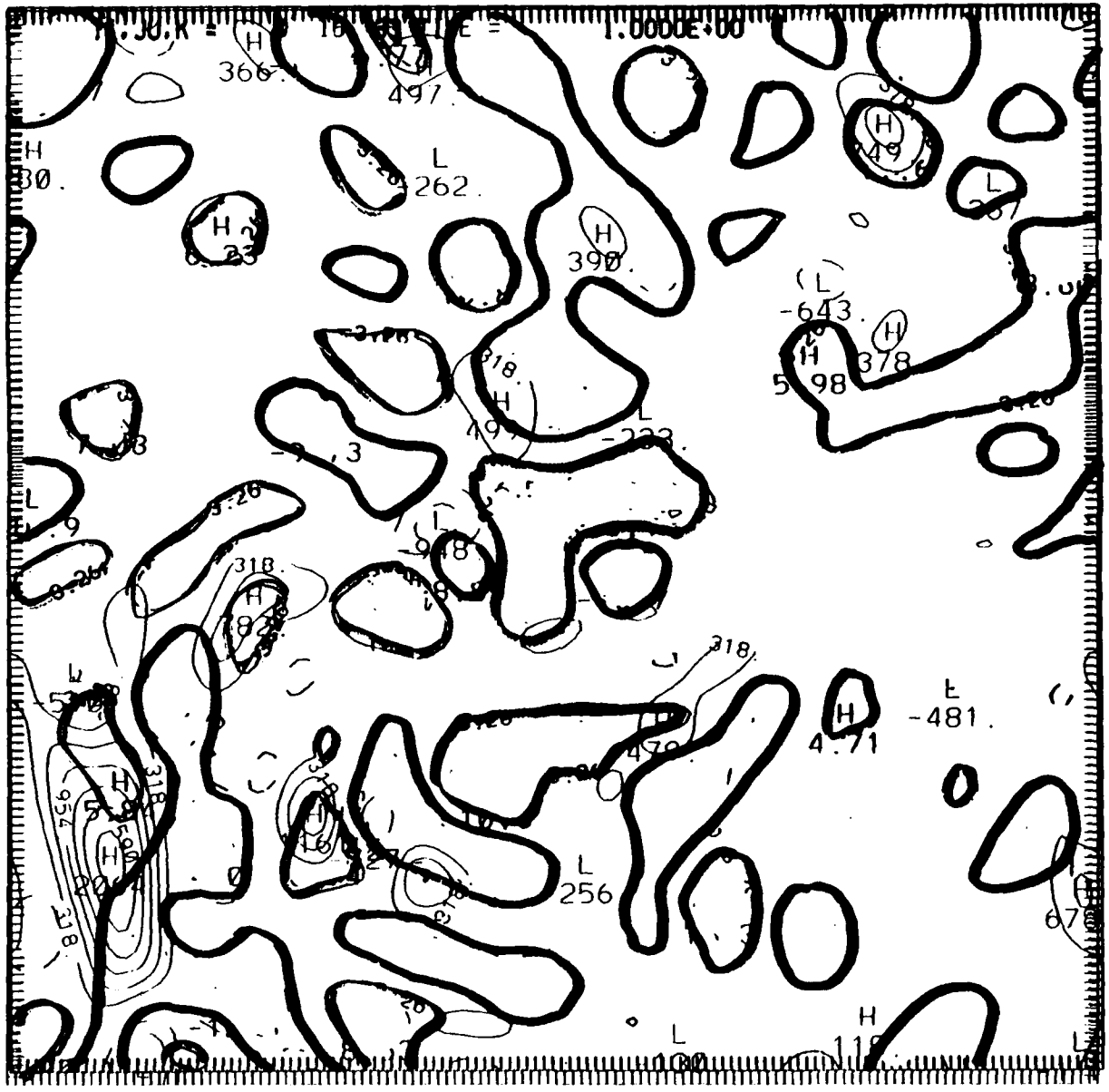

CONTOUR FROM -202889 TO -9.9888 CONTOUR INTERVAL OF 3.2689 P(13,31)= 6.1198
CONTOUR FROM -317598 TO -498749 CONTOUR INTERVAL OF 317.98 P(13,31)= 84.473

Fig-8

second invariant

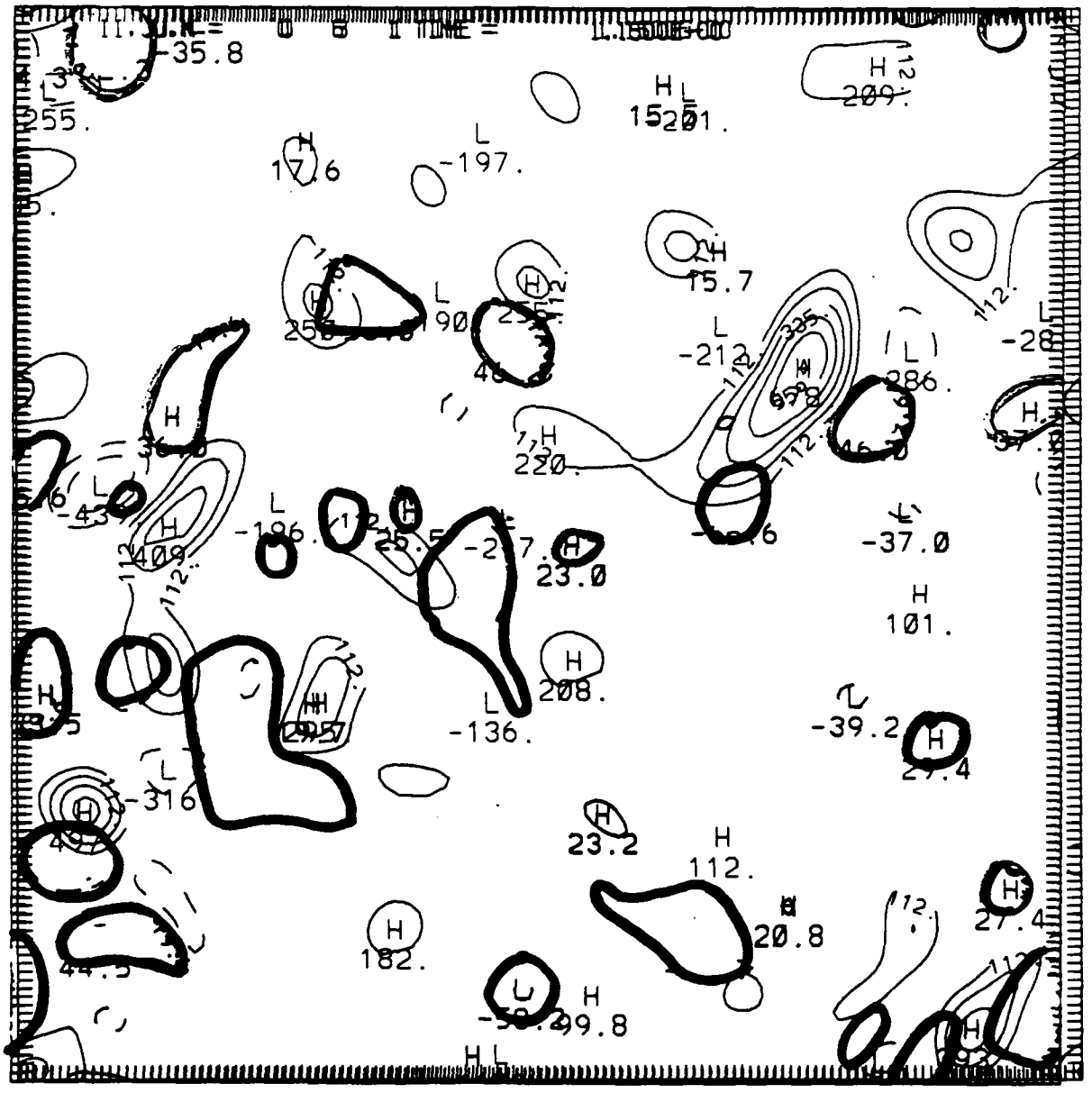

Fig. 9

Smagorinsky's transfer

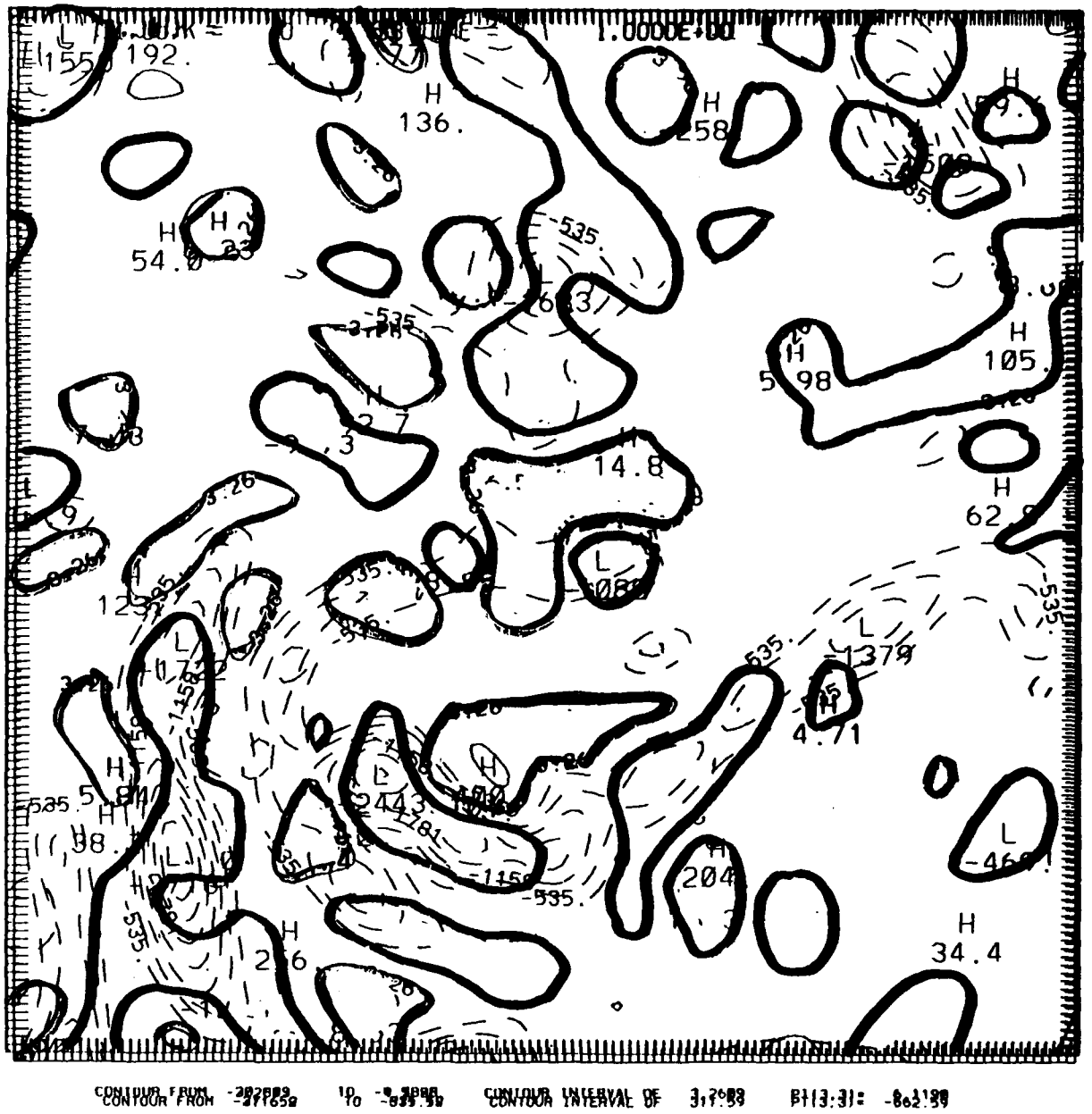

Fig. 10.